

Design and Synthesis of Chalcone and Chromone Derivatives as Novel Anticancer Agents

CHRISTINE DYRAGER



UNIVERSITY OF GOTHENBURG

Department of Chemistry
University of Gothenburg
2012

DOCTORAL THESIS

Submitted for fulfillment of the requirements for the degree of
Doctor of Philosophy in Chemistry

Design and Synthesis of Chalcone and Chromone Derivatives as Novel Anticancer Agents

CHRISTINE DYRAGER

Cover illustration: Suggested interactions between **59** and the ATP-binding site of p38 α (Chapter 5.2, Paper III).

© Christine Dyrager

ISBN: 978-91-628-8399-7

Available online at: <http://hdl.handle.net/2077/28110>

Department of Chemistry
SE-412 96 Göteborg
Sweden

Printed by Ale Tryckteam
Bohus, 2012

"My goal is simple. It is a complete understanding of the universe, why it is as it is and why it exists at all."

Stephen Hawking

Abstract

This thesis comprises the design and synthesis of chalcone and chromone derivatives and their use in various biological applications, particularly as anticancer agents (targeting proteins associated with cancer pathogenesis) and as potential fluorophores for live-cell imaging. Conveniently, all structures presented were synthesized from commercially available 2'-hydroxyacetophenones. Different synthetic strategies were used to obtain an easily accessible chromone scaffold with appropriate handles that allows regioselective introduction of various substituents. Structural diversity was accomplished by using palladium-mediated reactions for the incorporation of suitable substituents for the generation of chromone derivatives that possess different biological activities.

Challenging synthesis provided a series of fluorescent 2,6,8-trisubstituted 3-hydroxychromone derivatives with high quantum yields and molar extinction coefficients. Two of these derivatives were studied as fluorophores in live-cell imaging and showed rapid absorption, non-cytotoxic profiles and excellent fluorescent properties in a cellular environment.

Synthetic chromone precursors, i.e. chalcones, and related dienones were evaluated as antiproliferative agents that interfere with the tubulin-microtubule equilibrium, crucial for cellular mitosis. It was shown that several of the synthesized compounds destabilize tubulin assembly. However, one of the compounds was instead found to stabilize tubulin to the same extent as the known anticancer drug docetaxel, thus representing the first chalcone with microtubule stabilizing activity. Molecular docking was used in order to theoretically investigate the interactions of the chalcones with β -tubulin mainly focusing on binding modes, potential interactions and specific binding sites.

Structural-based design and extensive synthesis provided chromone-based derivatives that target two different MAP kinases (p38 α and MEK1), involved in essential cellular signal transduction pathways. The study resulted in a series of highly selective ATP-competitive chromone-based p38 α inhibitors with IC₅₀ values in the nanomolar range. Among those, two derivatives also showed inhibition of p38 signaling in human breast cancer cells. Furthermore, molecular docking was used to study potential structural modifications on the chromone structure in order to obtain highly potent derivatives that selectively target the allosteric pocket on MEK1. Initial studies provided a first generation of non-ATP-competitive chromone derivatives that prevents the activation of MEK1 with micromolar activities.

Keywords: Chalcones, Chromones, Fluorescence, Fluorophore, Cellular imaging, Anticancer, Tubulin, Microtubule, Kinase inhibitors, p38, MEK1, Palladium-mediated reactions, Molecular modeling, Structure-Activity Relationships.

List of Publications

This thesis is based on the following papers, which are referred to by the Roman numerals I-IV.

I 2,6,8-Trisubstituted 3-Hydroxychromone Derivatives as Fluorophores for Live-cell Imaging

Christine Dyrager, Annika Friberg, Kristian Dahlén, Maria Fridén-Saxin, Karl Börjesson, L. Marcus Wilhelmsson, Maria Smedh, Morten Grøtli and Kristina Luthman

Chemistry a European Journal **2009**, *15*, 9417-9423

II Inhibitors and Promoters of Tubulin Polymerization: Synthesis and Biological Evaluation of Chalcones and Related Dienones as Potential Anticancer Agents

Christine Dyrager, Malin Wickström, Maria Fridén-Saxin, Annika Friberg, Kristian Dahlén, Erik A. A Wallén, Joachim Gullbo, Morten Grøtli and Kristina Luthman

Bioorganic and Medicinal Chemistry **2011**, *19*, 2659-2665

III Design, Synthesis and Biological Evaluation of Chromone-based p38 MAP Kinase Inhibitors

Christine Dyrager, Linda Nilsson Möllers, Linda Karlsson Kjäll, Peter Dinér, Fredrik F. Wallner and Morten Grøtli

The Journal of Medicinal Chemistry **2011**, *54*, 7427-7431

IV Towards the Development of Chromone-based MEK1 Modulators

Christine Dyrager, Carlos Solano, Peter Dinér, Laure Voisin, Sylvain Meloche and Morten Grøtli

Manuscript

The publications **I-III** are reprinted with kind permission from the publishers.

Publications related to, but not discussed in this thesis:

Synthesis and Photophysical Characterisation of Fluorescent 8-(1*H*-1,2,3-Triazol-4-yl)adenosine Derivatives

Christine Dyrager, Karl Börjesson, Peter Dinér, Annelie Elf, Bo Albinsson, L. Marcus Wilhelmsson and Morten Grøtli

European Journal of Organic Chemistry **2009**, *10*, 1515-1521

Synthesis of 2-Alkyl-Substituted Chromone Derivatives Using Microwave Irradiation

Maria Fridén-Saxin, Nils Pemberton, Krystle da Silva Andersson, Christine Dyrager, Annika Friberg, Morten Grøtli and Kristina Luthman

Journal of Organic Chemistry, **2009**, *74*, 2755-2759

The Authors' Contribution to Papers I-IV

- I** Contributed to the formulation of the research problem; contributed to the synthetic work; participated during the fluorescence measurements and the fluorescence microscopy experiments; interpreted the results and wrote the manuscript.
- II** Contributed to the formulation of the research problem; contributed to the experimental work; performed the molecular modeling; interpreted the results and wrote the manuscript.
- III** Contributed to the formulation of the research problem; performed or supervised the experimental work including synthesis and molecular modeling; interpreted the results and wrote the manuscript.
- IV** Contributed to the formulation of the research problem; contributed to the synthesis of the flavone scaffold; performed the molecular modeling; interpreted the results and wrote the manuscript.

Abbreviations

1PE	One-photon excitation
2PE	Two-photon excitation
3D	Three-dimensional
ADP	Adenosine diphosphate
Ac	Acetyl
AFO	Agar-Flynn-Oyamada
AIBN	2,2'-Azobisisobutyronitrile
Ala	Alanine
aq	Aqueous
Arg	Arginine
Asn	Asparagine
Asp	Aspartate
ATP	Adenosine triphosphate
BEMP	2- <i>tert</i> -Butylimino-2-diethylamino-1,3-dimethylperhydro-1,3,2-diazaphosphorine
Boc	<i>tert</i> -butyloxycarbonyl
CAN	Cerium(IV) ammonium nitrate
Cys	Cysteine
DBU	1,8-Diazabicyclo[5.4.0]undec-7-ene
DFG	Asp-Phe-Gly
DIPA	Diisopropylamine
DME	1,2-Dimethoxyethane
DMF	<i>N,N</i> -Dimethylformamide
DMSO	Dimethyl sulfoxide
DNA	Deoxyribonucleic acid
DSK	Dual specific kinase
equiv.	Equivalents
ERK	Extracellular signal-regulated kinase
ESIPT	Excited intramolecular proton transfer
Et	Ethyl
FDA	Fluorescein diacetate
FMCA	Fluorometric microculture cytotoxicity assay
GDP	Guanosine diphosphate
Gln	Glutamine
Glu	Glutamate
Gly	Glycine
GPCR	G protein-coupled receptor
GTP	Guanosine triphosphate
h	hours
HBSS	Hank's balanced salt solution
HeLa Cells	Cervical cancer cells that originate from Henrietta Lacks (1920-1951)
His	Histidine
hp	Hydrophobic pocket
IC ₅₀	The concentration of an inhibitor required to inhibit an enzyme by 50%
IL-1	Interleukine-1
Ile	Isoleucine
JNK	c-Jun <i>N</i> -terminal kinase
LDA	Lithium diisopropylamide

Leu	Leucine
LPS	Lipopolysaccharide
Lys	Lysine
MAOS	Microwave assisted organic synthesis
MAPK	Mitogen activated protein kinase
MAPKK	Mitogen activated protein kinase kinase
MAPKKK	Mitogen activated protein kinase kinase kinase
Me	Methyl
MEK	Mitogen-activated ERK-regulating kinase
Met	Methionine
min	Minutes
MPE	Multiphoton excitation
mw	Microwave heating
N*	Normal excited species
NBS	<i>N</i> -Bromosuccinimide
<i>n</i> -Bu	<i>n</i> -Butyl
n.d.	Not determined
NIS	<i>N</i> -Iodosuccinimide
NMR	Nuclear magnetic resonance
n.r.	No reaction
PBS	Phosphate buffered saline
PDB	Protein Data Bank
Phe	Phenylalanine
Pro	Proline
PSTK	Protein serine/threonine kinase
PTK	Protein tyrosine kinase
QSAR	Quantitative structure-activity relationship
RA	Rheumatoid arthritis
rt	Room temperature
SAR	Structure-activity relationship
SDS-PAGE	Sodium dodecyl sulfate polyacrylamide gel electrophoresis
Ser	Serine
T*	Excited tautomer
TFA	Trifluoroacetic acid
THF	Tetrahydrofuran
Thr	Threonine
TLC	Thin layer chromatography
TNF- α	Tumor necrosis factor- α
Trp	Tryptophan
Tyr	Tyrosine
UV	Ultraviolet
Val	Valine

Table of Contents

1. GENERAL INTRODUCTION AND AIMS OF THE THESIS.....	1
2. BACKGROUND	3
2.1. FLAVONOIDS AND RELATED COMPOUNDS	3
2.1.1 Chalcones.....	3
2.1.2 Chromones	4
2.2 PALLADIUM-MEDIATED COUPLING REACTIONS.....	6
2.2.1 Palladium-catalyzed couplings in organic synthesis	7
2.3 MOLECULAR MODELING IN DRUG DISCOVERY	9
2.3.1 Molecular docking	10
3. 3-HYDROXYCHROMONE DERIVATIVES AS FLUOROPHORES FOR LIVE-CELL IMAGING (PAPER I)	11
3.1 INTRODUCTION	11
3.1.1 Fluorescence spectroscopy.....	11
3.1.2 Multiphoton excitation and fluorescent microscopy	12
3.1.3 Fluorescent characteristics and applications of 3-hydroxychromone derivatives	13
3.2 RESULTS AND DISCUSSION	14
3.2.1 Synthesis of 2,6,8-trisubstituted 3-hydroxychromone derivatives	14
3.2.2 Photophysical characterization	19
3.2.3 Live-cell imaging of compounds 29 and 30, using 2PE microscopy	23
3.3 CONCLUSIONS.....	25
4. CHALCONES AND RELATED DIENONES AS INHIBITORS OR PROMOTERS OF TUBULIN POLYMERIZATION (PAPER II)	27
4.1 INTRODUCTION	27
4.1.1 Tubulin and microtubules	27
4.1.2 Tubulin as a target for antimetabolic agents	28
4.1.3 Chalcones as microtubule destabilizing agents	29
4.2 RESULTS AND DISCUSSION	30
4.2.1 Synthesis of dihalogenated dienones 34-35.....	30
4.2.2 Cytotoxicity and antiproliferative studies.....	31
4.2.3 The effect on tubulin polymerization.....	33
4.2.4 Molecular modeling and docking studies.....	34
4.2.5 Study of the chemical reactivity with glutathione.....	38
4.3 CONCLUSIONS.....	38
5. DEVELOPMENT OF CHROMONE-BASED KINASE INHIBITORS AND MODULATORS (PAPERS III AND IV).....	39
5.1 INTRODUCTION	39
5.1.1 Protein kinases	39
5.1.2 MAP Kinases.....	41
5.1.3 Protein kinases as drug targets.....	42
5.1.4 The p38 MAP Kinase	43
5.1.5 The MEK1/2 MAP kinase kinases.....	46
5.2 DEVELOPMENT OF p38 α MAP KINASE INHIBITORS (PAPER III)	47
5.2.1 Docking studies of the ATP-binding site of p38 α	47
5.2.2 Synthetic strategy A	48
5.2.3 Synthetic strategy B	50
5.2.4 Biological evaluation of compounds 57-65 toward p38 α	57

5.2.5 Kinase selectivity screening of 59 and 63	57
5.2.6 Studies on the effect of p38 kinase signaling in human breast cancer cells	59
5.3 DEVELOPMENT OF ALLOSTERIC MEK1 MODULATORS (PAPER IV)	60
5.3.1 Docking studies into the allosteric pocket of MEK1	60
5.3.2 Synthesis of PD98059 analogs.....	62
5.3.3 Biological evaluation of compounds 80, 81 and 85 as MEK1 modulators.....	65
5.4 CONCLUSIONS.....	66
6. CONCLUDING REMARKS AND FUTURE PERSPECTIVES	69
ACKNOWLEDGEMENTS	71
REFERENCES AND NOTES	73
APPENDIX.....	87

1. General Introduction and Aims of the Thesis

Proteins are essential components in signal transduction pathways and play crucial roles in various processes within the cell cycle. Consequently, dysregulation of protein function related to cell growth, mitosis, proliferation, and apoptosis is strongly associated with human cancers. Furthermore, the understanding of cancer pathogenesis on a molecular level has improved during the last decades, thus increased the identification of small molecular inhibitors that target cancer-specific pathways. As a result, contemporary development of novel anticancer agents focuses on compounds that bind to specific biological targets instead of non-selective strategies such as radiation or chemotherapy.

This thesis includes the design and synthesis of chalcones and chromone derivatives that target mitogen activated protein kinases (proteins that are involved in various processes to maintain cell viability) and the tubulin-microtubule equilibrium, which is crucial for cellular mitosis. The general aim of the study was to develop efficient synthetic strategies to afford structurally diverse chromone derivatives, involving Pd-mediated cross-coupling reactions, and to investigate their utility for various applications. The specific objectives of the thesis were:

- To use a scaffold methodology in the pursuit to access diverse chromone derivatives, which could be decorated by introduction of various substituents using palladium mediated C-C coupling reactions.
- To study the spectroscopic properties of 2,6,8-trisubstituted 3-hydroxychromones and to investigate their ability as fluorescent probes in a cellular environment using live-cell imaging.
- To investigate if synthesized chromone precursors, i.e. chalcones, could interfere with the tubulin-microtubule equilibrium which is crucial for cellular mitosis.
- To use molecular docking as a tool for designing chromone-based kinase inhibitors/modulators and to evaluate their activity towards two specific kinases, p38 α and MEK1.

2. Background

2.1. FLAVONOIDS AND RELATED COMPOUNDS

Flavonoids belong to a large group of abundant plant secondary metabolites, which can be found in vascular plants such as ferns, conifers and flowering plants.¹⁻³ These natural compounds are generally divided into various classes on the basis of their molecular structures including chalcones, flavones, flavanones, flavanols, and anthocyanidins (Figure 1). Approximately, 4000 varieties of flavonoids have been identified and many of these are intense pigments, providing a spectrum of yellow, red and blue colors in flowers, fruits and leaves.³⁻⁶ Besides their contribution to plant color, flavonoids have several pharmacological benefits (e.g. anticancer, anti-inflammatory, anti-allergic, etc.) and are known as effective antioxidants, metal chelators and free radical scavengers.^{3, 7-12} Natural and synthetic flavonoids are therefore of considerable interest in the development of novel therapeutic agents for various diseases and are generally believed to be non-toxic compounds since they are widely distributed in the human diet.^{2, 5}

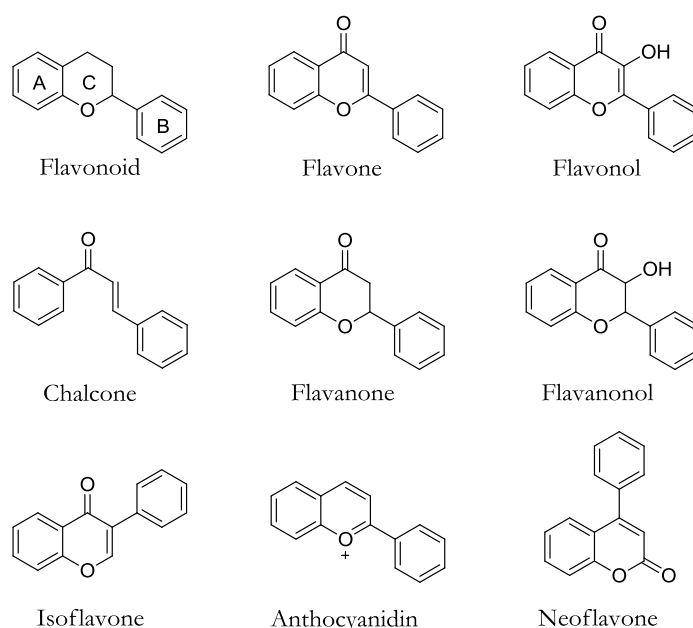


Figure 1. Examples of common flavonoids and their derivatives. A, B, and C describe the order of ring introduction or ring formation in the synthesis (biosynthesis or synthetic).^{1, 3, 13}

2.1.1 Chalcones

Chalcones, 1,3-diphenylpropenones (Figure 2), constitute one of the major classes of flavonoids with widespread distribution in vegetables, fruits, tea and soy.^{3, 14} Prehistoric

therapeutic applications of chalcones can be associated with the thousand-year old use of plants and herbs for the treatment of different medical disorders.¹⁵ Contemporary studies report a generous variation of significant pharmacological activities of chalcones including antiproliferative, antioxidant, anti-inflammatory and anticancer effects.^{14, 16-18}

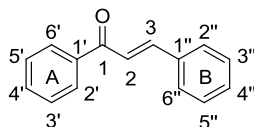


Figure 2. The general structure and numbering of chalcones. A and B describe the order of ring introduction or ring formation in the synthesis.¹⁹

Chalcones are important precursors in the biosynthesis of flavones and flavanones and are usually synthesized from acetophenones and benzaldehydes via the Claisen-Schmidt condensation, using base in a polar solvent (Figure 3).¹⁹⁻²¹ In addition, more exotic synthetic protocols have been reported, such as the palladium-mediated Suzuki coupling between cinnamoyl chloride and phenyl boronic acids or the carbonylative Heck coupling with aryl halides and styrenes in the presence of carbon monoxide.^{22, 23}

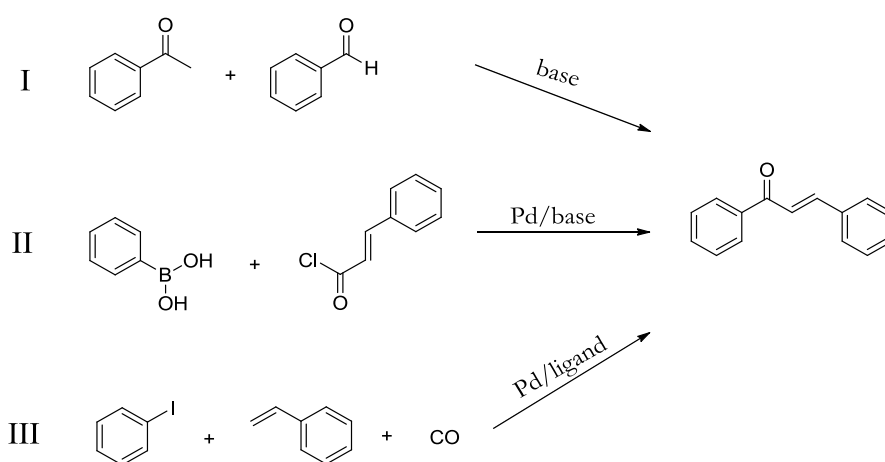


Figure 3. Examples of synthetic routes toward chalcones. I) Claisen-Schmidt condensation. II) Suzuki cross-coupling. III) Carbonylative Heck reaction.²⁰⁻²³

2.1.2 Chromones

The chromone ring system, 1-benzopyran-4-one (Figure 4), is the core fragment in several flavonoids, such as flavones, flavonols and isoflavones.²⁴ The word chromone can be derived from the Greek word *chroma*, meaning “color”, which indicates that many chromone derivatives exhibit a broad variation of colors.

The rigid bicyclic chromone fragment has been classified as a privileged structure in drug discovery (i.e. a molecular framework able to provide ligands for diverse receptors), due to its use in a wide variety of pharmacologically active compounds such as anticancer,

anti-HIV, antibacterial and anti-inflammatory agents.²⁵⁻³⁴ Several chromone derivatives have also been reported to act as kinase inhibitors, to bind to benzodiazepine receptors and as efficient agents in the treatment of cystic fibrosis.³⁵⁻³⁷

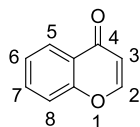


Figure 4. The general structure and numbering of chromones.^{24, 38}

Although there are a large number of chromone derivatives known for their pharmacological properties there are only a few examples that have been or that are used as therapeutic agents today. Khellin (Figure 5), extracted from the seeds of the plant *Ammi visnaga*, was the first chromone in clinical practice and it has been used for centuries in the Mediterranean area as a diuretic to relieve renal colic.³⁸ Furthermore, around the 1950s, khellin was used as a smooth muscle relaxant in the treatment of angina pectoris and asthma.³⁹ However, present use of khellin as a therapeutic agent focuses on the treatment of vitiligo, a pigmentation disorder.⁴⁰ Other, current medical treatments with chromone derivatives can be exemplified by sodium cromoglycate (Lomudal®) used as a mast cell stabilizer in allergic rhinitis, asthma and allergic conjunctivitis, diosmin (Daflon®) for the treatment of venous diseases and flavoxate a smooth muscle relaxant to treat urge incontinence (Figure 5).^{38, 41-45}

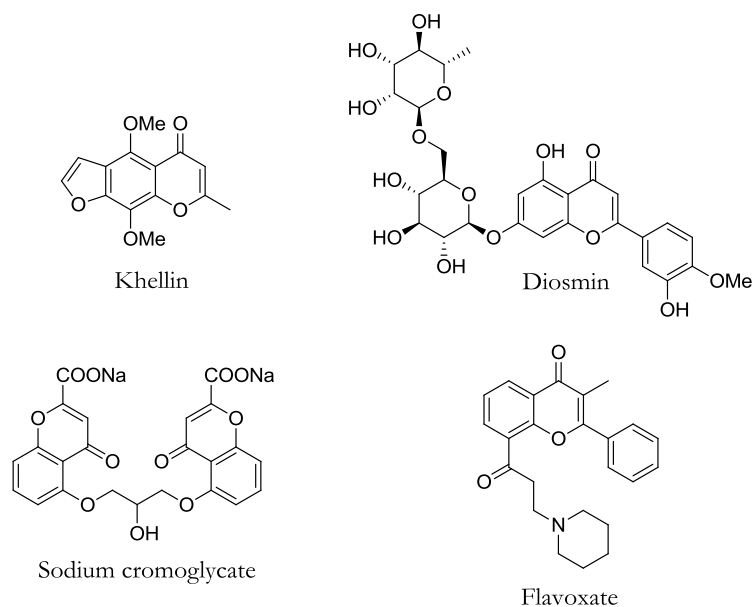


Figure 5. Examples of chromone-based compounds that have been or that are used as pharmaceutical agents. Khellin has previously been used for the treatment of angina pectoris and is currently used in the treatment of vitiligo. Diosmin is a therapeutic agent for venous diseases, sodium cromoglycate is utilized as a mast cell stabilizer in allergic rhinitis, asthma and allergic conjunctivitis and flavoxate is a smooth muscle relaxant to treat urge incontinence.

Besides their diversity as structural scaffolds, possible to modify to achieve different pharmacological activities, several chromone derivatives also exhibit a wide range of fluorescent properties. In particular, the 3-hydroxyflavones have been used as hydrogen bonding sensors, fluorescent probes for DNA-binding affinity studies and as fluorophores for protein labeling and apoptosis.⁴⁶⁻⁴⁹

The most common synthetic routes to the chromone structure occur via a chalcone intermediate or via the Baker-Venkataraman rearrangement (Figure 6).^{24, 50-53} The chalcone pathway implicates the base-catalyzed aldol condensation of 2'-hydroxyacetophenones with aromatic or conjugated aldehydes. The resulting chalcone can then be cyclized to a flavone (e.g. in the presence of iodine) or to the corresponding 3-hydroxyflavone, using alkaline hydrogen peroxide solution, via the Algar-Flynn-Oyamada (AFO) reaction.^{54, 55} The Baker-Venkataraman approach involves rearrangement of *O*-acetylated 2'-hydroxyacetophenones to *ortho*-hydroxy 1,3-diketones via enolate formation followed by a base-promoted acyl transfer. The chromone structure can then be obtained via acid catalyzed cyclization.²⁴ Several alternative routes to obtain chromones and flavones have been reported over the recent years, such as the cyclization of alkynyl-ketones (either base promoted or using iodine monochloride) or palladium-mediated cyclocarbonylation of *ortho*-iodophenols with terminal acetylenes in the presence of carbon monoxide.^{24, 56, 57}

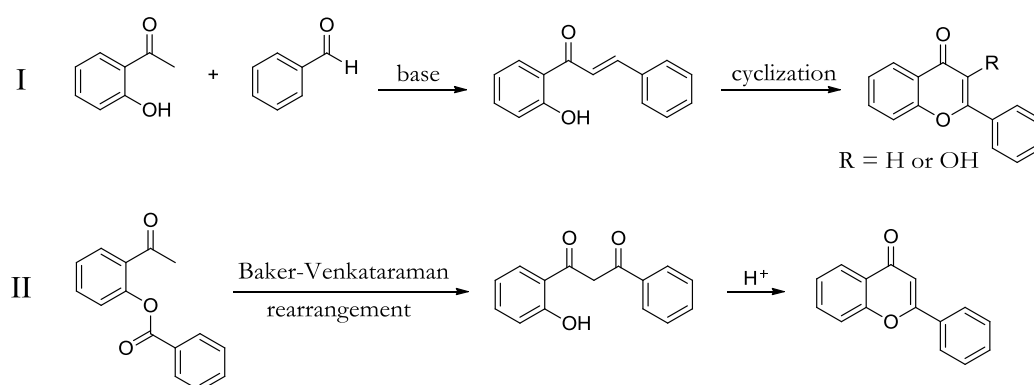


Figure 6. Common synthetic routes to obtain the chromone structure. I) Synthesis via a chalcone intermediate followed by cyclization, e.g. in the presence of iodine or alkaline hydrogen peroxide. II) Synthesis via the Baker-Venkataraman rearrangement followed by acid-catalyzed cyclization.

2.2 PALLADIUM-MEDIATED COUPLING REACTIONS

Transition metals, such as palladium, copper, nickel, iron and rhodium play an important role in organic synthesis since they can catalyze the formation of new bonds, especially C-C bonds. A large number of transition metal-mediated reactions have been reported during the past decades and many of these have become essential in the synthesis of complex organic molecules including biologically active compounds such as natural products and steroids.^{24, 58, 59}

This thesis includes introduction of various substituents on the chromone scaffold via various palladium-mediated coupling reactions, in particular the Heck, Sonogashira, Suzuki and Buchwald-Hartwig reactions, which will be discussed further in the following chapters.

2.2.1 Palladium-catalyzed couplings in organic synthesis

Palladium is by far the most important and frequently used transition metal in organic coupling reactions.⁶⁰ Thus, the 2010 Nobel Prize in chemistry was awarded to Richard F. Heck, Ei-ichi Negishi and Akira Suzuki for the development of palladium-catalyzed cross-coupling reactions in organic synthesis.⁶¹ Well-known coupling reactions with palladium as a catalyst are illustrated in Figure 7.

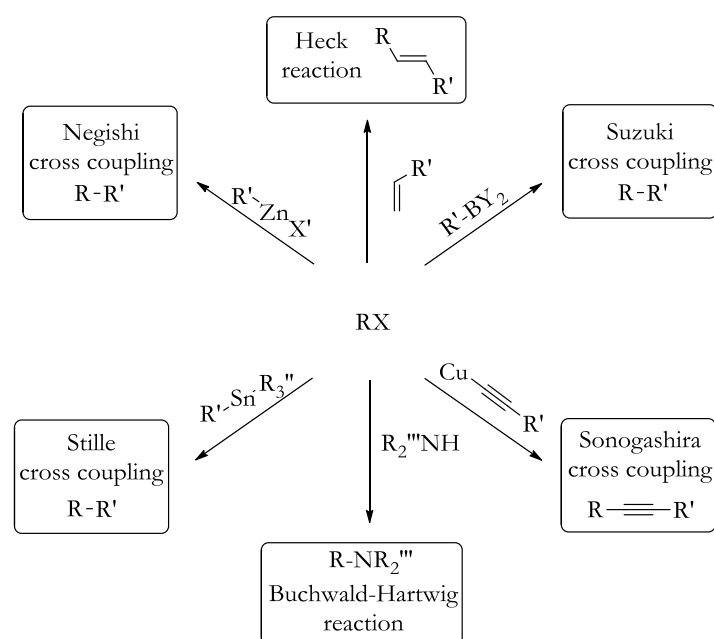


Figure 7. Examples of common palladium-catalyzed reactions in organic synthesis.²⁴

The general mechanism for Pd-catalyzed cross-coupling reactions with organometallic reagents (e.g. the Sonogashira, Negishi, Stille and Suzuki reactions) involves three stages: oxidative addition, transmetalation and reductive elimination (Figure 8). The cycle starts with a zerovalent catalyst, Pd(0), generally constructed of palladium and ligands such as phosphines, amines or *N*-heterocyclic carbenes. However, Pd(II) complexes are frequently used as pre-catalysts since they are generally more stable than the Pd(0) species. Nevertheless, these pre-catalysts need to be reduced to Pd(0), which can be done as an initial step in situ, before the catalytic cycle can begin. The oxidative addition step involves insertion of Pd(0) into the R-X bond along with a simultaneous oxidation of Pd(0) to Pd(II). In terms of chemoselectivity and relative rate, the reaction is dependent on X according to the trend: X = I > Br ~ OTf >> Cl >> F. Subsequent transmetalation with a nucleophilic organometallic reagent, such as copper acetylides or boronic acids, involves transfer of the R-group to palladium with displacement of X. In the last step, the

unstable intermediate is subjected to reductive elimination creating a carbon-carbon bond and regeneration of the palladium(0) complex.^{58, 59}

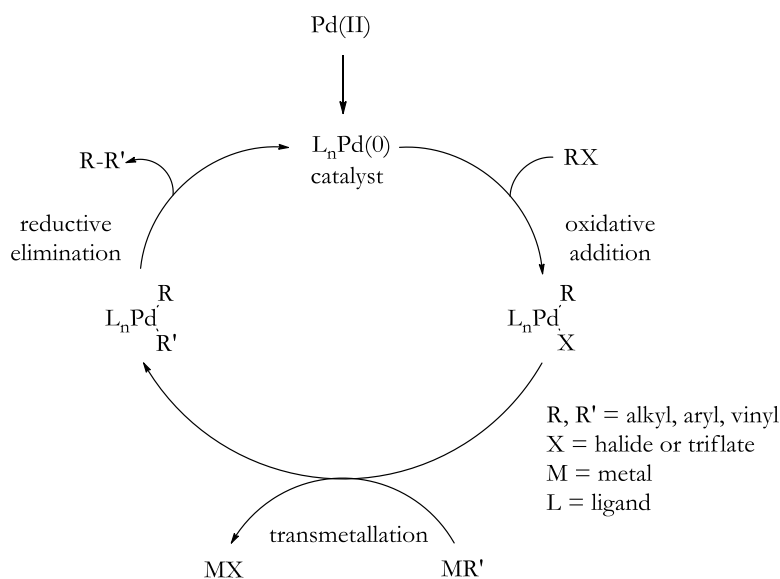


Figure 8. General catalytic cycle for palladium-mediated cross-coupling reactions.⁵⁸

The Heck reaction, with olefins and alkyl or aryl halides, does not involve organometallic reagents, which results in a slightly different mechanism than the one described above.⁶²⁻⁶⁵ As illustrated in Figure 9, the olefin forms a π -complex with the palladium catalyst after the oxidative addition step. Subsequently, the R-group on palladium migrates to one of the olefin carbons at the same time as the palladium gets attached via a σ -bond to the other carbon. The generated alkylpalladium intermediate then undergoes a β -hydride elimination giving an R-substituted olefin product and a hydridopalladium halide. Finally, the palladium complex undergoes a reductive elimination in the presence of base to regenerate the palladium(0) catalyst.^{58, 59}

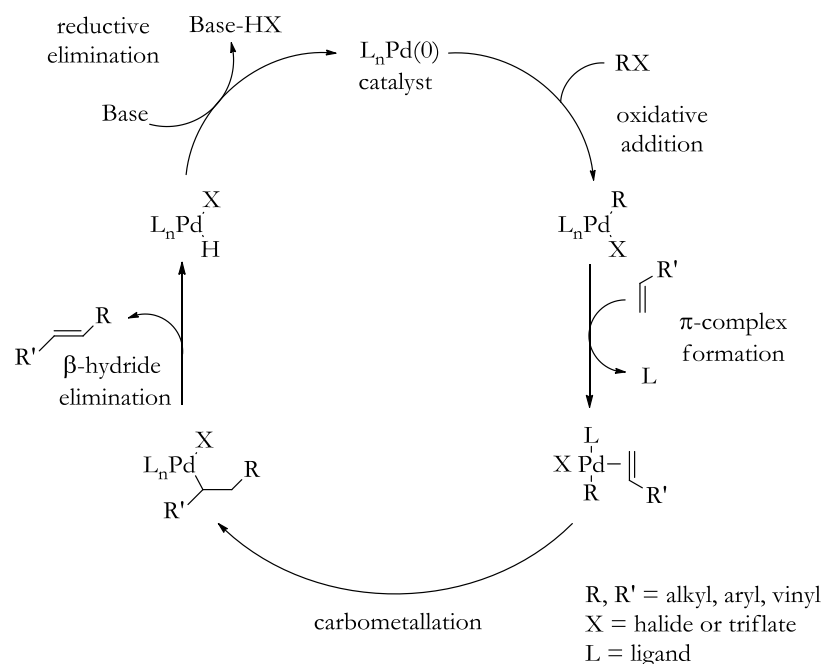


Figure 9. General catalytic cycle for the Heck reaction.⁵⁸

2.3 MOLECULAR MODELING IN DRUG DISCOVERY

The term molecular modeling includes theoretical methods and computational methodologies that are used to mimic or predict the behavior of molecules and molecular systems. These methods usually involve molecular mechanics, quantum mechanics, conformation analysis, and molecular dynamics.⁶⁶ Molecular modeling technologies have mainly been developed during the past decades, due to the development of fast computers, and are today essential tools in drug development used for protein structure determination, sequence analysis, protein folding, homology modeling, docking studies and pharmacophore determination.

Currently, two major modeling strategies are used for the design of new drugs and these are generally based on whether three-dimensional (3D) structures of the biological targets or related proteins are available or not:

Structure-based (direct) drug design is generally performed using a known 3D structure of a specific biological target (e.g. a receptor or an enzyme), information that is usually provided by techniques such as NMR spectroscopy or X-ray crystallography.^{67, 68} Alternatively, if the 3D structure of a specific target is unavailable, it is possible to generate a homology model based on a related protein. Three-dimensional data of target proteins bound to known inhibitors or antagonists provide invaluable information that allows active site determination, identification of important binding interactions within the active site and further possibilities for docking of other compounds.

Ligand-based (indirect) drug design is generally used if the 3D structure of a particular target is unavailable. This strategy relies on known active compounds that bind to the biological target of interest and that are complementary with a hypothetical active

site.⁶⁸ These together with known inactive compounds can be used to create a pharmacophore model that defines essential structural features for binding and activity.⁶⁹ In addition, incorporating inactive compounds into the model can give information about forbidden volumes with the aim to constrain the prototype. Furthermore, known ligands can be used for the development of a target specific quantitative structure-activity relationship (QSAR) model that uses molecular descriptors as numerical representations of chemical structures. Thus, physicochemical properties of compounds are correlated with their pharmacological activity and the calculated mathematical relationship can predict the activity of novel compounds.

2.3.1 Molecular docking

Molecular docking is commonly used in the field of drug design to predict the binding of small molecules to biological protein targets. This method gives the possibility to study an active site in detail and can be used for hit identification, virtual screening, binding mode determination, and lead optimization. Generally, the docking methodology is used to fit a compound into an artificial model or to a known three-dimensional binding site, which can be utilized to explore ligand conformation, orientation and feasible molecular interactions such as hydrogen bonding and hydrophobic interactions. Thus, molecular docking is a powerful tool for the design of ligands toward a specific protein target. Although, molecular docking is a useful tool in drug design it should be used with common sense since it comprise artificial models of complex structures with high flexibility and dynamics.

3. 3-Hydroxychromone Derivatives as Fluorophores for Live-Cell Imaging (Paper I)

3.1 INTRODUCTION

3.1.1 Fluorescence spectroscopy

Fluorescence is a photoluminescence phenomenon in which spontaneous emission of electromagnetic radiation normally occurs within a few nanoseconds after an atom or a molecule is being excited to a higher state.^{70, 71} Structural features (generally in polyaromatic hydrocarbons or heterocycles) that are responsible for the fluorescent mechanism are called fluorophores, and molecules that exhibit fluorescence properties are commonly designated as fluorophores or fluorescent dyes.⁷²

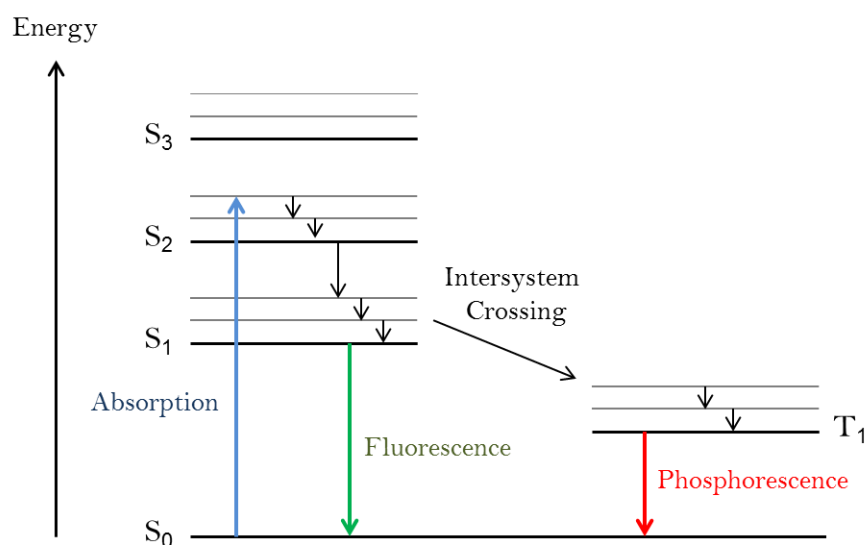


Figure 10. Jablonski diagram.⁷⁰ Following photon absorption, a fluorophore is generally excited from its singlet ground electronic state (S_0) to a higher energy level such as S_1 or S_2 . Subsequently, the fluorophore relaxes to the ground state (S_0), via fluorescence or phosphorescence, by emitting a photon.

The photophysical relationship between absorption and emission is usually described by the Jablonski diagram, which illustrates the electronic states of a molecule and the transitions between them (Figure 10). Following photon absorption, a fluorophore is generally excited from its singlet ground electronic state (S_0) to a higher energy level such as S_1 or S_2 . In each electronic state, the fluorophore can exist in a number of vibrational levels. In the excited state, the fluorophore is subjected to collisions with the surrounding molecules, which results in energy loss as it descends the vibrational ladder to the lowest

level of that state. Further deactivation via internal conversion to lower lying excited states and vibrational relaxation to the lowest vibrational level of S_1 then occurs. Subsequently, the fluorophore relaxes to the ground state (S_0) via the fluorescence pathway by emitting a photon. The difference in energy between the maxima of the spectral absorption and emission bands is commonly referred to as the Stokes shift, which is an effect of rearrangements of the solvent around the fluorophore. Additionally, in phosphorescence, the photon emission can occur for longer periods as a result of spin conversion to a forbidden triplet state (T_1) via an intersystem crossing process followed by further relaxation in another spin-forbidden process from T_1 to S_0 .^{70, 71}

The efficiency of the fluorescence process is generally described by the quantum yield (Φ_F), defined as the ratio of the number of photons emitted to the number of photons absorbed. The maximum fluorescence quantum yield is 1.0 (100%), which can be reached if the number of photons absorbed is equal to the number of photons emitted. The fluorescence intensity can be decreased by various quenching mechanisms such as contact with collisional quenchers (e.g. molecular oxygen, halogens and specific amines) and complex formation with a molecule that generates a nonfluorescent complex.⁷⁰

Fluorescence methodologies are used in a large range of valuable biochemical applications, including structural determination of proteins, DNA sequencing, medical diagnostics, and organelle staining in living cells.⁷⁰ A large number of fluorophores have been developed and discovered during the last decades, e.g. fluorescein, rhodamine and quinine (Figure 11).⁷²

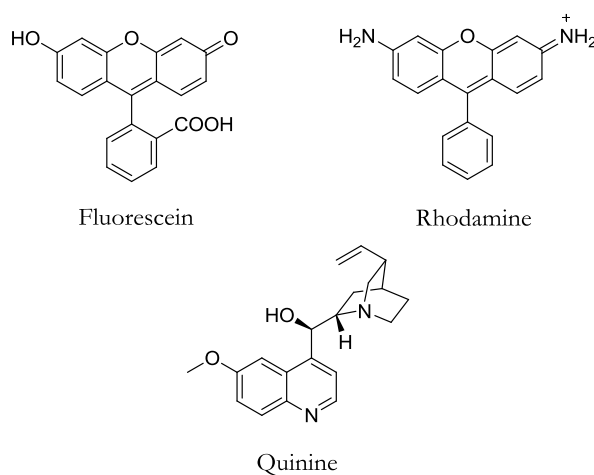


Figure 11. Fluorescein, rhodamine and quinine are examples of fluorescent dyes with applicable photophysical properties, such as high quantum yields (e.g. $\Phi_{\text{Fluorescein}} = 0.92$ and $\Phi_{\text{Quinine}} = 0.55$).⁷²⁻⁷⁴

3.1.2 Multiphoton excitation and fluorescent microscopy

Besides one-photon excitation, fluorophores can reach the excited state by simultaneous absorption of two-photons or more, known as multiphoton excitation (MPE).⁷⁰ This can be achieved by using a high energy pulsed laser, which provides a high stream of photons.

MPE, in particular two-photon excitation (2PE), is predominantly used in fluorescence microscopy for the investigation of biological systems, due to several important advantages over one-photon excitation (1PE) techniques. 2PE is achieved by using longer wavelengths, i.e. infrared light, to avoid the much stronger single-photon absorption of the fluorophore and to decrease effects of light scattering by the cell content. 2PE microscopy increases the cell viability and allows the use of an optimal excitation wavelength. Moreover, almost all fluorophores are photobleached upon continuous illumination, especially in fluorescence microscopy where the light intensities are high. Thus, the use of 2PE minimizes photobleaching and phototoxicity, which are limiting factors in fluorescence microscopy of living cells and tissues.^{70, 75}

3.1.3 Fluorescent characteristics and applications of 3-hydroxychromone derivatives

In 1979, Sengupta and Kasha reported the characteristic dual fluorescent behavior of 3-hydroxyflavones.⁷⁶ Upon excitation, the 3-hydroxychromone fluorophore exhibits two well-separated emission bands, originating from the excited normal species (N^*) and the phototautomer (T^*) formed via an excited state intramolecular proton transfer (ESIPT) (Figure 12).^{77, 78}

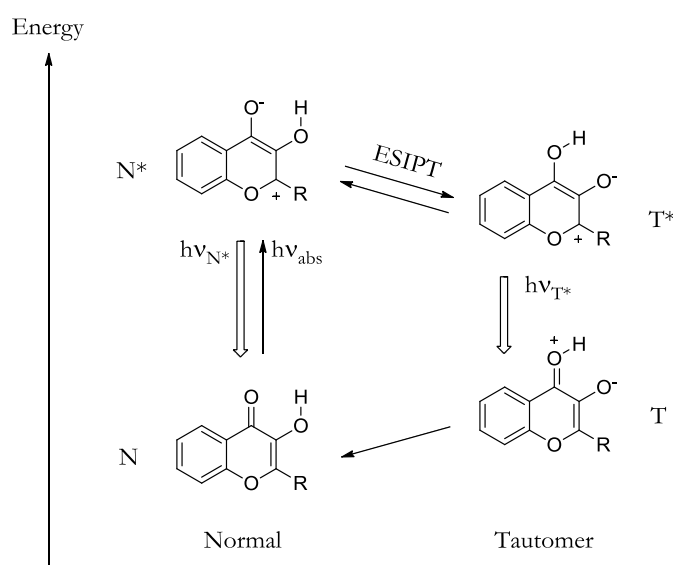


Figure 12. The dual fluorescent behavior of 3-hydroxychromones represented in an energy diagram.⁷⁶ Upon excitation, the normal excited species (N^*) undergoes an excited intramolecular proton transfer (ESIPT) to give the excited tautomer (T^*). The R-group in the figure is generally an aromatic moiety, e.g. phenyl.

Due to their characteristic fluorescence behavior, 3-hydroxychromone derivatives have been used as biosensors, hydrogen bonding sensors, and as fluorescent probes for dipotential (Ψ_D) measurements in lipid bilayers.⁷⁹⁻⁸⁵ They have also been used for studies of DNA interactions and as photochemical dyes for protein labeling and apoptosis.^{47, 86-88}

The photophysical behavior of 3-hydroxychromones has been carefully studied and efforts have been made to develop derivatives with improved and exceptional fluorescent properties. For example, a strong electron donating substituent in the *para*-position on the B-phenyl ring, such as in 2-(4-diethylaminophenyl)-3-hydroxychromones, have shown to be beneficial for the fluorescent behavior (Figure 13).^{78, 89} The electron-rich diethylamine functionality contributes to a significant change in the electron distribution resulting in derivatives with high quantum yields ($\Phi_F \sim 0.5$). It has also been proposed that the S_1 state for 2-(4-diethylaminophenyl)-3-hydroxychromones is represented by a zwitterionic excited species, which is induced via charge transfer (Figure 13).⁸⁹

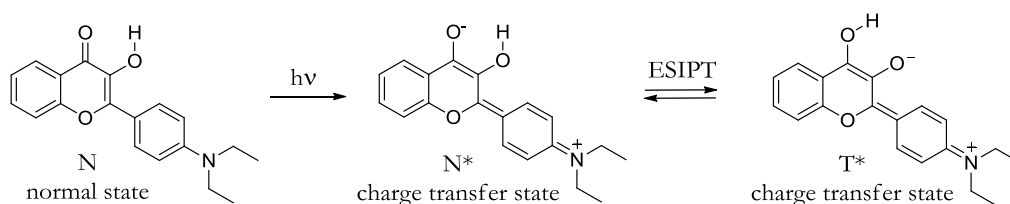


Figure 13. 2-(4-Diethylaminophenyl)-3-hydroxychromones exhibit interesting fluorescence properties. In addition to the ESIPT mechanism, they are able to adopt a zwitterionic excited state, which is induced via charge transfer.⁸⁹

3.2 RESULTS AND DISCUSSION

In a project aimed at the development of novel chromone-based peptidomimetics, we came across a series of fluorescent 3-hydroxychromone derivatives with electron withdrawing and donating aromatic or conjugated substituents in the 2-position.^{90, 91} Thus, we wanted to characterize the fluorescent properties of these derivatives and investigate how various substituents in the 2-position affect the ESIPT process, the absorption/emission maxima, and the fluorescence quantum yields. One aim was to extend the series with a few 2-(4-diethylaminophenyl)-3-hydroxychromone derivatives, due to their known and interesting fluorescence properties.⁸⁹ In addition, we also wanted to explore the utility of 3-hydroxychromone derivatives as fluorophores for live-cell imaging. However, the use of living cells implicates a number of important aspects that need to be taken into consideration such as permeability, solubility and UV-exposure. Considering this, the idea was to extend the conjugation of the chromone chromophore and to enhance the polarity by introducing an aminopropyl group to the A-ring. We also thought that the amine functionality could be used as a handle for the attachment of other compounds, i.e. probing, for various applications within the field of bioimaging.

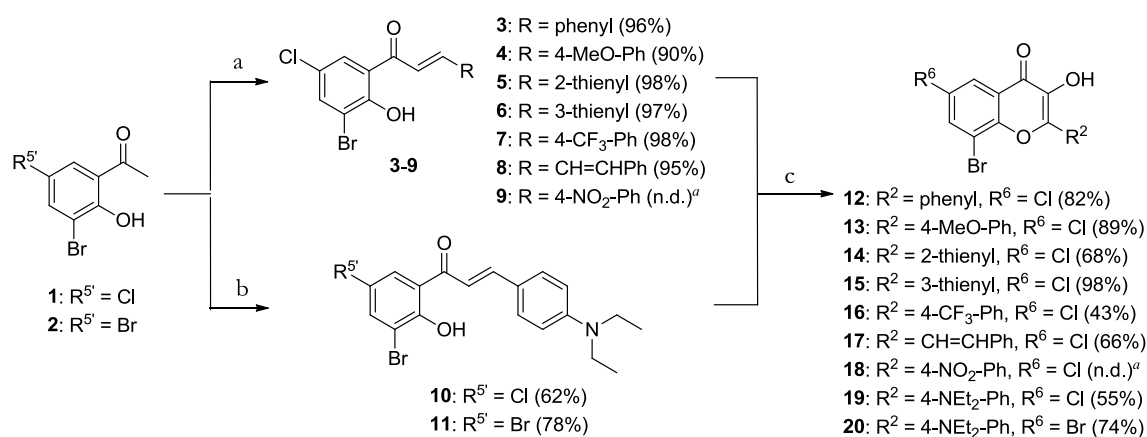
3.2.1 Synthesis of 2,6,8-trisubstituted 3-hydroxychromone derivatives

In 2006, Dahlén et al. reported a scaffold approach toward 3,6,8-trisubstituted flavones using 3'-bromo-5'-chloro-2'-hydroxyacetophenone (**1**) as starting material.⁹¹ This flavone scaffold enables regioselective introduction of substituents at the given positions as well as construction of a series of structural diverse derivatives that could be used for various applications. Moreover, the synthetic route also involves efficient generation of fluorescent 3-hydroxychromone derivatives with various aromatic or conjugated

substituents in the 2-position. Consequently, we wanted to use this scaffold methodology in the present study.

3.2.1.1 Synthesis of the chromone scaffold

Chalcones **3-7** and the dienone **8** were prepared via a Claisen-Schmidt condensation, from commercially available 3'-bromo-5'-chloro-2'-hydroxyacetophenone **1** and various aromatic or conjugated aldehydes with electron-deficient or donating properties, using KOH in EtOH (Scheme 1).^{90, 91} Compounds **3-8** were obtained in high yields (90-98%), after efficient recrystallization from EtOH. Initially, it was anticipated that the same reaction conditions also could be used to provide the diethylamino derivatives (Figure 13). However, no product could be traced or isolated when using 4-diethylaminobenzaldehyde in the condensation reaction. A possible explanation for this could be that, the strong electron donating diethylamino group in the *para*-position makes the aldehyde less electrophilic, which aggravates the essential nucleophilic attack at the carbonyl carbon. Similar protocols but with other bases were attempted, such as Ba(OH)₂ in MeOH or NaOMe in DMF, but disappointingly without any product formation.^{92, 93}



Scheme 1. Synthesis of dihalogenated 3-hydroxychromone derivatives **12-20**. Reagents and conditions: (a) the appropriate aldehyde, KOH, EtOH, 50 °C → rt, overnight; (b) 4-diethylaminobenzaldehyde, aqueous NaOH (60%), MeOH, rt, overnight; (c) NaOH, aqueous H₂O₂ (30%), MeOH/THF (1:1), 0 °C → rt, overnight. ^aNot determined due to purification problems.

Due to problems in the synthesis of the diethylamino derivatives, a new synthetic strategy was developed. According to the new approach, based on the retrosynthetic analysis illustrated in Figure 14, the diethylamino containing compounds could be provided from the corresponding 4-nitrophenyl derivatives with the aim to later convert the nitro group to diethylamine via chemoselective reduction and subsequent *N*-diethylation. Chalcone **9** was obtained using the Claisen-Schmidt reaction conditions described above (Scheme 1). However, the product was difficult to purify, mainly due to severe solubility problems in an array of solvents (polar and non-polar). Thus, the crude product of **9** was used in the next reaction step without any further purification.

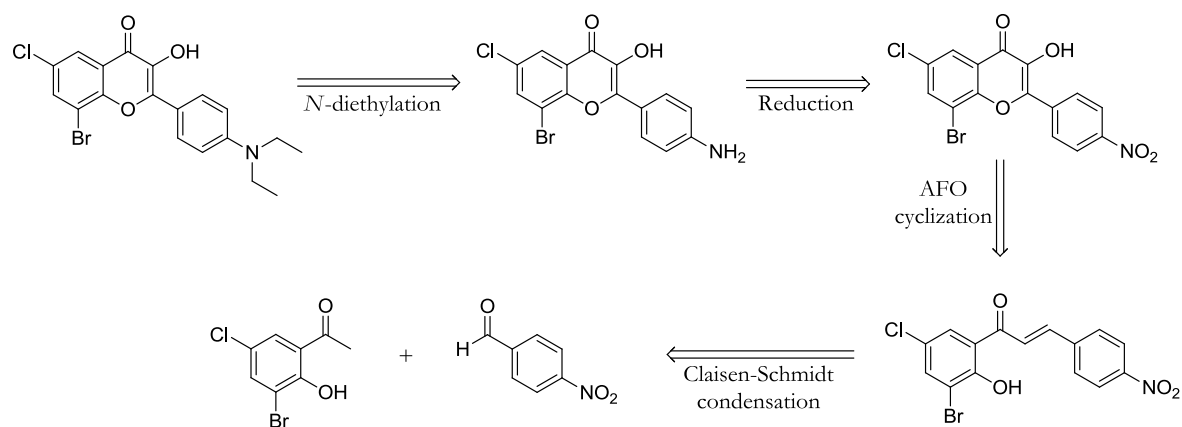


Figure 14. Retrosynthetic analysis for the synthesis of 2-(4-diethylaminophenyl)-3-hydroxychromones via the corresponding nitro derivatives.

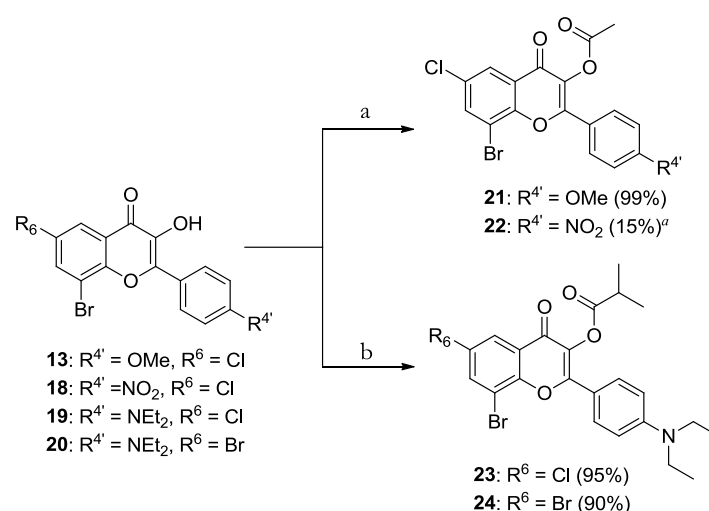
Chalcones, **3-7** and **9**, and the dienone **8** were cyclized to the corresponding 3-hydroxychromones **12-18** via the Algar-Flynn-Oyamada (AFO) reaction, using aqueous hydrogen peroxide (30%) and 4M NaOH in a 1:1 mixture of THF and MeOH (Scheme 1).^{90, 91} Subsequent recrystallization from EtOH gave the chromones **12-18** in moderate to high yields (43-98%). However, once again we faced solubility problems with the nitro derivative **18**. Hence, the crude product of **18** was used in the next reaction step without any further purification.

Next, the focus was directed towards the preparation of new 3-hydroxychromone derivatives with applicable fluorescence properties. Compound **13** and **18** were selected for further synthesis, since they possess groups that are or that easily can be converted into electron-rich moieties. To avoid purifications problems on silica the hydroxyl functionality in the 3-position of **13** and **18** was acetylated. Two similar protocols, with different solvents, were used for the protection step (Scheme 2). Compound **13** was treated with acetyl chloride and triethylamine in dichloromethane, whereas the protection of **18** was conducted using the same acetylation agent and base in DMF. The protocols gave **21** and **22** in moderate or high yields, respectively.⁹⁴ However, the latter was preferable since the convenient work up, addition of water, gave precipitation of the pure product, which could be isolated after filtration.

After dealing with problems related to solubility and purification, the acetylated nitro derivative **22** was finally obtained (as described above). However, attempts to perform the subsequent Sonogashira reaction in the 8-position of **22** failed and only the starting material could be regenerated (not shown). Consequently, no further synthetic efforts were made with the nitro derivatives. Hence, the focus was once again to synthesize the 2-(4-diethylaminophenyl)-3-hydroxychromone derivatives by using the 4-diethylamino-benzaldehyde. New attempts, with stronger alkaline conditions, were performed. Consequently, the diethylamino derivatives **10-11** were successfully obtained from dihalogenated 2'-hydroxyacetophenones **1-2**, using aqueous sodium hydroxide (60%) in

MeOH (Scheme 1).⁹² Furthermore, the corresponding 3-hydroxychromone derivatives **19-20** were obtained by the AFO reaction using the same conditions as described above.

The 2-(4-diethylaminophenyl)-3-hydroxychromones **19-20** were first successfully protected as acetyl esters using acetyl chloride and triethylamine in DMF. However, the subsequent Sonogashira cross-coupling in the 8-position (described below) gave products that decomposed (ring-opened) on silica gel during the purification process. Instead, **19-20** were protected as the more stable isobutyric esters **23-24**, using isobutyric anhydride in pyridine (Scheme 2).



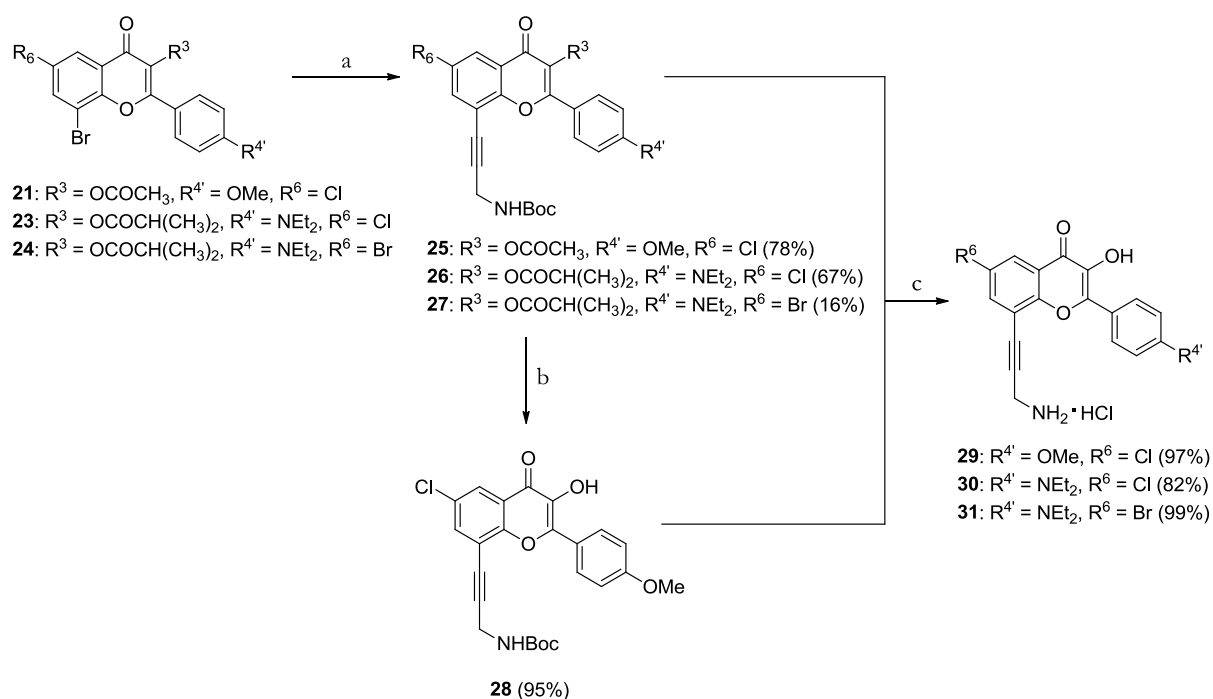
Scheme 2. Protection of the hydroxyl functionality in the 3-position to obtain **21-24**. Reagents and conditions: (a) acetyl chloride, Et₃N, dichloromethane, rt, overnight or acetyl chloride, Et₃N, DMF, rt, 24 h; (b) isobutyric anhydride, pyridine, rt, 18-36 h. ^aCalculated yield over three steps, starting from compound **1** (Scheme 1).

3.2.1.2 Synthesis of the final compounds via the Sonogashira reaction

The general Sonogashira reaction was first reported in 1975, and involves cross-coupling between terminal alkynes and aryl or alkenyl halides or triflates in the presence of a Pd-catalyst, a base and generally copper iodide as a co-catalyst.^{95, 96} Furthermore, the use of microwave assisted organic synthesis (MAOS) in transition-metal-catalyzed reactions, such as the construction of C-C bonds, has shown several beneficial aspects over conventional heating.^{97, 98} MAOS generates efficient internal heating in sealed vessels, which allows high temperature and high pressure. Accordingly, organic reactions can be accelerated giving enhanced reaction rates and reduced reaction times.

Microwave-assisted Pd-couplings, in particular on the chromone ring system, have frequently been used and studied in our research group.^{90, 99, 100} Hence, a microwave-assisted Sonogashira reaction was used for the regioselective introduction of *N*-Boc-protected propargylamines in the 8-position of the chromone scaffold. Compounds **25-27** were prepared from **21** and **23-24**, in a microwave cavity at 120 °C, in the presence of *N*-Boc-propargylamine, PdCl₂P(Ph)₃, triethylamine and copper iodide in THF (Scheme 3).

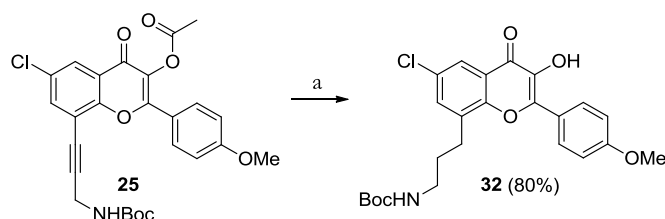
Two equivalents of the terminal alkyne were used for the coupling of **21** to give **25**, whereas four equivalents were required for the diethylamino derivatives **23** and **24** to obtain the products **26-27**. As expected, the coupling of the dibromo derivative **24** also resulted in the dicoupled product, giving a lower yield of the monocoupled derivative **27** (16%). However, the dicoupled derivative was not completely characterized due to purification problems. Compound **25** was purified by column chromatography, on silica gel, whereas the diethylamino derivatives **26-27** were purified on neutral aluminum oxide, to avoid decomposition during the purification process. Furthermore, two important aspects were noticed for the Sonogashira reaction. First, 120 °C is an optimal reaction temperature, since higher temperature results in Boc-deprotection and lower gives decreased yields. Secondly, the addition order of the reagents is crucial, the products could only be obtained when the co-catalyst (CuI) was added last, a few seconds prior to vessel capping.



Scheme 3. Synthesis of the final compounds **29-31** via the Sonogashira reaction. Reagents and conditions: (a) *N*-Boc-propargylamine, PdCl₂(PPh₃)₂, NEt₃, CuI, THF, 120 °C, 20 min, microwave heating; (b) NaOMe, MeOH, rt, 5h; (c) HCl, MeOH, rt, 6-40 h.

Compound **29** was obtained by using two consecutive deprotecting protocols. The acetyl ester in **25** was hydrolyzed with NaOMe in MeOH, to produce the corresponding 3-hydroxychromone derivative **28** (Scheme 3). Furthermore, deprotection of the Boc-group in **28** was performed by HCl in MeOH to give the primary amine **29**. However, it was later found that the first deprotection step with NaOMe was unnecessary since the target compounds **30-31** could be obtained directly from **26-27** using acidic conditions. Thus, dual deprotection of **26-27**, using HCl in MeOH, gave the HCl salts of the amines **30-31** in high yields (82 and 99%, respectively).

Additionally, in order to study the difference in fluorescence properties between conjugated and non-conjugated substituents in the 8-position, the alkyne in **25** was reduced to the corresponding alkyl derivative (**32**). The conversion was performed by catalytic hydrogenation over Pd/C (5%) in a 1:1 mixture of dioxane/MeOH (Scheme 4). As a consequence of the reducing conditions, the acetyl ester in the 3-position was simultaneously cleaved off via hydrogenolysis giving **32** in 80% yield.

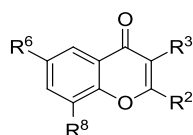


Scheme 4. Conversion of the alkyne in **25** to the corresponding alkyl **32**. Reagents and conditions: (a) H₂, Pd/C (5%), MeOH/dioxane (1:1), room temperature, 15 h.

3.2.2 Photophysical characterization

The synthesized 3-hydroxychromones, **12-17**, **19-20**, **29-32**, with electron-withdrawing and donating aromatic or conjugated substituents in the 2-position and the protected 2-(4-diethylaminophenyl)-3-isobutyroxychromone derivatives, **23-24** and **26-27**, were characterized for their photophysical properties (Table 1). All measurements were performed in ethanol solutions (95%) due to a favorable solubility profile. Absorption and emission spectra of the compounds were collected using highly diluted samples of unknown concentrations. The majority of the 3-hydroxychromone derivatives, **12-17**, **29** and **32**, showed low energy absorption maxima centered around 360 nm and two well-separated emission maxima originating from the normal excited species (N^{*}) and the excited phototautomer (T^{*}) centered at ~ 440 nm and ~ 555 nm, respectively (Figure 15). As expected, the 2-(4-diethylaminophenyl)chromone derivatives, **19-20** and **30-31**, shifted the absorption (~ 440 nm) and emission maxima to longer wavelengths (red-shift) and gave a single defined emission maximum, representing the excited normal species (N^{*}), centered at ~ 565 nm (Figure 16). The red-shifted single emission band for **19-20** and **30-31** is an effect when using a strongly polar and protic solvent, such as ethanol, due to strong charge transfer properties, perturbation and solvatochromism.⁸⁹ In detail, solvent stabilization of zwitterionic species in the excited charge transfer state, with a positive charge on the 4'-diethylamino group and a negative charge on the carbonyl oxygen, possess lower energy than T^{*} and are therefore more energetically favorable than ESIPT. In contrast, it has been demonstrated that decreasing the solvent polarity from ethanol to hexane results in a significantly increased formation of the excited tautomer (T^{*}).^{93, 101} In other words, the dual emission for 2-(4-diethylaminophenyl)-3-hydroxychromone derivatives is strongly dependent on the polarity of the solvent.

Table 1. Photophysical data of 2,6,8-trisubstituted 3-hydroxychromones **12-17**, **19-20** and **29-32**, and 2,6,8-trisubstituted 3-isobutyroxychromones **23-24** and **26-27**.^a



Compd	R ²	R ³	R ⁶	R ⁸	λ_{abs} (nm)	λ_{em} (nm) ^b		ϵ (M ⁻¹ cm ⁻¹)	Φ_{F}
						N*	T*		
12	Phenyl	OH	Cl	Br	355	435	550	12000	0.07
13	4-MeO-Ph	OH	Cl	Br	370	446	554	23000	0.06
14	2-Thienyl	OH	Cl	Br	372	438	560	19000	0.09
15	3-Thienyl	OH	Cl	Br	358	434	548	17000	0.13
16	4-CF ₃ -Ph	OH	Cl	Br	354	436	553	14000	0.03
17	CH=CHPh	OH	Cl	Br	381	446	544	12000	0.05
19	4-NEt ₂ -Ph	OH	Cl	Br	438	564		27000	0.43
20	4-NEt ₂ -Ph	OH	Br	Br	439	565		27000	0.42
23	4-NEt ₂ -Ph	OCOCH(CH ₃) ₂	Cl	Br	417	556		36000	0.04
24	4-NEt ₂ -Ph	OCOCH(CH ₃) ₂	Br	Br	418	560		32000	0.06
26	4-NEt ₂ -Ph	OCOCH(CH ₃) ₂	Cl	C≡CCH ₂ NHBoc	420	554		33000	0.12
27	4-NEt ₂ -Ph	OCOCH(CH ₃) ₂	Br	C≡CCH ₂ NHBoc	420	553		30000	0.12
29	4-MeO-Ph	OH	Cl	C≡CCH ₂ NH ₂	372	444	556	14000	0.10
30	4-NEt ₂ -Ph	OH	Cl	C≡CCH ₂ NH ₂	441	568		21000	0.49
31	4-NEt ₂ -Ph	OH	Br	C≡CCH ₂ NH ₂	443	570		18000	0.48
32	4-MeO-Ph	OH	Cl	(CH ₂) ₃ NHBoc	362	434	542	16000	0.07

^aPhotophysical data measured in 95% ethanol. ^bEmission values originating from the normal excited form (N*) and the phototautomer (T*), which is formed via an excited state intramolecular proton transfer (ESIPT).

However, the excitation of the 2-(4-diethylaminophenyl)-3-hydroxychromone derivatives show lower solvent polarity dependence compared to Nile Red, a known solvatochromic dye, while the emission shows higher solvent polarity dependence.^{102, 103} Furthermore, the emission maximum for 4'-diethylamino-3-hydroxyflavone has been reported to have much shorter wavelength (~ 505 nm) than those observed for **19-20** and **30-31**.⁸⁹ However, in studies where electron-withdrawing groups (e.g. methoxycarbonylvinyl) are attached to the 7-position of the chromone both the absorption and emission maxima are significantly red-shifted, therefore the shift to longer wavelengths observed for our compounds was expected since Cl, Br and 3-amino-1-propynyl groups are all electron withdrawing.¹⁰⁴

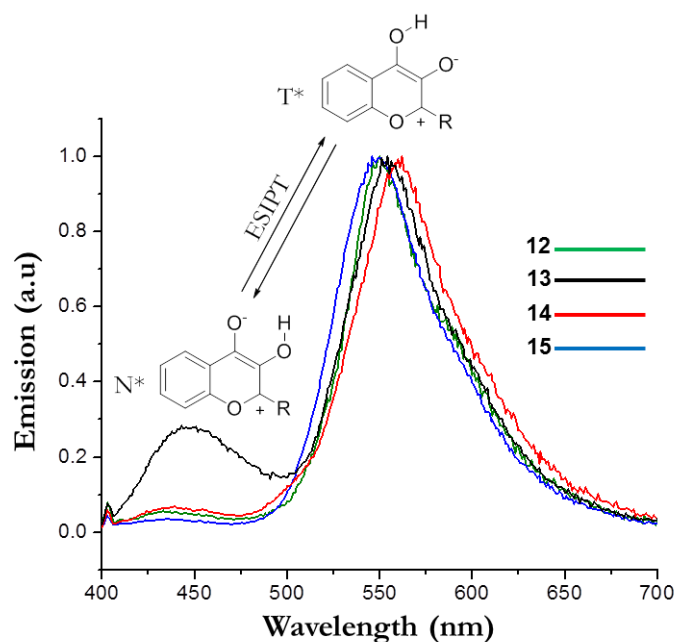


Figure 15. Emission spectra for the 3-hydroxychromone derivatives **12-15**. These derivatives exhibit dual fluorescence behavior giving two well-separated emission maxima originating from the normal excited species (N^*) and the phototautomer (T^*).

The fluorescent quantum yields (Φ_F) were measured relative to fluorescein or quinine sulfate with an excitation wavelength of 465 or 360 nm, respectively. The results showed that the quantum yield is highly dependent on the electronic properties of the substituent in the 2-position of the 3-hydroxychromone system (Table 1). For example, the introduction of a strong electron withdrawing 4'-CF₃-phenyl group, as in **16**, results in the lowest quantum efficiency ($\Phi_F = 0.03$) among all the derivatives. However, the trend is not completely obvious when comparing **12-17**, showing increasing Φ_F values (between $\Phi_F = 0.03-0.13$) in the series 4'-CF₃-Ph < CH=CHPh < 4'-MeO-Ph < phenyl < 2'-thienyl < 3'-thienyl. On the other hand, introduction of a 4'-diethylaminophenyl substituent, as in **19-20**, increases the quantum yield dramatically ($\Phi_F = 0.42-0.43$) due to the strong electron donating properties from the *para*-diethylamino group thus facilitating charge transfer and dielectric stabilization. The *para*-positioned methoxy group, as in **13**, does not

show the same electron donating ability leading to a considerably lower quantum yield ($\Phi_F = 0.06$). In comparison with the 8-bromo-analogs **13** and **19-20**, the introduction of an electron-withdrawing 3-amino-1-propynyl substituent in the 8-position, as in **29-31**, resulted in only minor variations in absorption and emission values and in quantum yields. Similar results were also observed for the reduced 3-(*tert*-butoxy-carbonylamino)propyl derivative **32**.

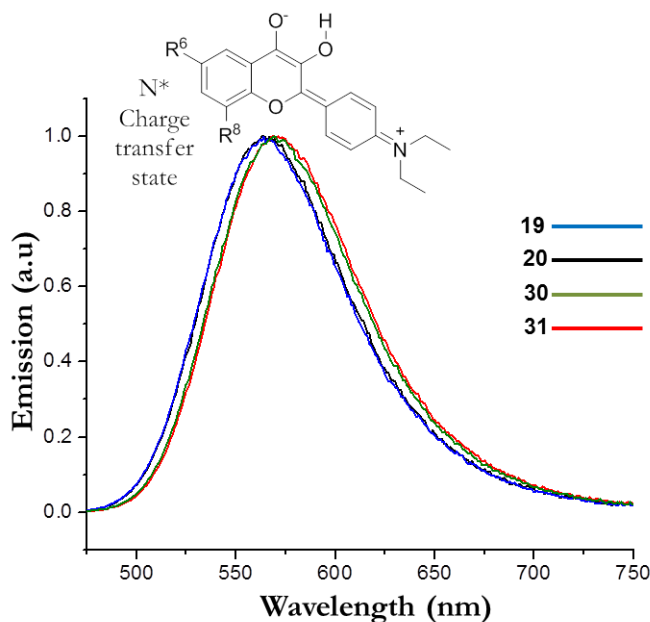


Figure 16. Emission spectra for the 2-(4-diethylaminophenyl)chromone derivatives **19-20** and **30-31**. These compounds exhibit single defined emission maxima (N^*) in ethanol due to strong charge transfer properties, perturbation and solvatochromism.

To investigate the importance of the free hydroxyl group in the 3-position and its ability to undergo ESIPt for the fluorescence capacity, the protected 3-isobutyroxychromone derivatives, **23-24** and **26-27**, were also photophysically characterized. These derivatives are not able to exhibit dual fluorescence. Thus, as expected, the spectra of **23-24** and **26-27** exhibit one single defined emission band, assigned to the normal excited species (N^*), centered at ~ 555 nm. Moreover, the similarity in emission maxima compared with the unprotected derivatives, **19-20** and **30-31**, confirm that the single emission band for the 2-(4-diethylaminophenyl)chromone derivatives originates from the N^* state. In addition, when comparing **23-24** and **26-27** with the unprotected derivatives **19-20** and **30-31**, we observed higher molecular extinction coefficients and dramatically decreased quantum yields (from Φ_F of 0.4-0.5 to 0.1) (Table 1). In spite of this, the results indicate that esterification of the 3-hydroxyl group results in compounds with acceptable and useful fluorescence properties.

Extinction coefficients (ϵ) were determined from samples with known concentrations of test compounds (typically 20 μM). All the 3-hydroxychromone derivatives, **12-17**, **19-20**,

29-32 showed high extinction coefficient values ($\epsilon > 12,000 \text{ M}^{-1} \text{ cm}^{-1}$), with the highest values for **19-20** ($\epsilon = 27,000 \text{ M}^{-1} \text{ cm}^{-1}$). However, as mentioned above, the difference in quantum yields between the derivatives is more pronounced. Interestingly, the extinction coefficients for the 3-isobutyroxychromone derivatives **23-24** and **26-27** were even higher ($\epsilon = 30,000\text{-}36,000 \text{ M}^{-1} \text{ cm}^{-1}$) than those for **19-20** ($\epsilon = 27,000 \text{ M}^{-1} \text{ cm}^{-1}$), but again the quantum yields are much lower. Thus, the 3-hydroxy group is important for obtaining high quantum yields, but it is evidentially possible to use esterified derivatives for fluorescence studies.

With the aim to use 3-hydroxychromones as fluorophores for live-cell imaging, the fluorescence quantum yields of the more hydrophilic **30** and **31** were also measured in water. Interestingly, the quantum yield for these derivatives was found to be zero. However, this kind of observation has been reported earlier. It has been shown that the quantum yield for 4'-diethylamino-3-hydroxyflavones in ethyl acetate decreases with the addition of water, and becomes completely quenched in pure water.^{105, 106} In contrast, 2-(2-furyl)- and 2-(2-benzofuryl)-3-hydroxychromones have shown ESIP1 in water and the increase in quantum yields was especially pronounced for derivatives containing an electron-donating substituent in the 7-position.¹⁰⁶ However, we reasoned that the quenching in water for **30** and **31** could be used as an advantage since they would not be detectable in a hydrophilic cellular environment but instead exhibit fluorescence properties when moving into more hydrophobic areas, e.g. into a hydrophobic active site, a hydrophobic receptor binding pocket or into membrane structures. Theoretically, these derivatives could be used as indicators for protein interactions and receptor binding studies.

3.2.3 Live-cell imaging of compounds **29** and **30**, using 2PE microscopy

In 2004, Shynkar et al. reported the use of 3-hydroxychromones as fluorescent probes for live-cell imaging in plasma membranes.^{85, 107} Thus, we wanted to investigate the potential use of our synthesized compounds in such applications and observe their photochemical and biochemical behavior in terms of photostability, transport, permeability, localization and distribution in a cellular environment.

Compounds **29** and **30** were dissolved in a minimum amount of DMSO to avoid cytotoxicity and cell leakage. The DMSO solutions were further diluted (with Hank's balanced salt solution, HBSS) to generate appropriate concentrations (0.5 mM and 0.1 mM, respectively). A monolayer of HeLa cells (in 1.8 mL cell medium) were stained with solutions of either **29** or **30** at 37 °C and the viability of the cells was monitored during approximately one hour. The fluorescence was observed by multi-photon laser scanning microscopy in the 500-700 nm region by using 2PE excitation at 750 and 900 nm, respectively.¹⁰⁸ Images of the cells were collected at regular and increasingly time intervals.

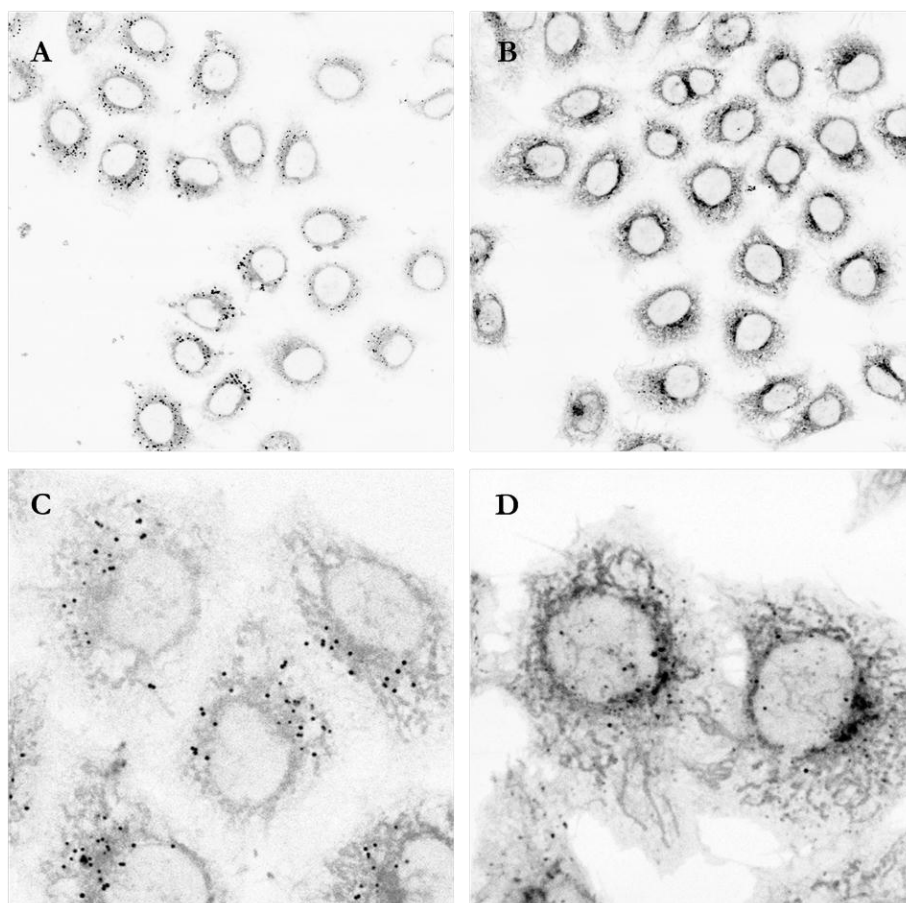


Figure 17. Live-cell imaging of HeLa cells, stained with **29** (A and C) or **30** (B and D), using two-photon excitation (2PE). Panels A and B: Single planes, larger field of view ($215 \times 215 \mu\text{m}^2$), after approximately 20 minutes. Panels C and D: Uptake after 12 min, single planes, ($74 \times 74 \mu\text{m}^2$) from the middle of $9 \mu\text{m}$ thick z stacks. The images have been modified for clarity (negative picture mode).

Figure 17 depicts the cellular uptake of **29** and **30** at two different time points. Figure 17A and B, show larger fields after approximately 20 min, whereas Figure 17C and D display enlarged fields with a few cells and their uptake after 12 min. The imaging revealed rapid penetration with an observed cellular uptake within a minute after the incubation (data not shown). Both compounds are accumulated between the cellular membrane and the nucleolus and they seem to be taken up by endosomal structures, indicated by the bright punctuate structures in the images, and by weaker fluorescent membrane network structures that resemble the endoplasmic reticulum. This observation suggests that the cellular uptake occurs via an active endocytotic mechanism. Thus, additional experiments were conducted in order to investigate the transport mechanism and to confirm our hypothesis. HeLa cells were fixed and stained with either **29** or **30** at $4 \text{ }^\circ\text{C}$. The experiments showed no cellular uptake at the given temperature, which satisfyingly support the assumption regarding endocytosis as the pivotal transport mechanism since endocytosis cannot occur at low temperatures.¹⁰⁹ Moreover, cross-section images through the z-stacks established the fact that the compounds are located inside the cell and not in the cellular membrane. Additionally, there was no indication of cytotoxic effects after fluorophore incubation for approximately two hours. The significant difference in

photophysical properties between **29** and **30**, such as extinction coefficients (ϵ) (14000 vs. 21000 M⁻¹ cm⁻¹), quantum yields (Φ_F) (0.10 vs. 0.49) and cross-section values (0.13 vs. 12 GM),¹¹⁰ could easily be visualized during the experiments. Despite the fact, that the added concentration of **30** was lower than **29** (0.01 mM and 0.05 mM, respectively). The intensity of **30** is clearly stronger than **29**, however both compounds exhibit interesting and adaptable photophysical properties that could be used for various applications within the field of fluorescence microscopy.

3.3 CONCLUSIONS

In conclusion, the work presented in this chapter demonstrates that multifunctionalized 3-hydroxychromone derivatives constitute a new promising class of fluorophores useful for live-cell imaging. Two of the synthesized derivatives, **29** and **30**, with adequate and high fluorescence quantum yields (0.10 and 0.49, respectively) show rapid permeability and non-toxic profiles in living cells. The fluorescence microscopy studies revealed that the derivatives are accumulated between the cellular membrane and the nucleolus, and that the cellular uptake probably occurs via endocytosis. The fluorescence quenching observed in water for **30** and **31** gives opportunities to use these derivatives as probes for receptor-binding studies, i.e. to study the movement from hydrophilic areas into more hydrophobic compartments. Further studies of 3-hydroxychromones as fluorophores for live-cell imaging could involve applications such as protein labeling, examination of specific binding interactions to target proteins, and/or the cellular localization coupled to other compounds targeted for specific organelles. Alternatively, due to the designation as privileged structures, it could be interesting to combine biological activity and fluorescent properties, for example, to design fluorescent chromone-based enzyme inhibitors and to follow their uptake and accumulation in living cells by using fluorescence microscopy.

4. Chalcones and Related Dienones as Inhibitors or Promoters of Tubulin Polymerization (Paper II)

4.1 INTRODUCTION

4.1.1 Tubulin and microtubules

Microtubules are filamentous components of the cytoskeleton, constructed by tube-shaped protein polymers, formed by α - and β -tubulin heterodimers (Figure 18).¹¹¹⁻¹¹⁴ In eukaryotic cells, microtubules form a dynamic network that is essential in cellular processes such as mitosis, maintenance of cell shape, cytoplasmic organelle movement and cell replication.

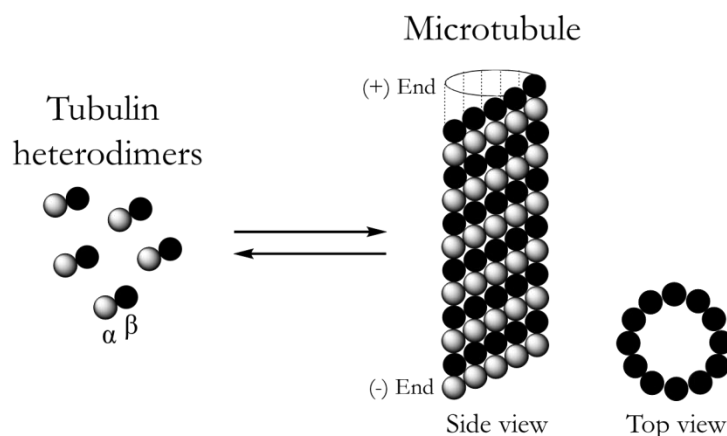


Figure 18. The structure and formation of microtubules. Tubulin exists in two forms within the cell, either as free protein heterodimers or as tube-shaped assemblies, referred to as microtubules.^{17, 111} These structures are constantly changing through polymerization and depolymerization, at the (+) and (-) ends, respectively, a dynamic feature that is essential in various cellular processes, such as mitosis.

The structure of microtubules is consistently changing, i.e. they alternate between growing and shrinking through the addition and removal of tubulin molecules at the (+) and (-) ends, respectively. Thus, the function of microtubules is strongly associated with their stability and the dynamic character of the tubulin-microtubule equilibrium.¹⁷ Moreover, the microtubule assembly requires the association of two guanosine triphosphate (GTP) molecules for each tubulin heterodimer.¹¹⁵ One of them binds to an exchangeable site on the β -tubulin subunit where it can be hydrolyzed to guanosine diphosphate (GDP), essential for microtubule elongation. In contrast, the other GTP nucleotide, which binds to α -tubulin, is stable to hydrolysis and appears to have a structural role instead.¹¹³ The dynamic behavior of microtubules is essential for normal cell function and growth and is

affected by several factors including the intracellular GTP/GDP ratio, the ionic microenvironment and the presence of stabilizing microtubule-associated proteins.¹¹⁶

The importance of tubulin and microtubules in chromosome segregation during cell division makes them attractive targets for anticancer drug design, i.e. in the development of antimetabolic agents.¹¹¹ Beneficially, the interference of tubulin/microtubule polymerization dynamics has two pivotal anticancer effects: i) inhibition of cancer cell proliferation through interruption of mitotic spindle formation, which leads to apoptosis, and ii) disruption of cell signaling pathways involved in regulating and maintaining the cytoskeleton of endothelial cells in tumor vasculature.¹¹⁷

4.1.2 Tubulin as a target for antimetabolic agents

In general, antimetabolic agents that interfere with tubulin dynamics act by targeting three different sites on the β -tubulin subunit: the colchicine, the vinca alkaloid and the paclitaxel binding sites (Figure 19).^{17, 111} Agents that bind to the colchicine binding site (e.g. colchicine and podophyllotoxin, Figure 20) or to the vinca alkaloid domain (e.g. vincristine) induce depolymerization of tubulin and are therefore defined as inhibitors of tubulin assembly. In contrast, agents that target the paclitaxel binding site (e.g. taxanes such as paclitaxel and docetaxel, Figure 20) are known to stabilize the microtubule cytoskeleton against depolymerization, thus promoting tubulin assembly. Despite different mechanisms, both types of agents provide the same antimetabolic effect, due to the conflict with tubulin/microtubule dynamics.

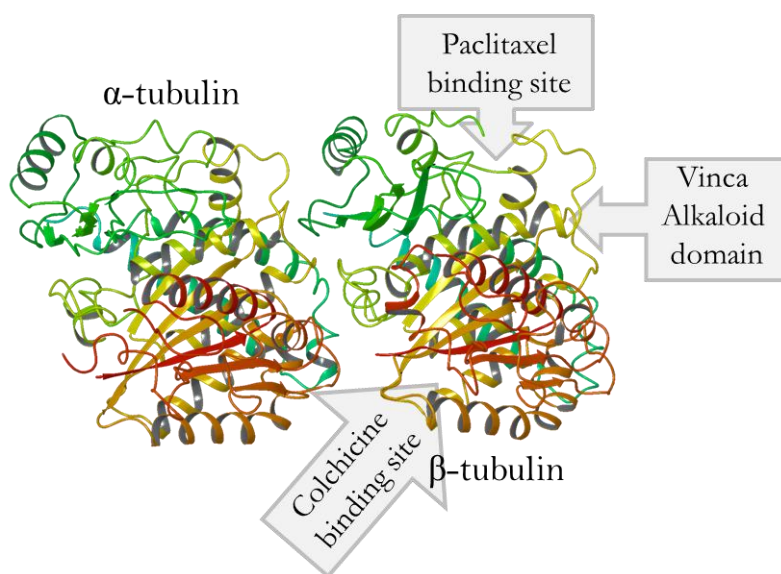


Figure 19. Illustration of the tubulin α,β -heterodimer with three major binding sites on the β -tubulin subunit: the colchicine binding site, the paclitaxel binding site, and the vinca alkaloid domain.¹¹⁸

As depicted in Figure 20, antimetabolic agents that target the tubulin heterodimer are obviously dominated by complicated natural occurring structures. Besides limited access via extraction from natural sources, such complex derivatives could be obtained using time-consuming total synthesis.^{119, 120} Consequently, the development of small, synthetic, and easily accessible compounds is of great interest in the field of oncology and in the development of tubulin modulators.¹¹¹

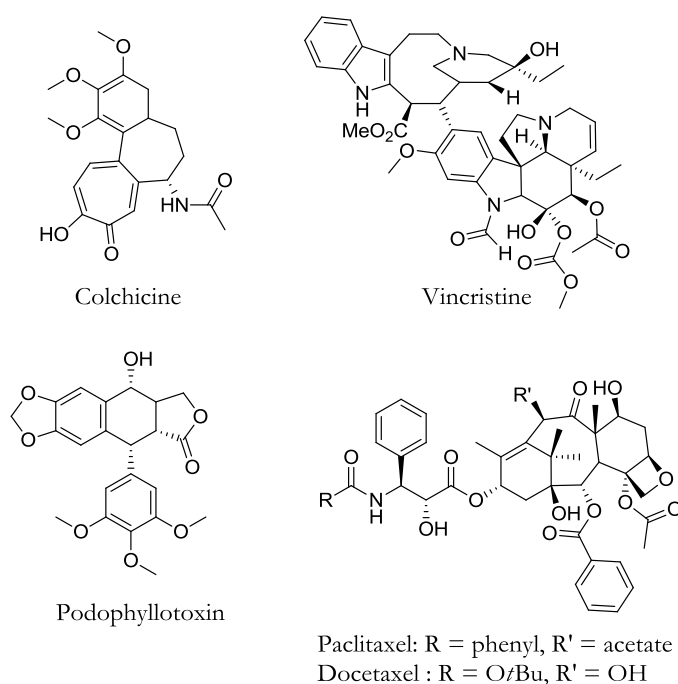


Figure 20. Chemical structures of known natural products that target tubulin and acts as antimetabolic agents. Colchicine, vincristine and podophyllotoxin destabilize microtubule assembly, whereas paclitaxel and docetaxel act as promoters of tubulin polymerization.

4.1.3 Chalcones as microtubule destabilizing agents

Several chalcones have been reported to act as cytotoxic or microtubule destabilizing agents, preventing tubulin from polymerizing into microtubules.¹²¹⁻¹²⁴ The majority of these are natural occurring compounds substituted with electron donating hydroxy and/or methoxy groups at various positions.^{16, 122, 125-127} However, the interest and development of synthetic chalcone derivatives as tubulin inhibitors has increased in recent years in order to establish more advanced structure-activity relationships and to generate novel compounds with diverse substituent patterns. For example, MDL 27048 (Figure 21) was one of the first synthetic chalcone-based tubulin inhibitors reported in the literature.¹²³ Since its discovery in 1989, considerable efforts have been dedicated to identify new potential chalcone-based drug candidates within the field of oncology.¹²⁸ Despite this, MDL 27048 is still, to this date, one of the most potent synthetic inhibitors toward tubulin polymerization ($IC_{50} = 12 \text{ nM}$).¹²⁹

The pharmacological profile for chalcone derivatives has shown to be similar to the analogous combretastatins (Figure 21), a class of natural stilbenoids known for the activity as tumor vascular disrupting agents.^{17, 125, 130} Like colchicine and podophyllotoxin, combretastatins and chalcones bind to the colchicine binding site on β -tubulin, thus inducing depolymerization of tubulin assembly.^{124, 131-133} It should be noted that, besides the interference of tubulin assembly, the cytotoxicity of chalcones can originate from other mechanisms involving inhibition of the tumor suppressor protein p53 (leading to dysregulation of the cell cycle in various tumor cell lines), blockage of nitric oxide production (important in macrophage-induced cytotoxicity) and inhibition of cytochrome P450 enzymes that are associated with the activation of procarcinogens.^{126, 134}

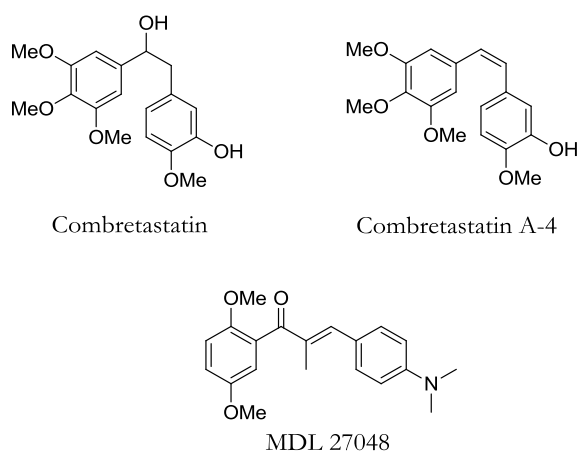


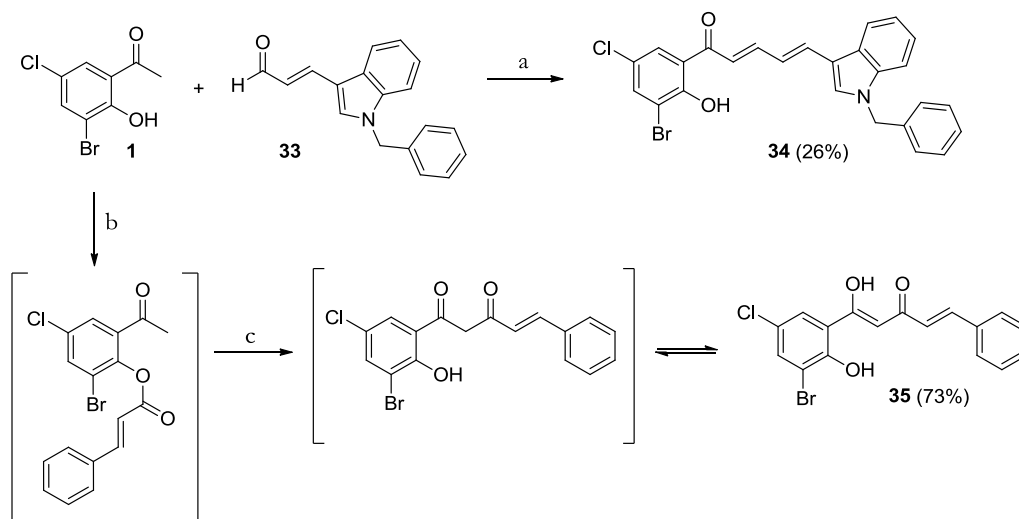
Figure 21. Chalcones are structurally related to combretastatins, natural occurring compounds that are known for their cytotoxic activity and inhibition of tubulin assembly. Furthermore, MDL 27048 was one of the first reported synthetic chalcone-based tubulin inhibitors.

4.2 RESULTS AND DISCUSSION

The synthesis toward fluorescent and bioactive chromone-based compounds (Chapter 3, Paper I) generated a series of dihalogenated chalcone derivatives with various aromatic or conjugated B-rings. Due to numerous reports of chalcones and their anticancer activities, particularly as destabilizing agents of tubulin polymerization, we decided to investigate if our synthetic derivatives could act as tubulin inhibitors and/or cytotoxic agents.

4.2.1 Synthesis of dihalogenated dienones 34-35

As described earlier (section 3.2.1.1, Scheme 1), chalcones **3-5**, **7**, **10**, **11** and dienone **8** were prepared via a Claisen-Schmidt condensation of dihalogenated-2'-hydroxyacetophenones **1-2** and various aromatic or conjugated aldehydes using aqueous NaOH (60%) in MeOH or KOH in EtOH.⁹⁰⁻⁹² The series were extended with two dienone derivatives, **34** and **35**. Compound **34** was obtained in low yields (26%), due to purification problems, using the latter reaction conditions described above (Scheme 5). The enol tautomer of **35** was synthesized in two steps from 3'-bromo-5'-chloro-2'-hydroxyacetophenone **1** via esterification with benzoyl chloride, followed by a base-promoted intramolecular Baker-Venkataraman rearrangement (Scheme 5).^{135, 136}



Scheme 5. Synthesis of dienones **34** and **35**. Reagents and conditions: (a) KOH, EtOH, 50 °C → rt, overnight; (b) *trans*-cinnamoyl chloride, pyridine, rt, 48 h; (c) K₂CO₃, 2-butanone, reflux, 3.5 h.

4.2.2 Cytotoxicity and antiproliferative studies

The antiproliferative activity of compounds **3-5**, **7**, **8**, **10**, **11**, **34** and **35** was evaluated using a fluorometric microculture cytotoxicity assay (FMCA), performed by co-workers at Uppsala University Hospital.^{137, 138} FMCA is a total cell kill assay, based on the ability of cells with intact cell membranes to convert non-fluorescent fluorescein diacetate (FDA) to fluorescent fluorescein. A panel of ten human cancer cell lines was used for the study, consisting of: RPMI 8226 (myeloma), CCRF-CEM (leukemia), U937-GTB (lymphoma) and NCI-H69 (small-cell lung cancer) along with the drug resistant sublines 8226/Dox40 (doxorubicin resistant myeloma), 8226/LR5 (melphalan resistant myeloma), CEM/VM1 (teniposide resistant leukemia), U937/Vcr (vincristine resistant lymphoma), H69AR (doxorubicin resistant small-cell lung cancer) and the primary resistant ACHN (renal adenocarcinoma) cell line. This panel has been designed to represent different histologies and different mechanisms of drug resistance.¹³⁹ The cell suspensions (10,000-20,000 cells per mL) were exposed, at 37 °C, to varying concentrations of the test substances (0.016, 0.08, 0.04, 2.00, 10.0 and 50.0 μM dissolved in DMSO with maximum 1% DMSO in cell suspensions) in 96-well microtiter plates for 72 h. Each compound concentration was tested in duplicate and the experiments were repeated twice. The cells were washed with phosphate-buffered saline (PBS) followed by the addition of FDA (dissolved in DMSO and diluted with physiological buffer to 10 μg/mL). The fluorescence, which is proportional to the number of living cells, was measured after 40 min incubation at 485/520 nm, and the results were presented as survival index.

The results, depicted in Table 2, showed that all the assayed chalcones **3-5**, **7**, **10**, **11**, and dienones **8**, **34**, and **35**, exhibit cytotoxic activities with noticeable differences in IC₅₀ values due to structural diversity. As expected, compounds **10** and **11** showed similar activity profiles in the majority of the cell lines, with the highest activity against NCI-H69 (IC₅₀ 5.2 and 7.1 μM, respectively). However, the difference in cytotoxicity between **10** and **11** in the renal adenocarcinoma cell line (ACHN) (IC₅₀ 164 and 69 μM, respectively) suggests that ACHN is sensitive to size modifications in the 5'-position of the chalcone structure. When comparing **4** and **7** (4-MeO-phenyl vs. 4-CF₃-phenyl) the electron donating 4-methoxy group was unfavorable in three of the tested cell lines: CCRF-CEM, U973/Vcr and RPMI 8226. This result is more likely due to the difference in size between the trifluoromethyl and the methoxy group than the difference in electronic properties since the cytotoxic activity of **3** (no substituent on the phenyl group) is similar to that of **7**. Moreover, the 2-thienyl derivative **5** showed decreased activity in several of the cell lines in comparison with the slightly larger bioisosteric phenyl derivative **3**, most noticeable in CCRF-CEM (IC₅₀ 152 vs. 37.6 μM). Elongation of the carbon chain between the aromatic moieties in **3** to obtain **8** also resulted in decreased activities. However, the introduction of a diketone/enol fragment as in **35** improved the activity with IC₅₀ values corresponding to those of **3**. Moreover, introducing an additional aromatic moiety, such as in **34**, gave low activity in several of the tested cell lines, e.g. CCRF-CEM (IC₅₀ 280 μM), while a higher activity was observed toward the small-cell lung cancer cell line (NCI-H69) (IC₅₀ 11.1 μM). Interestingly, **34** showed the highest activity among the tested compounds toward the ACHN cell line (IC₅₀ 17.0 μM), known for its aggressive growth and high resistance profile.¹⁴⁰

Table 2. Cytotoxicity data of chalcones **3-5**, **7**, **10-11** and dienones **8**, **34-35** against ten human cancer cell lines.

Cmpd	Cytotoxicity, IC ₅₀ (μM)									
	CCRF-CEM	CEM/VM1	ACHN	U937GTB	U973/Vcr	RPMI 8226	8226/Dox40	8226/LR5	NCI-H69	H69A R
3	37.6	22.3	48.9	20.0	24.2	18.7	12.4	13.2	10.3	26.4
4	111 ^a	45.8	49.4	45.0	77 ^a	80 ^a	16.9	46.0	16.4	42.6
5	152 ^a	48.9	44.2	42.5	32.6	79 ^a	26.5	23.3	20.0	56.1
7	15.4	31.1	49.4	14.9	24.4	20.8	22.5	22.3	11.5	33.2
8	129 ^a	48.6	93 ^a	36.6	31.7	48.8	14.2	23.4	19.9	n.d. ^b
10	14.8	14.5	164 ^a	9.3	8.8	29.4	9.7	9.4	5.2	24.5
11	20.1	13.1	69 ^a	8.2	9.6	26.1	7.7	9.9	7.1	38.8
34	280 ^a	89 ^a	17.0	49.0	54 ^a	119 ^a	42.3	70 ^a	11.1	48.5
35	34.1	24.1	37.8	18.1	23.9	27.9	19.1	33.5	9.4	25.5

^a Extrapolated values (highest tested concentration of 50 μM). ^b Not determined (no cytotoxic effect was observed).

4.2.3 The effect on tubulin polymerization

Effects on tubulin polymerization were monitored using a commercial Tubulin Polymerization Assay Kit (porcine tubulin and fluorescence based), performed by co-workers at Uppsala University Hospital.^{141, 142} The chalcones **3-5**, **7**, **10**, **11**, and dienones, **8**, **34**, and **35** (dissolved in DMSO) were evaluated at 5 and 25 μM , and the experiments were performed twice (mean values are presented). Docetaxel and vincristine (3 μM , diluted in PBS) were used as positive stabilizing and destabilizing controls, respectively.

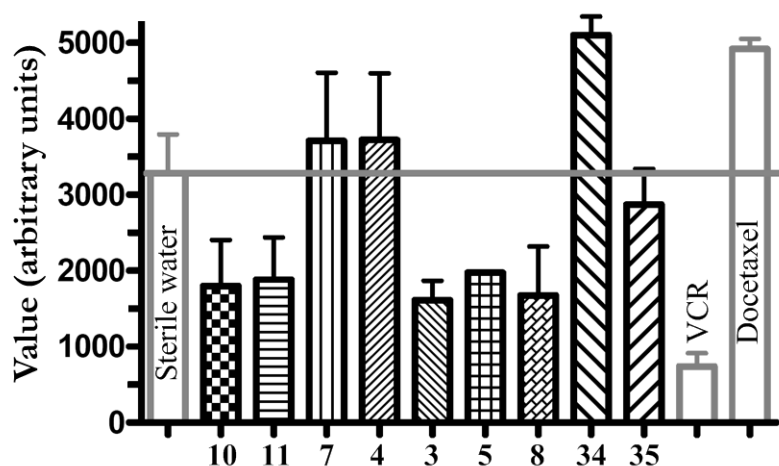
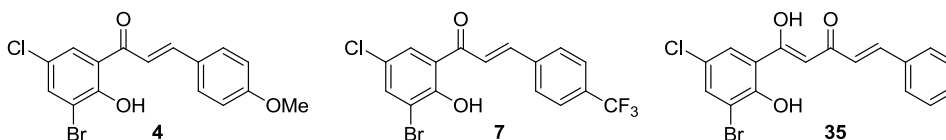


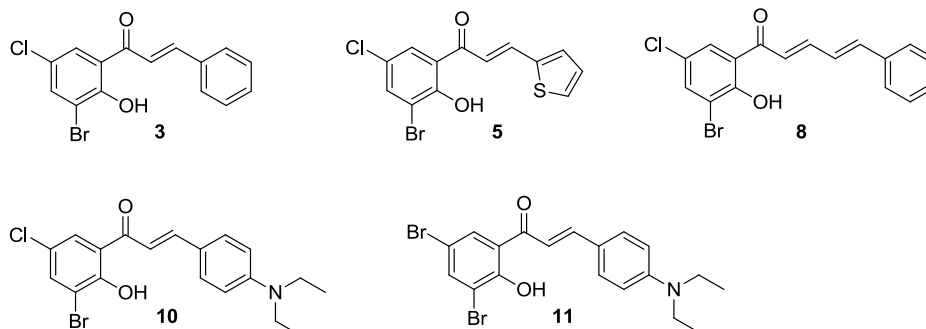
Figure 22. Tubulin polymerization activity in the presence of compounds **3-5**, **7**, **8**, **10**, **11**, **34** and **35** (at 5 or 25 μM , mean values presented) with vincristine and docetaxel (at 3 μM) as reference compounds. Stacks below the horizontal (grey) line indicate tubulin inhibition, stacks above indicate tubulin stabilization and stacks close to the horizontal line are considered to represent inactive compounds. The y-axis demonstrates tubulin polymerization activity measured at 15 min (arbitrary units) in the growth phase of the tubulin polymerization curve.

The tubulin polymerization activity of compounds **3-5**, **7**, **8**, **10**, **11**, **34**, and **35** is depicted in Figures 22 and 23. Compounds **4**, **7**, and **35** showed no significant activity toward tubulin assembly, which suggests a different mechanism for their observed cytotoxic activity. However, chalcones **3**, **5**, **10**, and **11** along with dienone **8** were identified as tubulin-destabilizing agents. In contrast, chalcone **34** displayed microtubule-stabilizing activity comparable to the well-established antimetabolic chemotherapeutic drug docetaxel, which is used in the treatment of several types of cancer.¹⁴³ Interestingly, to the best of our knowledge, compound **34** is the first reported chalcone with microtubule-stabilizing activity.

INACTIVE COMPOUNDS



DESTABILIZING AGENTS



STABILIZING AGENTS

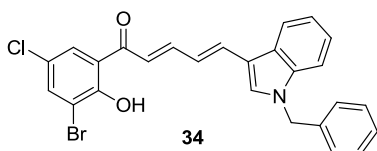


Figure 23. Chemical structures of compounds 3-5, 7-8, 10-11, 34-35, and their activity toward tubulin dynamics.

4.2.4 Molecular modeling and docking studies

Molecular docking was performed in order to explore possible binding modes and orientations for the chalcones and the dienones that showed activity toward tubulin polymerization. The docking was accomplished using the Schrödinger Package with the MAESTRO interface.¹⁴⁴ The structure of tubulin in complex with podophyllotoxin (PDB 1SA1) and the structure of tubulin in complex with taxol (PDB 1JFF) were used for the study.^{114, 145, 146}

4.2.4.1 Docking into the colchicine binding site of β -tubulin

Several chalcones have been reported to act as antimetabolic agents, targeting the colchicine binding site on β -tubulin.^{17, 124} Therefore, it seemed reasonable to assume the same thing for our synthetic derivatives. Thus, the microtubule destabilizing compounds **3**, **5**, **8**, **10** and **11** along with the co-crystallized ligand podophyllotoxin, were docked into the colchicine binding site of tubulin using the podophyllotoxin-tubulin complex (PDB 1SA1) as template.^{145, 146} Podophyllotoxin binds into a hydrophobic cavity on β -tubulin, which includes two hydrophobic pockets, I and II (Figure 24A); The benzodioxole fragment is located in the hydrophobic pocket I (hpI), surrounded by Met259, Ala316 and Lys352, whereas the trimethoxyphenyl moiety is located in the hydrophobic pocket II

(hpII), enclosed by Leu242, Ala250 and Leu255.¹⁴⁷ The docking study suggested that chalcones **3** and **5** bind to the colchicine binding site by directing the phenyl or 2-thienyl moieties, respectively, into hpI (Figure 24B and C). Simultaneously, the 4-bromo-3-chloro-2-hydroxyphenyl moieties could tentatively fit into the other hydrophobic pocket, hpII. Moreover, compounds **8**, **10** and **11** are more elongated and are therefore not able to adopt a conformation that utilizes both hydrophobic areas. Instead, the styryl group in **8** is directed out from the binding site and placed into the gap that leads to the hydrophobic areas (Figure 24D). However, the 4-bromo-3-chloro-2-hydroxyphenyl moiety is located in the same hydrophobic pocket (hpII) as the corresponding moiety in chalcone **3**, but it seems to be buried deeper inside the pocket and thereby utilizes the area more efficiently. In contrast, compounds **10** and **11** bind in a flipped fashion; the 4-diethylaminophenyl group is placed into the hpII and the rest of the molecule is directed outwards from the active site (Figure 24E).

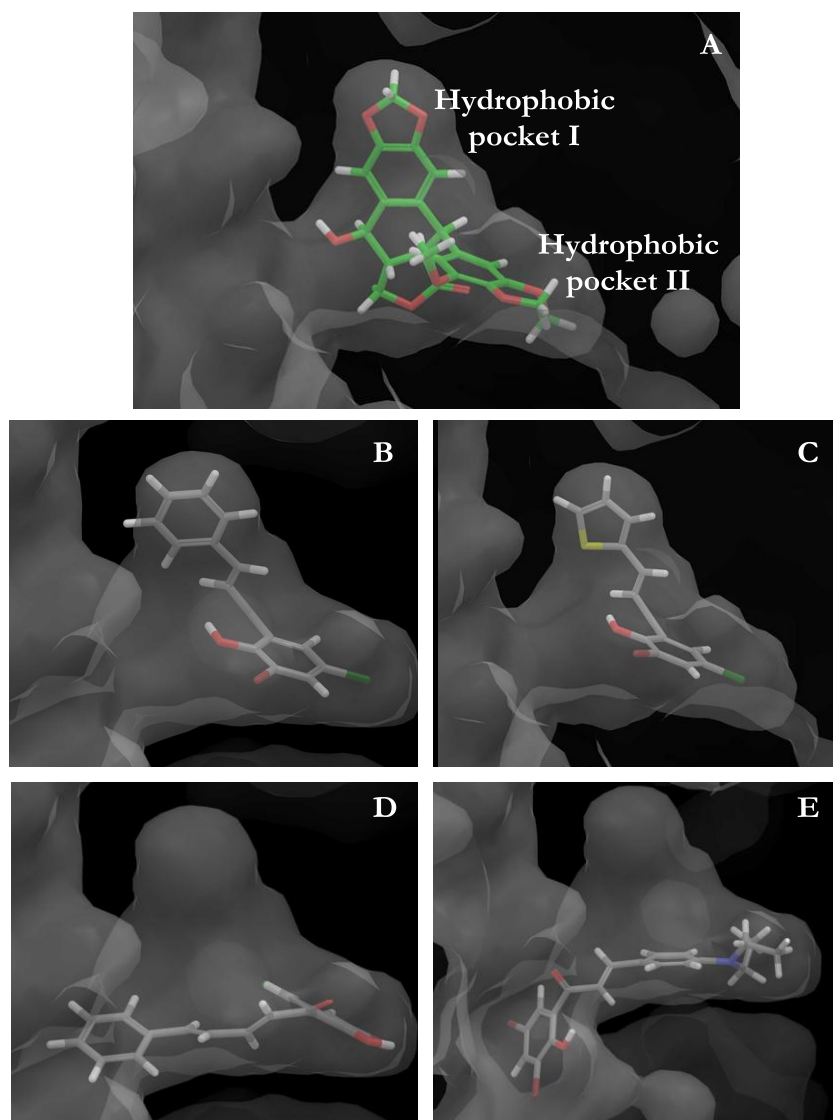


Figure 24. Docking of the synthesized destabilizing agents and podophyllotoxin in the colchicine binding site of β -tubulin: (A) podophyllotoxin, (B) compound **3**, (C) compound **5**, (D) compound **8**, (E) compound **11**.

The inactive compounds, **4**, **7** and **35**, were also docked into the colchicine binding site of tubulin in order to find an explanation why these do not possess the same destabilizing activity against tubulin assembly as **3**, **5**, **8**, **10** and **11**. Interestingly, compounds **4** and **7** (Figure 25 A and B) adopt the same flipped binding mode as **10** and **11** (Figure 24E). However, the methoxy or the trifluoromethyl group is not able to achieve contact with the hydrophobic pocket to the same extent as the diethylamino moiety in **10** and **11**. Additionally, compound **35** (Figure 25C) was directed in a similar manner as **3** (Figure 24B) but the 4-bromo-3-chloro-2-hydroxyphenyl moiety seems to adopt a slightly different angle and could therefore not reach as far into the pocket as the corresponding moiety in **3**.

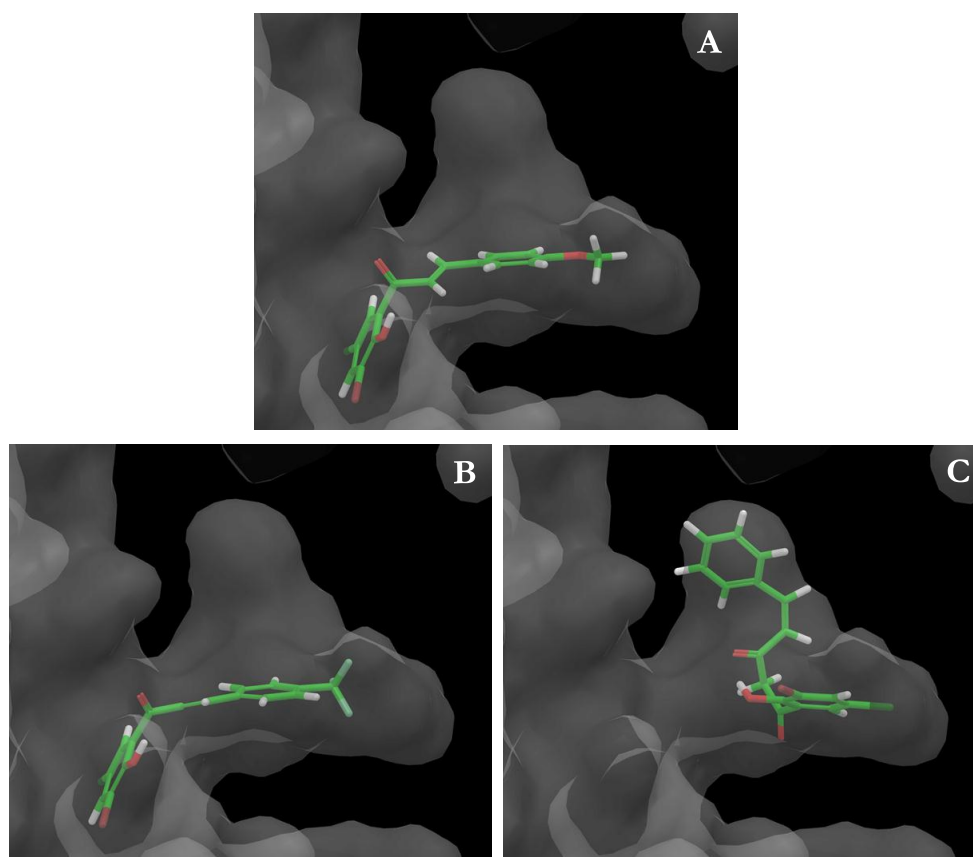


Figure 25. Docking of the inactive compounds into the colchicine binding site of β -tubulin: (A) compound **4**, (B) compound **7** and (C) compound **35**.

4.2.4.2 Docking into the paclitaxel binding site of β -tubulin

Drugs that target the paclitaxel-binding site on β -tubulin are known to act as promoters of tubulin assembly. Accordingly, the microtubule stabilizing dienone **34** and the co-crystallized ligand paclitaxel, were docked into the paclitaxel binding site of β -tubulin using the paclitaxel-tubulin crystal structure (PDB 1JFF).^{114, 145} The large and complex structure of paclitaxel binds to β -tubulin through multiple hydrophobic interactions (Figure 26A). The phenyl ring of the 2-benzoyl ester moiety is located in a hydrophobic cavity surrounded by Leu217, Leu219, Asp226, His229 and Leu230. Residues Val23,

Ala233, Ser236 and Phe272 generate a hydrophobic pocket occupied by the 3'-phenyl ring whereas the voluminous taxane ring is enclosed by the Pro274, Leu275, Thr276, Ser277, Arg278, Pro360, Arg369, Gly370 and Leu371 residues. Furthermore, the phenyl ring of the 3'-benzamido group is close to Val23 and the oxetane oxygen participates in hydrogen bonding with the backbone N-H of Thr276 (Figure 26C). Since dienone **34** is considerably smaller than paclitaxel, it is not able to fill the binding pocket to the same extent. However, the docking study showed that the three different aromatic moieties in **34** are directed towards different hydrophobic regions in the paclitaxel binding site (Figure 26B). The indole fragment is buried inside the hydrophobic pocket that binds to the 3'-phenyl ring in paclitaxel. The *N*'-benzyl moiety enters the same pocket as the 2-benzoyl phenyl group and the 4-bromo-3-chloro-2-hydroxyphenyl moiety is directed, via the alkene linker, down into a hydrophobic area, enclosed by Pro274, Thr276, Arg278, Gln282, Arg284, Leu286, and Leu371. Interestingly, the modeling study also suggested that **34** could interact via two hydrogen bonds with Thr276: one between the phenolic hydrogen and the alcohol oxygen (2.31 Å, -OH...O, 134°) and one hydrogen bond between the carbonyl oxygen and N-H in the protein backbone (2.14 Å, C=O...H-N, 171°) (Figure 26D).

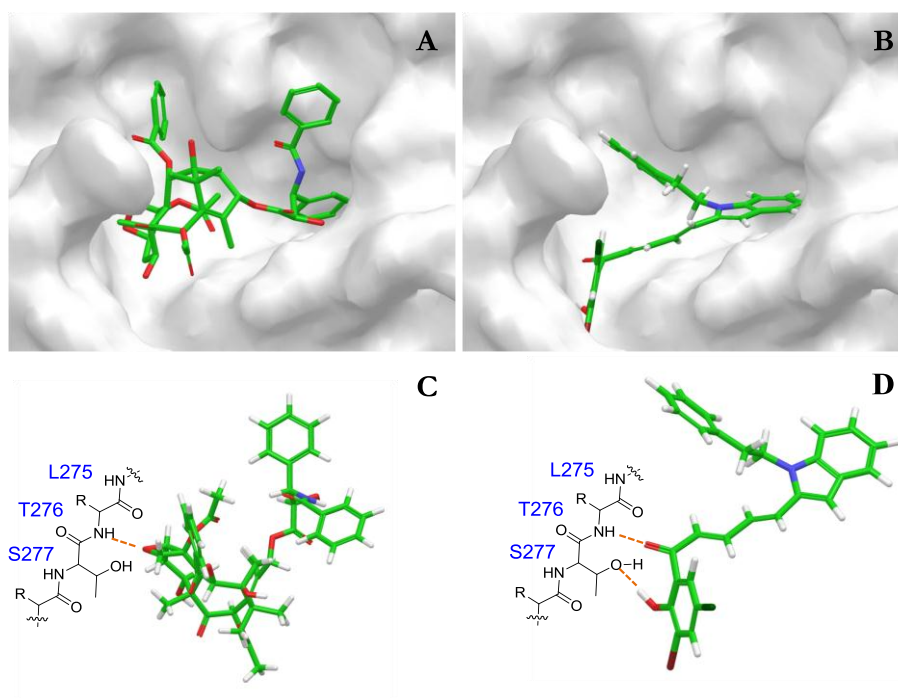


Figure 26. Paclitaxel (A) and dienone **34** (B) docked into the paclitaxel binding site of tubulin. Panels C and D depict potential hydrogen bonding interactions (orange dashed lines) between paclitaxel or **34** and the Thr276 residue in the active site on the β -tubulin subunit.

4.2.5 Study of the chemical reactivity with glutathione

Chalcones are known Michael acceptors and the observed effects toward tubulin assembly may be due to their reactivity as α,β -unsaturated electrophiles.¹²² For instance, several reports of chalcones binding to β -tubulin suggest the interaction with nucleophilic cysteine residues in the colchicine binding site, in particular Cys241.^{130, 148} Accordingly, the reactivity towards thiols has been established in the presence of glutathione, a nucleophilic intracellular tripeptide with an essential role in xenobiotic metabolism and detoxification.^{126, 148} For that reason, a synthetic experiment was conducted in order to investigate the reactivity of the dihalogenated chalcone derivatives in the present study. A mixture of glutathione and compound **10** in THF was stirred at 37 °C for 2 hours.¹⁴⁹ However, subsequent TLC analysis of the reaction mixture showed that no glutathione conjugate was formed. Additionally, the result was supported by the docking study where none of the destabilizing compounds, **3**, **5**, **8**, **10** and **11**, appeared to interact with Cys241 due to the large distance between the electrophilic α,β -unsaturated fragment and the nucleophilic thiol residue. In summary, the observed activity of the destabilizing agents toward tubulin dynamics is probably not a result of the reaction with cysteine residues in the colchicine binding site on β -tubulin.

4.3 CONCLUSIONS

This study comprises a series of dihalogenated chalcones and related dienones with antiproliferative activities against ten individual cancer cell lines. Five compounds were established as inhibitors of tubulin assembly, and surprisingly, one dienone derivative was instead found to stabilize tubulin to the same extent as the well-known anticancer drug docetaxel. The remaining three compounds showed no significant effect on tubulin dynamics, which suggests a different mechanism for their observed cytotoxicity profiles. Disruption of tubulin assembly was favored by compounds containing unsubstituted aromatic B-rings (i.e., phenyl or 2-thienyl as in **3** or **5**), an electron rich 4-diethylaminophenyl group (as in **10** and **11**) or an elongated styryl moiety in the 3-position of the chalcone structure (as in **8**). Stabilization of tubulin polymerization was obtained in the presence of the significantly larger dienone structure **34** containing an additional aromatic moiety. Molecular docking studies suggested that the tubulin inhibitors bind into the colchicine binding site of β -tubulin while the novel tubulin-stabilizing agent seems to interact with the paclitaxel binding site. To the best of our knowledge, compound **34** is the first reported chalcone with microtubule-stabilizing activity, which could be a starting point for the development of novel small molecule microtubule-stabilizing agents.

5. Development of Chromone-Based Kinase Inhibitors and Modulators (Papers III and IV)

5.1 INTRODUCTION

5.1.1 Protein kinases

Protein kinases belong to a ubiquitous class of structurally related enzymes, expressed by 518 genes encoded by the human genome, referred to as “the human kinome”. The protein kinase complement of the human kinome constitutes approximately 1.7% of all human genes, thus representing one of the largest families of genes in eukaryotes.^{150, 151}

Protein kinases catalyze the phosphorylation of specific proteins by transferring the γ -phosphate from adenosine-5'-triphosphate (ATP) to the hydroxyl groups of serine, threonine or tyrosine residues (Figure 27). Hence, protein kinases are generally divided into two major classes: protein serine/threonine kinases (PSTKs) and protein tyrosine kinases (PTKs), and a minor class of dual specific kinases (DSKs), which utilize all three residues as substrates.¹⁵²⁻¹⁵⁵ Additionally, there are protein kinases that phosphorylate other amino acid residues, e.g. the histidine kinases. These enzymes have been found in eukaryotes but are primarily present in prokaryotes, plants and fungi.^{156, 157}

Phosphorylation of proteins is essential in signal transduction pathways and is involved in cellular processes such as DNA-replication, cell growth, metabolism, differentiation, motility, and apoptosis.^{150, 152, 158, 159} The reverse process can be achieved by phosphatases that dephosphorylate proteins. Consequently, the phosphorylation-dephosphorylation process acts as a molecular switch, turning the protein activity on and off to obtain different biological responses.^{160, 161} Approximately 30% of all cellular proteins are phosphorylated on at least one amino acid residue. This fact, together with the estimation of 10,000 different proteins in a conventional eukaryotic cell with an average length of ~400 amino acids (17% which are serine, threonine or tyrosine residues), give ~70,000 potential phosphorylation sites for any given kinase.¹⁵³

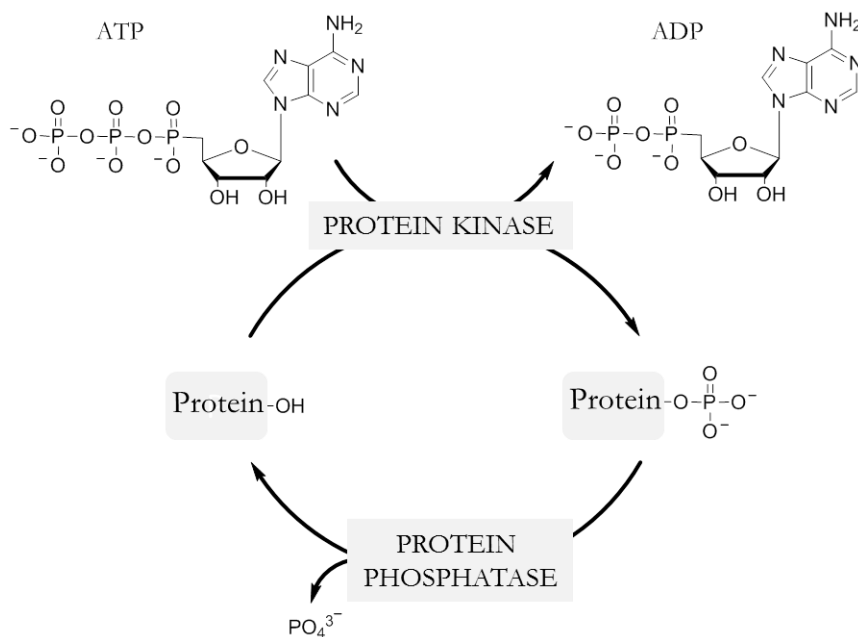


Figure 27. The catalytic cycle of phosphorylation and dephosphorylation of proteins, which generally occurs on serine, threonine and tyrosine residues.

Several common structural features of protein kinases have been identified from numerous X-ray studies.^{159, 162} In general, the characteristic protein kinase fold possesses a highly conserved catalytic domain, consisting of approximately 250 amino acids. These form a smaller *N*-terminal lobe of β -sheets and a larger *C*-terminal lobe of α -helices, which are connected via a linker that includes a short peptide fragment, referred to as the hinge region.^{152, 153, 159, 161, 163-166} ATP binds in a deep cleft located between the *N*- and the *C*-terminal lobes. The *N*-terminal lobe possesses a flexible glycine-rich loop that forms a lid on the top of ATP. This lid is crucial for catalysis and necessary for nucleotide positioning. Moreover, ATP-binding is characterized by two hydrogen bonds between the adenine moiety and the protein backbone of the hinge area (Figure 28). The ribose moiety is located in a polar pocket and interacts via hydrogen bonds to a carboxylate residue and to a backbone carbonyl oxygen within the kinase. Furthermore, the triphosphate group coordinates to a divalent metal ion, such as Mg^{2+} , which also binds to an aspartate residue in the well conserved DFG-motif (Asp-Phe-Gly).¹⁶¹

The DFG-sequence is located in the activation loop, which is an important site for substrate binding and protein phosphorylation. A large conformational change in the activation segment allows the kinase to transform between an active and inactive state. In the active state, the aspartate of the DFG-motif is directed into the ATP-binding site, referred to as “DFG-in”, and thus coordinates to the magnesium ion. At the same time, the phenylalanine residue of the DFG-motif is located in a hydrophobic pocket and is not accessible. In the inactive state, the aspartate residue points out from the ATP-binding

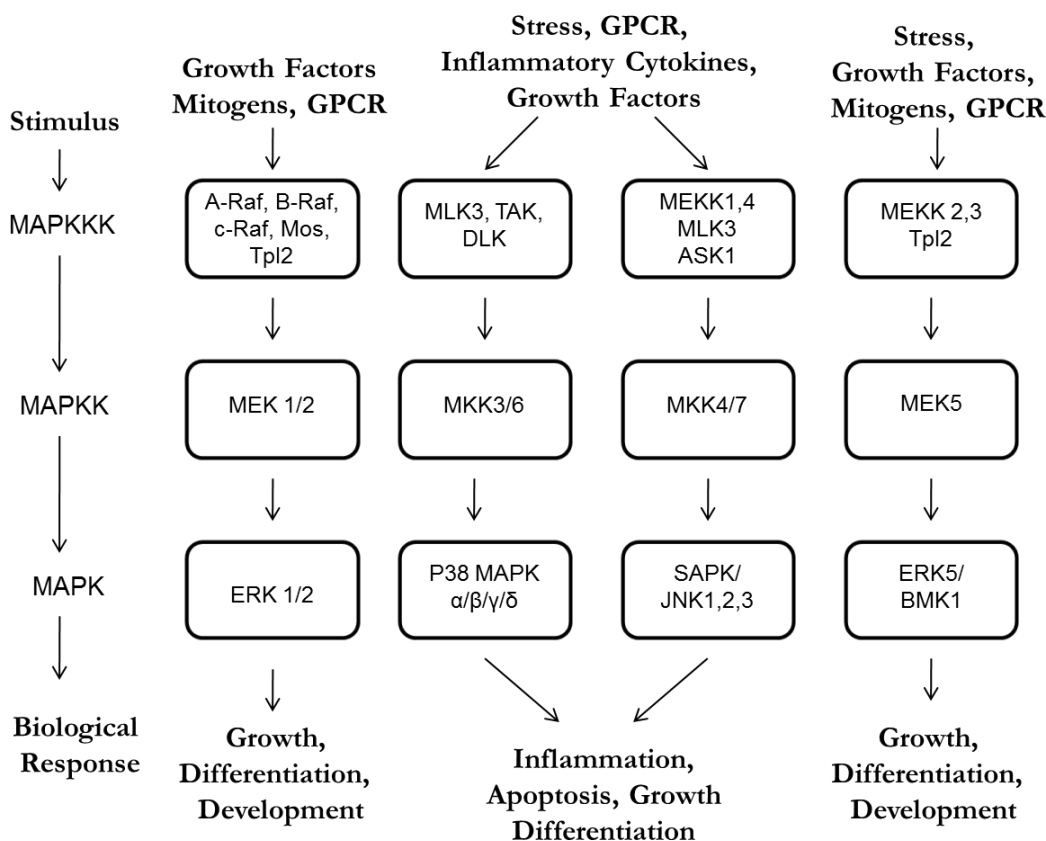


Figure 29. Schematic illustration of mammalian MAPK pathways. MAP kinases are activated by phosphorylation cascades, usually comprised of two upstream protein kinases (MAPKKK and MAPKK). The activated MAP kinase is transported into the nucleus, where it phosphorylates and regulates its target proteins, which further initiate gene transcription and cell proliferation.^{168, 174, 175}

5.1.3 Protein kinases as drug targets

Protein kinases are important regulators in signal transduction pathways and their catalytic activity is essential for the development and survival of eukaryotic organisms.¹⁵⁰ Dysregulation of kinase activity has been associated with a number of pathological pathways related to cancers, inflammation, autoimmune diseases and metabolic disorders.^{161, 165, 176} Thus, kinases constitute an important class of therapeutic targets in the pharmaceutical industry.^{161, 177} However, the design of kinase inhibitors is especially complex since the aim is to achieve selectivity for a small number of kinases within a family of more than 500 structurally related enzymes. Moreover, all kinases bind to the same cofactor, ATP, and they also exhibit proximate sequence homology with protein kinases of other organisms such as plants, fungi and yeasts.¹⁷⁸ As a consequence, inhibitors that target the ATP-binding site often suffer from low selectivity profiles and cross-reactivity with other protein kinases. They also have to compete with high molar concentrations of intracellular ATP (~ 1-10 mM).^{152, 165, 179, 180} Despite these drawbacks, the majority of small molecule kinase inhibitors reported to date targets the ATP-binding site.¹⁵² However, apart from ATP-antagonism, several other inhibition strategies and mechanisms have been applied, including allosteric or covalent inhibition along with direct or indirect blocking of substrate binding.¹⁸¹

5.1.3.1 Type I and type II inhibitors, targeting the ATP-binding site

The majority of small molecule protein kinase inhibitors target the ATP-binding site and act either as type I or type II inhibitors.¹⁶¹ Type I inhibitors are ATP-competitive, they generally bind to the active conformation of the protein kinase, i.e. to the DFG-in conformation. These inhibitors mimic the interactions of the adenine moiety of ATP, typically by the formation of 1-3 hydrogen bonds with backbone residues in the kinase hinge area. Potent and selective type I inhibitors can be developed through design of compounds that utilize specific regions in the ATP-binding site that are not occupied by ATP. Such a region is the back cavity (hydrophobic region I) guarded by the gatekeeper residue, which is located in the kinase hinge region (Figure 28).¹⁸² The nature and size of the gatekeeper regulates the shape and the conformation of the hydrophobic cavity. Thus, a bulky gatekeeper residue limits the size and generates a small inaccessible cavity, whereas a small gatekeeper allows the positioning of substituents in the large back cavity.^{164, 165, 183}

Type II inhibitors occupy the ATP binding pocket in the same manner as the type I inhibitors, but they also utilize an adjacent hydrophobic site present in the DFG-out conformation. Type II inhibitors preferentially bind to and stabilize the inactive conformation of the protein kinase, thus preventing activation.^{162, 164, 165} The development of type II inhibitors is preferable since it opens several opportunities to control selectivity and thereby to improve the use of such novel kinase inhibitors as drugs.

5.1.3.2 Allosteric, type III inhibitors

Type III inhibitors bind exclusively to a less conserved allosteric binding pocket on the kinase, which is spatially distinct from the ATP-binding site.¹⁸⁴ Several kinases possess such a cavity, also referred to as the DFG-out pocket, adjacent (but not overlapping) to the ATP-binding site. Inhibitors that bind to this site can lock the kinase in the inactive, DFG-out conformation, thus preventing phosphorylation. Furthermore, allosteric inhibitors usually possess high selectivity and potency since they utilize binding sites and regulatory mechanisms that are unique to a particular kinase.

5.1.4 The p38 MAP Kinase

The human p38 MAP kinases comprise a family of serine/threonine kinases consisting of four isoforms: α , β , γ and δ .¹⁸⁵⁻¹⁸⁹ The α -isoform, p38 α , is the best characterized and is known to be involved in the biosynthesis of pro-inflammatory cytokines such as interleukin-1 β (IL-1 β) and tumor-necrosis factor α (TNF- α) in lipopolysaccharide (LPS)-stimulated human monocytes.¹⁸⁶ Consequently, p38 α is strongly associated with chronic inflammatory diseases such as rheumatoid arthritis, Crohn's disease, and inflammatory bowel syndrome. The p38 MAPKs are activated by dual phosphorylation on Thr180 and Tyr182 residues, which are operated by upstream MAPKKs, in particular MKK3 and MKK6 (Figure 29). Indirectly, they are also activated by cellular stress such as osmotic

shock, UV-radiation, mechanic stress and lipopolysaccharide (LPS) exposure. Subsequently, p38 MAP kinases activate several substrates via phosphorylation including transcription factors (e.g. activating transcription factor 2, ATF2, and tumor suppressor protein p53) and proteins involved in various cellular processes such as cell cycle progression, stability and mRNA translation (e.g. heat shock protein 27, Hsp27).¹⁸⁷

Besides the strong association with inflammatory disorders, p38 kinases have been found to be overexpressed in human tumors and cancer cell lines.^{190, 191} For example, high concentrations of p38 kinases have been correlated with invasive and poor prognostic breast cancers.¹⁹² Notably, chronic inflammation is a potent cancer promoter and cytokines are important survival factors for cancer cells. Thus, inhibition of p38 kinases could be beneficial for the treatment of inflammatory-associated cancers.¹⁹⁰

5.1.4.1 p38 α MAP kinase inhibitors

The human p38 α MAP kinase was originally identified as the molecular target of pyridyl imidazole derivatives, a class of compounds known to inhibit the biosynthesis of inflammatory cytokines.^{185, 186, 193} Pyridyl imidazoles, in particular those containing a vicinal 4-fluoro/pyridyl motif (e.g. SB-203580 and SKF-86002, Figure 30), are known to interact with the ATP-binding site of p38 α , thus preventing the activation of downstream kinases.¹⁹⁴⁻¹⁹⁷ A key interaction for these ATP-competitive compounds is a hydrogen bond between the pyridin-4-yl nitrogen and the backbone NH group of Met109 in the hinge region (Figure 31A).^{195, 197, 198} Furthermore, to obtain selectivity, the 4-fluorophenyl moiety utilizes a hydrophobic pocket (I), which is guarded by the gatekeeper residue (Thr106).¹⁹⁵

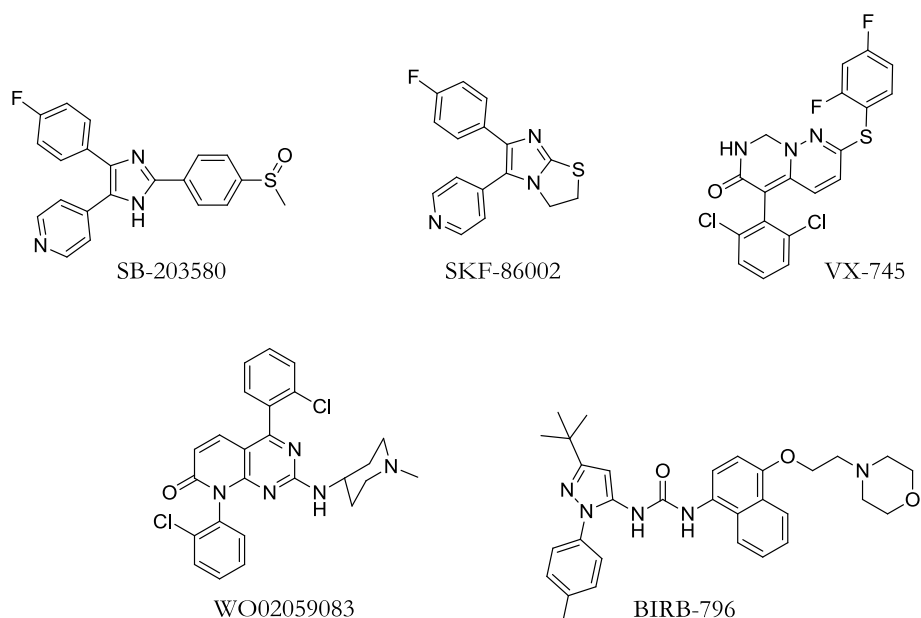


Figure 30. Structures of known p38 α inhibitors. SB203580, SKF-86002, VX-745 and WO02059083 bind to the ATP-binding site. In contrast, BIRB-796 is an allosteric inhibitor that binds to a pocket adjacent to the ATP-binding site.

Another class of compounds that binds to the ATP-binding site of p38 α is highly selective heteroaryl fused pyridones and derivatives thereof (e.g. VX-745 and WO02059083, Figure 30).¹⁹⁹⁻²⁰² These compounds are characterized by a non-complementary carbonyl hydrogen bond-accepting group opposite to a backbone carbonyl in the hinge area (Figure 31B).^{198, 202} To avoid repulsion, the carbonyl group of the inhibitor induces a peptide flip in the hinge region, thus allowing formation of two hydrogen bonds between the NH nitrogens in the backbone of Met109 and Gly110. Additionally, the adjacent pyridone NH group forms a hydrogen bond to the backbone carbonyl oxygen of His107.^{198, 202}

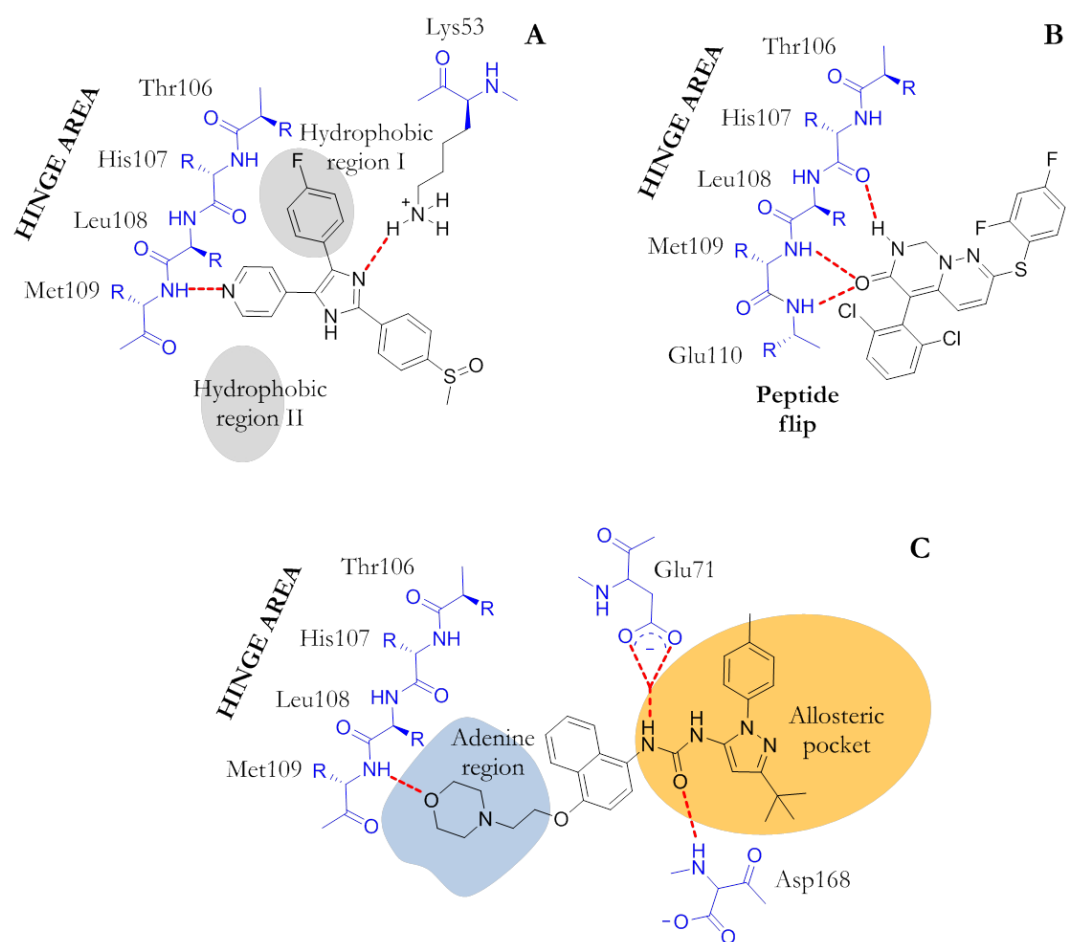


Figure 31. Binding features and key interactions for three well-known p38 α inhibitors. SB-203580 (A) and VX-745 (B) bind to the ATP-binding site of p38 α . However, VX-745 binds in a different manner than SB-203580 since it induces a peptide flip between Met109 and Glu110 in the hinge region. In contrast, BIRB-796 binds in an allosteric pocket adjacent to the ATP-binding site.

A third class of p38 α inhibitors bind to an allosteric binding site, adjacent to the ATP-binding pocket.¹⁶⁴ Among those, the *N,N'*-diaryl urea derivative BIRB-796 (Figure 30 and 31C) binds to the inactive conformation of p38 α in a selectivity pocket formed by the displacement of the Phe residue in the DFG-out motif.^{184, 203} Hence, BIRB-796 locks the protein in its inactive form and prevents ATP-binding due to steric overlap with the

The residue. Besides hydrophobic allosteric interaction, the urea group interacts via two hydrogen bonds: one between the NH hydrogen and the Glu71 side chain and one between the carbonyl oxygen and the backbone NH group of Asp168 in the DFG-motif.¹⁹⁸ Interestingly, BIRB-796 also extends into the adenine region of the ATP-binding site and forms a hydrogen bond between the morpholine oxygen and the backbone NH group of Met109 in the hinge region.^{164, 198}

5.1.5 The MEK1/2 MAP kinase kinases

The Ras/Raf/MEK/ERK mitogen-activated protein (MAP) kinase pathway plays an important role in control and regulation of cell proliferation, survival and differentiation.¹⁶⁸ Dysregulation of these kinases is strongly associated with oncogenesis in humans and are therefore attractive targets for the development of potential anticancer drugs.²⁰⁴ For example, high concentrations of activated MEK1/2 and ERK1/2 have been found in human tumors, particularly those present in colon, lung, pancreas, ovary and kidneys. MEK1/2 are dual specific MAP kinase kinases, which phosphorylate specific threonine and tyrosine residues on downstream ERK1 and ERK2, required for activation.^{205, 206} Furthermore, MEK1/2 are attractive targets in drug discovery since they possess restricted substrate specificity (ERK1/2), in comparison with other kinases.²⁰⁴ On the other hand, MEK1/2 are activated by several kinases, including Mos, A-raf, B-raf, Raf-1 and MEKK, which further is activated by growth factors, mitogens and GPCRs (Figure 29). Therefore, targeting MEK1/2, rather than upstream kinases, might offer a more efficient strategy toward the development of anticancer drugs than to target Ras/Raf/MEK/ERK signaling.

5.1.5.1 MEK1/2 inhibitors

MEK1 and MEK2 possess high sequence identity, with 86% homology in the catalytic domain.²⁰⁶ Thus, compounds that interact with MEK1/2 are non-selective between the two kinase isoforms. Several naturally occurring resorcylic acid lactones, e.g. L-783277 (Figure 32), have demonstrated ATP-competitive MEK1/2 inhibitory activity, targeting the ATP-binding site.²⁰⁴ A characteristic fragment for those compounds is the α,β -unsaturated *cis*-enone in the macrocycle that is associated with irreversible binding to nucleophilic cysteine residues in the active site. However, the most well-known and well-characterized MEK1/MEK2 inhibitors are non-competitive and bind to an allosteric pocket adjacent to the MgATP site. Among those, CI-1040, PD0325901, PD98059, and U0126 (Figure 32) bind to the inactive, dephosphorylated form of MEK1/2. Thereby the activation via upstream kinases is prevented by a conformational change that locks the kinase in its inactive form.^{162, 171, 204, 206, 207} In fact, these compounds are not MEK1/2 inhibitors. Instead, they are more correctly referred to as MEK1/2 modulators, since they inhibit the phosphorylation of MEK1/2, thus preventing its activation. Several CI-1040 and U0126 analogs have been synthesized and studied with the aim to investigate and characterize important structural features for the activity toward MEK1/2.^{206, 208, 209} However, only few investigations around the structure-activity relationships for the

chromone-based PD98059 have been performed considering the numerous reports of its *in vitro* and *in vivo* activity.^{210, 211}

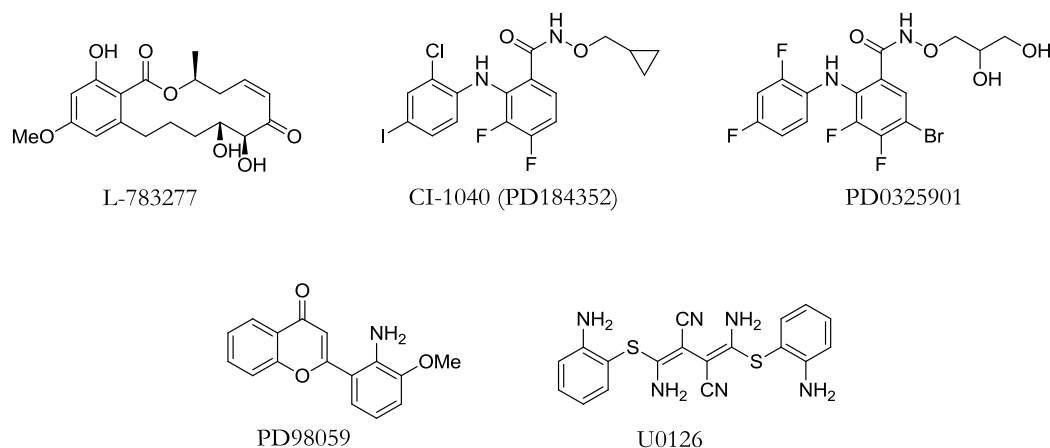


Figure 32. Chemical structures of known MEK1/2 inhibitors. L-783277 (MEK1 IC_{50} 4nM) binds to the ATP binding site of MEK1/2, whereas CI-1040 (MEK1/2 IC_{50} 17nM), PD0325901 (MEK1 and MEK2 IC_{50} 1.1 and 0.79 nM, respectively), PD98059 (MEK1 IC_{50} 10 μ M) and U0126 (MEK1 and MEK2 IC_{50} 72 and 58 nM, respectively) bind to an adjacent pocket and thereby act as allosteric modulators, preventing MEK1/2 activation.²⁰⁴

5.2 DEVELOPMENT OF p38 α MAP KINASE INHIBITORS (Paper III)

The ambition of the present study was to use structure-based design in order to develop chromone-based p38 α inhibitors. The aims were i) to evaluate if diarylated 4-fluorophenyl/pyridyl chromones can adopt the same binding mode as the imidazole-based SB203580 (Figure 31A), ii) to establish an appropriate substituent pattern on the chromone structure and iii) to study potential interactions with the ATP-binding site of p38 α to obtain inhibitory activity.

5.2.1 Docking studies of the ATP-binding site of p38 α

The docking study was performed using the Schrödinger Package, MAESTRO interface.¹⁴⁴ The structure of p38 α in complex with the inhibitor SB203580 (PDB 1A9U) was used for the study.^{145, 195} The study suggested that 3-(4-fluorophenyl)-2-(4-pyridyl)chromone derivatives (Figure 33) could adopt the same binding mode as the imidazole-based inhibitor SB203580 (Figure 31A). Accordingly, the pyridine-4-yl nitrogen could interact via a hydrogen bond to the backbone NH group of Met109 (2.14Å, N \cdots H-N, 163°) at the same time as the 4-fluorophenyl moiety is directed into the hydrophobic pocket I. Furthermore, the chromone carbonyl oxygen could participate in a hydrogen bond to the side chain of Lys53 (1.95Å, C=O \cdots H-N, 134°), in a similar fashion as one of the imidazole nitrogens in SB203580. The study also revealed that introduction of an amino functionality in the 2-position on the pyridyl moiety, such as an isopropylamine (compound **59**, Figure 33B), could provide an additional hydrogen bond to the hinge area, i.e. between the NH and the backbone carbonyl oxygen of Met109 (2.14 Å, N-H \cdots O=C, 139°).²¹²⁻²¹⁶ A suitable R-group on this amine could possibly utilize an adjacent

fluorophenyl moiety via a palladium-mediated Suzuki cross-coupling reaction. Finally, the target compounds could be obtained using Buchwald-Hartwig amination reactions for the introduction of various amines in the 2-position on the pyridyl moiety.

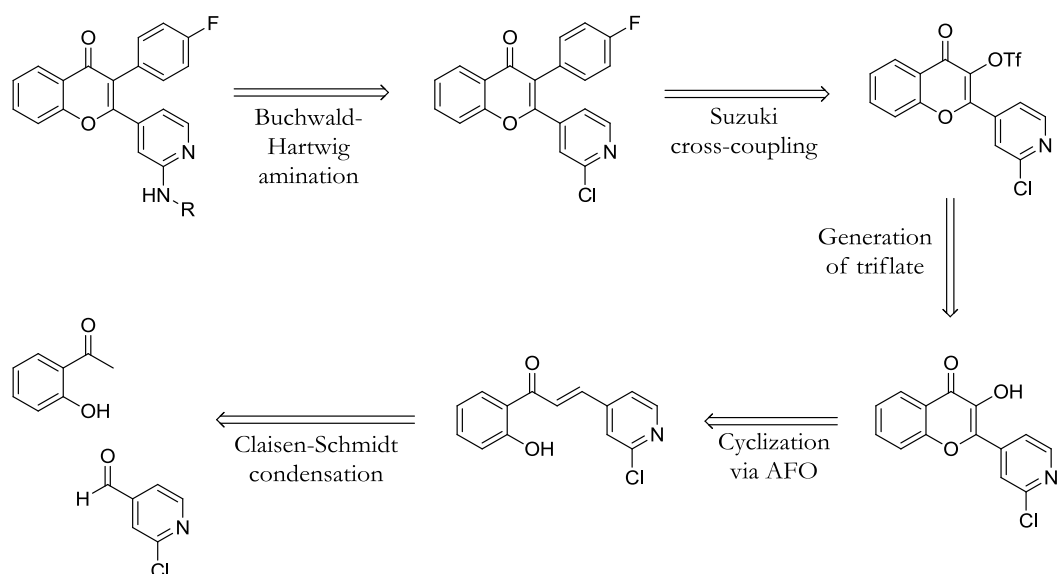
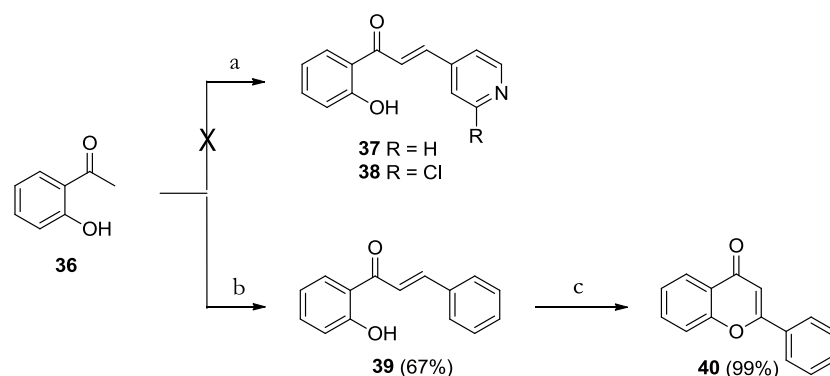


Figure 34. Retrosynthetic analysis for the synthesis of 2-(2-amino-4-pyridyl)-3-(4-fluorophenyl)chromone derivatives via the chalcone pathway.

The synthesis of the pyridylchalcone **37** has earlier been reported in the literature, using a base-promoted aldol condensation protocol with isonicotinaldehyde and KOH in ethanol.²¹⁷ However, after several attempts, we were not able to reproduce the reaction from the literature or isolate the desired products **37-38** (Scheme 6). The reaction was investigated using different conditions, such as stronger base (aqueous NaOH, 60%), varying reaction times and use of microwave heating, but unfortunately without any successful results. Thus, we had to change strategy and investigate alternative routes for the synthesis of the 2-(2-amino-4-pyridyl)-3-(4-fluorophenyl)chromone derivatives.



Scheme 6. Chromone synthesis via the chalcone pathway. Reagents and conditions: (a) The appropriate isonicotinaldehyde, KOH, EtOH, 50 °C→rt, overnight. (b) benzaldehyde, KOH, EtOH, 50 °C → rt, overnight (c) I₂, EtOH, 150 °C, microwave heating, 1h.

5.2.3 Synthetic strategy B

Due to synthetic problems via the chalcone pathway a new synthetic strategy was investigated (Figure 35). Instead, the desired derivatives could be generated via the Baker–Venkataraman rearrangement. Accordingly, the chromone ring system could be provided via esterification of 2'-hydroxyacetophenone with 2-chloroisonicotinoyl chloride followed by rearrangement to the corresponding diketone, which in turn could be cyclized to the 2-(2-chloro-4-pyridyl)chromone under acidic conditions. Similarly to the first synthetic strategy (Figure 34), the 4-fluorophenyl moiety could then be introduced in the 3-position via halogenation and Suzuki cross-coupling. Finally, the target compounds could be provided using Buchwald-Hartwig amination reactions for the introduction of various amines in the 2-position on the pyridyl moiety.

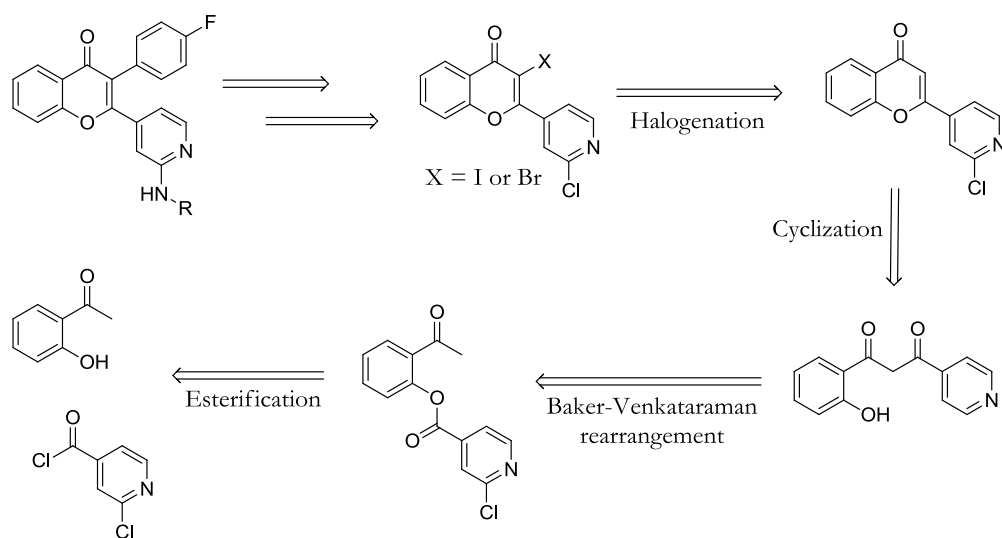
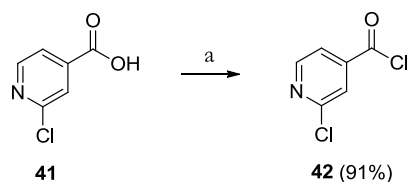


Figure 35. Retrosynthetic analysis for the synthesis of 2-(2-amino-4-pyridyl)-3-(4-fluorophenyl)chromone derivatives via the Baker-Venkataraman rearrangement.

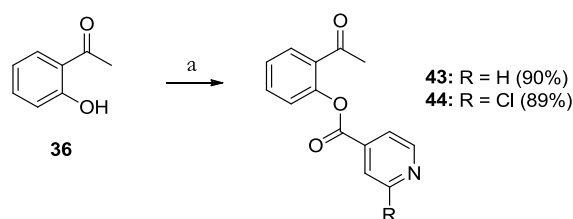
5.2.3.1 Synthesis of the chromone ring system

Initially, one of the starting materials, 2-chloroisonicotinoyl chloride **42** was synthesized prior to the first esterification step (described in Figure 35). The acid chloride **42** was obtained in excellent yields (91%) from the corresponding carboxylic acid **41** using neat thionyl chloride at reflux (Scheme 7).²¹⁸



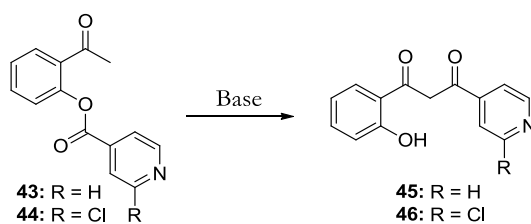
Scheme 7. Synthesis of 2-chloroisonicotinoyl chloride **42**. Reagents and conditions: (a) SOCl₂, reflux, 28 h.

Subsequently, esters **43-44** were successfully obtained (90 and 89%, respectively) from 2'-hydroxyacetophenone **36** and the appropriate acid chloride in pyridine at room temperature (Scheme 8).



Scheme 8. Esterification of 2'-hydroxyacetophenone **36** to generate **43** and **44**. Reagents and conditions: (a) isonicotinoyl chloride or 2-chloroisonicotinoyl chloride **42**, pyridine, 0 °C → rt, 2 h.

The subsequent Baker-Venkataraman rearrangement, to obtain diketones, is usually performed in the presence of KOH, with pyridine as a solvent, using conventional heating at 50 °C.^{90, 219} However, these reaction conditions gave diketone **45** in poor yields (19%) when using ester **43** (Table 3, Entry 1) and did not result in any product formation when using the chlorinated derivative **44** (Table 3, Entry 2). Other protocols in the literature reveal that the rearrangement can be accomplished using other bases such as DBU in pyridine or NaH in THF.^{220, 221} Thus, these protocols were tested in order to try to convert ester **44** to the corresponding diketone **46**. However, treatment of ester **44** with DBU in pyridine at 80 °C gave no indication of product formation (Table 3, Entry 3). In contrast, when using NaH in THF at 50 °C, all ester **44** was consumed in 50 min (Table 3, Entry 4) and the reaction time could be reduced to 10 min when using microwave heating at 65 °C (Table 3, Entry 5). However, when looking closer at the outcome of the reaction, we noticed that the major product was 2'-hydroxyacetophenone **36** formed as a result of hydride mediated ester cleavage. The diketones **45** and **46** could finally be obtained in acceptable and reproducible yields (85 and 60%, respectively), when using the KOH/pyridine protocol with microwave heating at 100 °C for 10 min (Table 3, Entries 6-7).

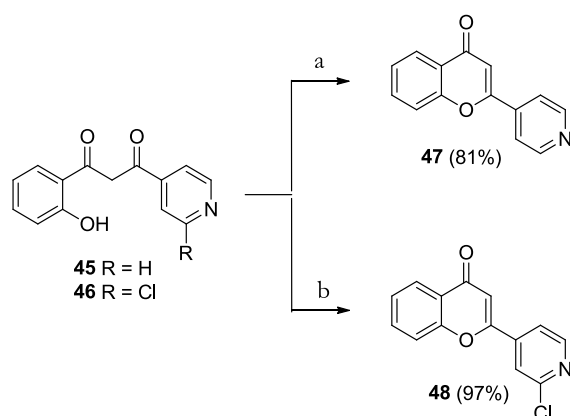
Table 3. Screening of reaction conditions for the Baker-Venkataraman rearrangement.

Entry	R	Base	Solvent	Temp. (°C) conditions	Reaction time (min)	Yield (%) ^a
1	H	KOH	Pyridine	50	120	19
2	Cl	KOH	Pyridine	50	120	n.r. ^b
3	Cl	DBU	Pyridine	80	overnight	n.r. ^b
4	Cl	NaH	THF	50	50	n.d. ^c
5	Cl	NaH	THF	65, mw ^d	10	n.d. ^c
6	H	KOH	Pyridine	100, mw ^d	15	85
7	Cl	KOH	Pyridine	100, mw ^d	10	60

^aIsolated yields. ^bn.r. = No reaction according to ¹H NMR spectra of the crude reaction mixture.

^cn.d. = Not determined, 2'-hydroxyacetophenone was generated during the reaction due to ester cleavage. ^dmw = microwave heating.

The 2-pyridylchromone derivatives **47-48** were provided in high yields (81 and 97%, respectively) via efficient acid-promoted cyclization in the microwave, using HCl in acetic acid at 60 °C for 30 min or concentrated sulfuric acid in ethanol at 100 °C for 15 min (Scheme 9).^{90, 99} Importantly, the latter reaction conditions could not be used for the cyclization of **45** since it only gave protonation of the pyridine nitrogen.



Scheme 9. Synthesis of **47** and **48** via acid-promoted cyclization. Reagents and conditions: (a) HCl, acetic acid, 60 °C, microwave heating, 30 min. (b) H₂SO₄, EtOH, 100 °C, microwave heating, 15 min.

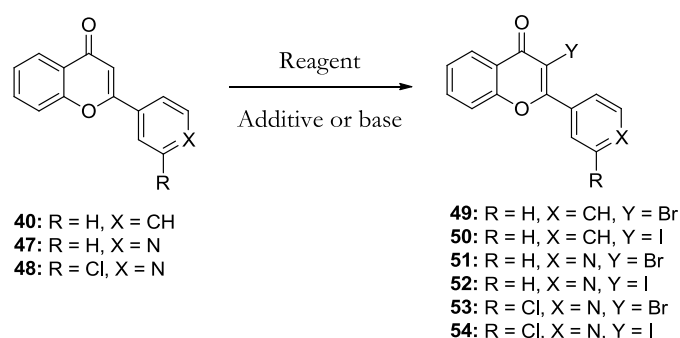
5.2.3.2 Halogenation in the 3-position

Flavone **40** was synthesized and used as a model compound for the screening of viable reaction conditions for the introduction of bromine or iodine in the 3-position of the chromone structure. Accordingly, 2'-hydroxychalcone **39** was obtained in 67% yield, via

the Claisen-Schmidt reaction using 2'-hydroxyacetophenone **36**, benzaldehyde, and KOH in ethanol (Scheme 6). Subsequently, microwave-assisted cyclization of **39** using molecular iodine in EtOH at 150 °C for 60 min gave flavone **40** in excellent yield (99%).^{222, 223}

Attempts to brominate **40** with molecular bromine in acetic acid at room temperature (Table 4, Entry 1) or with NBS in chloroform at 60 °C (Table 4, Entry 2) were unsuccessful and did not give any product formation.^{224, 225} However, treatment with NBS in DMF at 60 °C using microwave heating gave 3-bromoflavone **49** in low yields (22%) (Table 4, Entry 3). Furthermore, adjustment of the reaction time from 60 to 30 min increased the yield of **49** to 52% (Table 4, Entry 4). Nevertheless, using the same reaction conditions for the 2-pyridinechromone derivatives **47-48** were not as successful, giving the corresponding bromo derivatives **51** and **53** in 12 and 4%, respectively (Table 4, Entries 5-6). Instead, a couple of new halogenation protocols were tested, focusing on the introduction of iodine in the 3-position. Treatment of flavone **40** with NIS in DMF using microwave heating (Table 4, Entry 7) or molecular iodine and silver trifluoroacetate in dichloromethane at room temperature (Table 4, Entry 8) were unsuccessful.^{226, 227} On the other hand, using molecular iodine and CAN (cerium(IV) ammonium nitrate) in acetonitrile at 65 °C gave 3-iodoflavone **50** in 29% yield (Table 4, Entry 9), using microwave heating at 130 °C increased the yield to 67% (Table 4, Entry 10).²²⁸⁻²³¹ However, this procedure did not generate any product for the halogenation of the 2-chloropyridine derivative **48** (Table 4, Entry 11). Consequently, several other procedures were investigated using **48** as starting material, such as bromination with molecular bromine in pyridine (Table 4, Entry 12) or NBS and AIBN in carbon tetrachloride (Table 4, Entry 13).²³²⁻²³⁴ However these protocols were not successful and did not give the desired product. Furthermore, iodination attempts with molecular iodine and BEMP or BuLi in THF gave the same result, no product formation (Table 4, Entries 14-15). Finally, treatment of **48** with a commercial LDA solution (1.8 M) and molecular iodine gave **54** in 42% yield (Table 4, Entry 16). If instead using in situ generated LDA, prepared from diisopropylamine and BuLi, the yield of **54** increased to 50% (Table 4, Entry 17) and gave **52** in 88% yield (Table 4, Entry 18).²³⁵ Interestingly, the concentration of the reaction mixture proved to be important for the generation of **54** since dilution to 0.01M increased the yield to 80% (Table 4, Entry 19). However, we found that the reaction was not reproducible when using the 2-chloropyridine derivative **48**. Instead, microwave assisted bromination of **48** using excess NBS (5 equiv) in DMF at 80 °C for 60 min gave high and reproducible yields of **53** (94%) (Table 4, Entry 20).

Table 4. Screening for suitable reaction conditions for the introduction of halogens in the 3-position of the chromone structure.



Entry	R	X	Y	Reagent	Additive or base	Solvent	Temp. (°C) conditions	Reaction time (min)	Yield (%) ^a
1	H	CH	Br	Br ₂		Acetic acid	rt ^b	overnight	n.r. ^c
2	H	CH	Br	NBS ^d		CHCl ₃	60	300	n.r. ^c
3	H	CH	Br	NBS ^d		DMF	60, mw ^e	60	22
4	H	CH	Br	NBS ^d		DMF	60, mw ^e	30	52
5	H	N	Br	NBS ^d		DMF	60, mw ^e	30	12
6	Cl	N	Br	NBS ^d		DMF	60, mw ^e	30	4
7	H	CH	I	NIS		DMF	150, mw ^e	90	n.r. ^c
8	H	CH	I	I ₂	CF ₃ COOAg	CH ₂ Cl ₂	0 → rt ^b	overnight	n.r. ^c
9	H	CH	I	I ₂	CAN	Acetonitrile	65	overnight	29
10	H	CH	I	I ₂	CAN	Acetonitrile	130, mw ^e	60	67
11	Cl	N	I	I ₂	CAN	Acetonitrile	130, mw ^e	60	n.r. ^c
12	Cl	N	Br	Br ₂		Pyridine	rt ^b	overnight	n.r. ^c
13	Cl	N	Br	NBS	AIBN	CCl ₄	rt ^b	overnight	n.r. ^c
14	Cl	N	I	I ₂	BEMP	THF	rt ^b	overnight	n.r. ^c
15	Cl	N	I	I ₂	BuLi	THF	-78 → rt ^b	60	n.r. ^c
16	Cl	N	I	I ₂	LDA ^f	THF	-78 → rt ^b	15	42
17	Cl	N	I	I ₂	LDA ^g	THF ^h	-78 → rt ^b	15	50
18	H	N	I	I ₂	LDA ^g	THF ^h	-78 → rt. ^b	15	88
19	Cl	N	I	I ₂	LDA ^g	THF ⁱ	-78 → rt ^b	15	80 ^j
20	Cl	N	Br	NBS ^k		DMF	80, mw ^e	60	94

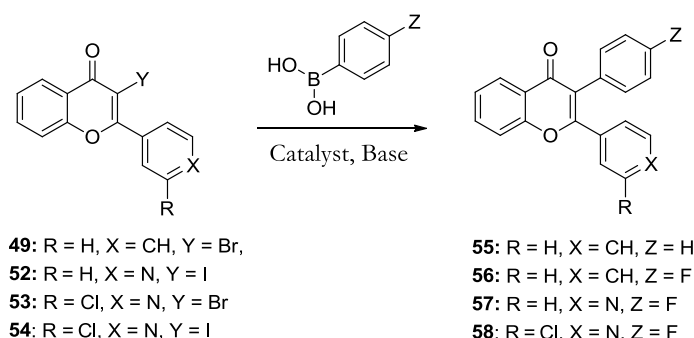
^aIsolated yields. ^brt = room temperature. ^cn.r. = No reaction, according to ¹H NMR spectra or TLC analysis of the crude reaction mixture. ^d1-2 equiv. ^emw = microwave heating. ^f1.8 M solution of LDA in THF/heptane/ethylbenzene. ^gIn situ generated LDA, from diisopropylamine and BuLi at -78 °C in THF. ^hConcentration of mixture = 0.03 M. ⁱConcentration of reaction mixture = 0.01 M. ^jThe reaction is not reproducible. ^k5 equiv.

5.2.3.3 Arylation in the 3-position via a Suzuki cross-coupling reaction

3-Bromoflavone **49** and phenylboronic acid were used as a model system in the search for viable reaction conditions for the introduction of aryl groups in the 3-position of the chromone structure. Notably, the introduction of various aryl groups on 3-iodochromones via Suzuki coupling has previously been reported using Pd₂(dpf)₂Cl₂ as a catalyst in dichloromethane.²²⁶ Instead, Pd(OAc)₂(PPh₃)₂ was used as a catalyst, due to

previous successful results within the research group. However, the reaction with **49** and phenylboronic acid did not generate the desired product after refluxing overnight (Table 5, Entry 1). The reaction was repeated with dichloroethane as a solvent, in order to increase the reaction temperature, but without any further improvement (Table 5, Entry 2). Consequently, the attention was directed towards a Suzuki coupling protocol that has earlier been successfully applied to 5-iodotriazole derivatives in our research group.²³⁶⁻²³⁸ However, following that procedure, using Pd(PPh₃)₄ and K₂CO₃ in DMF/H₂O (9:1) at 100 °C overnight, did not either generate the desired product (Table 5, Entry 3). Several other Suzuki protocols were explored, e.g. treatment with Pd/C (10%) and Na₂CO₃ in DME/ H₂O (1:1) (Table 5, Entry 4), but none of them resulted in product formation.²³⁹ Finally, product **55** was obtained in 65% yield via an oxygen-promoted ligand-free Suzuki procedure using palladium(II) acetate and K₂CO₃ in PEG-400 at 45 °C for 24 hours (Table 5, Entry 5).²⁴⁰⁻²⁴² The yield of **55** was increased to 84% using microwave heating at 60 °C for 30 min (Table 5, Entry 6). This procedure has been reported to involve the generation of highly active palladium nanoparticles, which are stabilized by oxygen.²⁴⁰ Additionally, the solvent, polyethylene glycol (PEG-400), acts as a reductant, reducing Pd(II) to Pd(0). Furthermore, the latter Suzuki protocol was also used for the introduction of the 4-fluorophenyl group in the 3-position of the flavone **49**, giving **56** in 17% (Table 5, Entry 7). Next, the 4-fluorophenyl moiety was introduced in the 3-position of the 3-iodo-2-pyridylchromone derivatives **52** and **54**. Accordingly, the Suzuki reactions were performed in the presence of 4-fluoroboronic acid, palladium(II)acetate and K₂CO₃ in PEG-400 using microwave heating at 60 °C for 90 min, affording **57** and **58** in 47 and 62% yield, respectively (Table 5, Entries 8-9). In addition, the same protocol was also used for the introduction of the 4-fluorophenyl group in the 3-position of the 3-bromo-2-pyridylchromone derivative **53**, which gave **58** in 59% yield (Table 5, Entry 10).

Table 5. Screening for viable Suzuki cross-coupling conditions for the introduction of aryl groups in the 3-position of the chromone ring system.



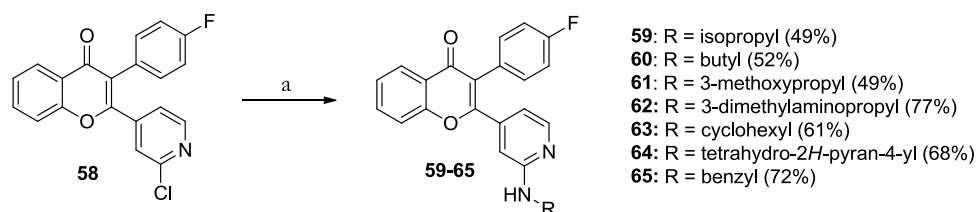
Entry	R	X	Y	Z	Catalyst	Base	Solvent	Temp. (°C) conditions	Reaction time (min)	Yield (%) ^a
1	H	CH	Br	H	Pd(OAc) ₂ (PPh ₃) ₂	K ₂ CO ₃	CH ₂ Cl ₂	reflux	overnight	n.r. ^b
2	H	CH	Br	H	Pd(OAc) ₂ (PPh ₃) ₂	K ₂ CO ₃	Dichloroethane	reflux	24 h	n.r. ^b
3	H	CH	Br	H	Pd(PPh ₃) ₄	K ₂ CO ₃	DMF/H ₂ O (9:1)	100	overnight	n.r. ^b
4	H	CH	Br	H	Pd/C (10%)	Na ₂ CO ₃	DME/H ₂ O (1:1)	80	overnight	n.r. ^b
5	H	CH	Br	H	Pd(OAc) ₂ ^c	K ₂ CO ₃	PEG-400	45	24 h	65
6	H	CH	Br	H	Pd(OAc) ₂ ^c	K ₂ CO ₃	PEG-400	60, mw ^d	30	84
7	H	CH	Br	F	Pd(OAc) ₂ ^c	K ₂ CO ₃	PEG-400	60, mw ^d	30	17
8	H	N	I	F	Pd(OAc) ₂ ^c	K ₂ CO ₃	PEG-400	60, mw ^d	90	47
9	Cl	N	I	F	Pd(OAc) ₂ ^c	K ₂ CO ₃	PEG-400	60, mw ^d	90	62
10	Cl	N	Br	F	Pd(OAc) ₂ ^e	K ₂ CO ₃	PEG-400	60, mw ^d	90	59

^aIsolated yields. ^bn.r. = No reaction, according to ¹H NMR or TLC analysis of the crude reaction mixture.

^c0.1 equiv. ^dmw = microwave heating. ^e0.3 equiv.

5.2.3.4 Introduction of amines via the Buchwald-Hartwig reaction

The final compounds **59-65** were obtained from the pyridyl chloride **58** using microwave assisted Buchwald-Hartwig amination in the presence of various primary amines (Scheme 10). Compound **59** was generated in 49% yield using isopropylamine, palladium(II) acetate, sodium *tert*-butoxide, and 2-(dicyclohexylphosphino)biphenyl in toluene at 130 °C for 90 min.²⁴³ However, for the introduction of other amines, a more efficient bidentate ligand was required and compounds **60-65** could be obtained in 49-77% yield using microwave heating in the presence of the appropriate amine, palladium(II)acetate, sodium *tert*-butoxide, and 1,3-bis(diphenylphosphino)propane in toluene at 130 °C for 90 min.²⁴⁴



Scheme 10. Synthesis of the final compounds **59-65** via Buchwald-Hartwig amination. Reagents and conditions: a) R-NH₂, NaO*t*-Bu, Pd(OAc)₂, 2-(dicyclohexylphosphino)biphenyl or 1,3-bis(diphenylphosphino)propane, toluene, 130 °C, 90 min, microwave heating.

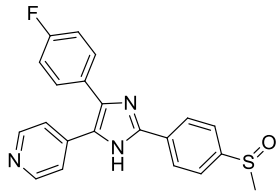
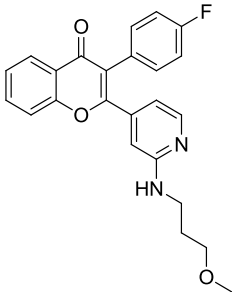
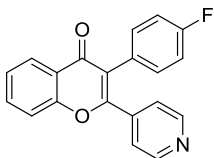
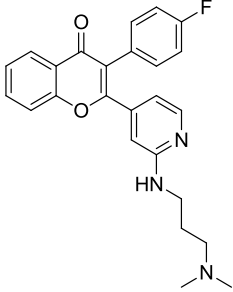
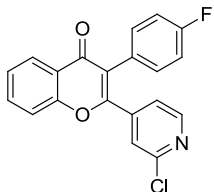
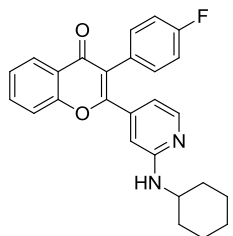
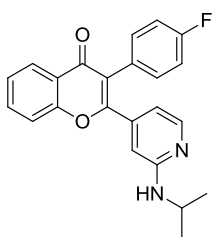
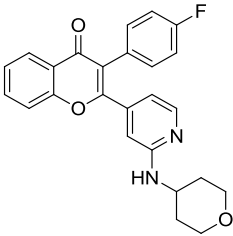
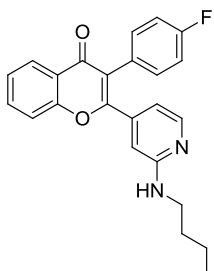
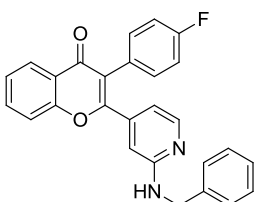
5.2.4 Biological evaluation of compounds **57-65** toward p38 α

Compounds **57-65** were evaluated using a commercial radiometric p38 α assay performed by Millipore KinaseProfiler™ service.²⁴⁵ It should be noted that a fluorescent-based assay could not be used since the compounds themselves exhibit fluorescent properties. As depicted in Table 6, all of the tested compounds **57-65** showed inhibitory activity toward the p38 α kinase and the IC₅₀ values were compared to the known p38 α inhibitor SB203580 (IC₅₀ 84 nM). Satisfyingly, the highest inhibitory activity in the series was observed for the isopropylamino derivative **59** (IC₅₀ 17 nM). The analogs **60-61** and **63-65** showed similar inhibitory potency (IC₅₀ 21-45 nM) indicating that p38 α is relatively flexible and can accept different amino groups in the 2-position of the pyridyl moiety. However, the 3-(dimethylamino)propylamino derivative **62** displayed a decreased activity (IC₅₀ 761 nM), which could imply that a polar group or a distal positive charge (at physiological pH) is disadvantageous for the activity. Furthermore, differences in the activity between **57** and **58** (IC₅₀ 813 and 1380, respectively) apparently originate from the electron withdrawing properties of the chlorine atom in **58**. Hence, the adjacent pyridine nitrogen becomes a less effective hydrogen bond acceptor resulting in a weaker interaction with the hinge area in the ATP-binding site of p38 α .

5.2.5 Kinase selectivity screening of **59** and **63**

Two of the inhibitors, **59** and **63**, were evaluated in a selectivity screen with a panel of 54 kinases chosen to represent the human kinome and eight kinases closely related to p38 α (Paper III, Supporting information).²⁴⁵ The study revealed an excellent selectivity profile for the p38 α and p38 β isoforms, with the exception for an observed activity against the JNK2 and JNK3 kinases (58 and 21% remaining activity, respectively for compound **59**). However, this kind of cross-reactivity, in particular with JNK3, has been reported earlier for chromone-based p38 α inhibitors.²⁴⁶ In addition, the observed selectivity for p38 α and p38 β over the closely related p38 γ and p38 δ isoforms was expected due to the nature of different gatekeeper residues in the selectivity pocket in the ATP-binding site (threonine in p38 α and p38 β , methionine in p38 γ and p38 δ).^{164, 198}

Table 6. Biological activity of **SB203580** and **57-65** against the p38 α MAP kinase.

Compound	Structure	IC ₅₀ (nM) p38 α	Compound	Structure	IC ₅₀ (nM) p38 α
SB203580		84	61		39
57		813	62		761
58		1380	63		34
59		17	64		45
60		21	65		35

Based on the results from the selectivity screen, the inhibitory activity for compounds **59** and **63** were also established toward p38 β (IC₅₀ 36 and 154 nM, respectively) and JNK3 (IC₅₀ 505 and 394, respectively).²⁴⁵ Interestingly, the difference in activity between **59** and **63** against p38 β suggests that the β -isoform, unlike p38 α , is sensitive to size modifications (isopropylamino vs. cyclohexylamino) in the 2-position of the pyridyl moiety. The lower activity toward JNK3 can also be explained, as stated earlier, by the nature of the gatekeeper residue. As for p38 γ and p38 δ , the JNK family possesses a methionine gatekeeper residue that blocks the entrance to the selectivity pocket (hydrophobic pocket I, Figure 31A).¹⁹⁸

5.2.6 Studies on the effect of p38 kinase signaling in human breast cancer cells

The p38 kinases are highly expressed in severe breast cancers and studies have shown that inhibition of the p38 kinases suppresses the proliferation of human breast cancer cells.¹⁹² Thus, the efficiency of compound **63** was evaluate in a cell-based assay with human derived MCF-7 breast cancer cells.²⁴⁷ The study showed that anisomycin-induced activation of p38 signaling, as shown for the p38 phosphorylation targets: activating transcription factor 2 (ATF2) and heat shock protein 27 (HSP27), was inhibited by doses as low as 0.5 μ M, and maximal inhibition was observed at 10 μ M (Figure 36). Interestingly, **63** also inhibits phosphorylation of p38 itself, which occurs without affecting the total levels of the enzyme, ruling out an effect on protein stability of the inhibitor as the mechanism.

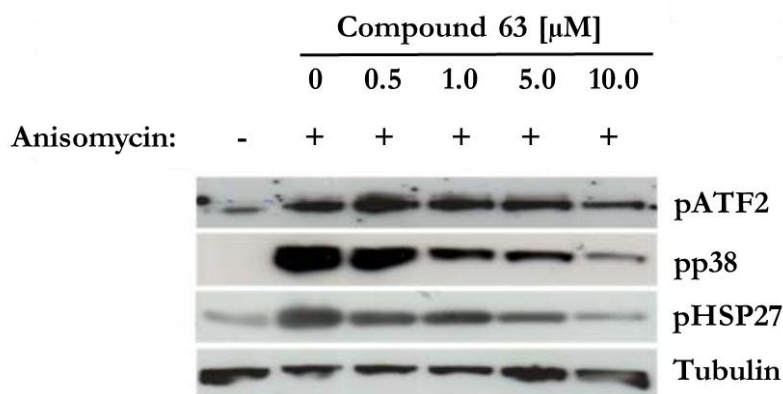


Figure 36. Compound **63** inhibits p38 kinase activation and signaling in human MCF-7 breast cancer cells. MCF-7 cells were preincubated with the indicated doses of **63** for 30 min and subsequently exposed to 10 μ g/mL anisomycin for another 30 min. Total cell lysates were resolved by SDS-PAGE and membranes were probed with antibodies directed against phosphorylated ATF2, p38, and HSP27. Tubulin was used as a loading control.

An additional experiment showed that phosphorylation of MKK3 and MKK6, the upstream activators of p38, was unaffected by **63** (Figure 37). Thus, the loss of p38 phosphorylation, induced by **63**, does not appear to result from the inhibition of upstream signaling. Furthermore, **59** and **63** did not significantly affect the proliferation of MCF-7 or MDA-MB436 cells, neither of the compounds enhanced sensitivity to anisomycin or doxorubicin in MCF-7 cells (Paper III, Supporting information). However,

both **59** and **63** appeared to suppress the sensitivity of MDA-MB436 cells, harboring a p53-mutation, to doxorubicin. This observation was unexpected since p38 kinase activity has previously been shown to suppress sensitivity to genotoxic agents in p53 negative cells.²⁴⁸

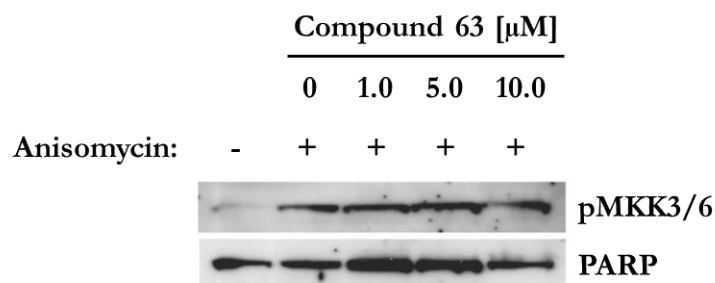


Figure 37. Phosphorylation of the MAP kinase kinase MKK3/6 is unaffected by **63**. MCF-7 breast cancer cells were preincubated with the indicated concentrations of **63** for 30 min and subsequently exposed to 10 μ g/mL anisomycin for another 30 min. Total cell lysates were resolved by SDS-PAGE and membranes were probed with antibodies directed against phospho-MKK3/6 (Ser189/207). Antibodies directed against poly (ADP-ribose) polymerase (PARP) were used as a loading control.

5.3 DEVELOPMENT OF ALLOSTERIC MEK1 MODULATORS (Paper IV)

The objective of this study was to design and synthesize chromone-based allosteric MEK1 modulators. Thus, we wanted to use PD98059 (Figure 32) as a starting point since it is a well-known allosteric chromone-based MEK1/2 modulator (MEK1 IC₅₀ 10 μ M).^{204, 249-251} Several studies of PD98059 reveal a high selectivity profile against the MEK1/2 kinases, *in vitro* and *in vivo*, along with cytotoxic effects toward several different cancer cell lines including leukemic and breast cancer cells.^{252, 253} Furthermore, docetaxel-induced apoptosis of androgen-independent prostate cancer cells have shown to be greatly enhanced by its combination with PD98059.²⁵⁴ Despite numerous reports of PD98059 as a selective MEK1/2 inhibitor and its use as a chemotherapeutic agent against different types of cancers, there are few reports on PD98059 analogues and the structure-activity relationship toward MEK1/2.^{210, 211} Therefore, we wanted to use molecular docking in order to identify potential structural modifications of the PD98059 structure that would result in optimized and highly potent allosteric MEK1 modulators.

5.3.1 Docking studies into the allosteric pocket of MEK1

The docking study was performed using the Schrödinger Package, MAESTRO interface.¹⁴⁴ The structure of MEK1 bound to ATPMg in complex with the allosteric modulator PD0325901 (Figure 32) (PDB 1S9J) was used for the study.^{145, 255} The MEK1 structure, PD0325901, PD98059 and various chromone derivatives were prepared and energy minimized using ligand preparation. Molecular docking was performed using GLIDE with extra precision (XP) settings and standard parameters for ligand docking.

Figure 38 shows selected examples of molecules docked into the allosteric site of MEK1. For example, PD0325901 binds into the hydrophobic allosteric pocket of MEK1 (Figure 38A) via one hydrogen bond between the hydroxamic acid oxygen and the side chain of Lys97 (2.14 Å, O...H-N, 144°). Additionally, the dihydroxypropoxy moiety utilizes a hydrophobic cavity that links the allosteric pocket and the ATP-binding site. Thus, the diol fragment forms two hydrogen bonds with the triphosphate group in ATP, one between the primary alcohol and the α -phosphate group (1.84 Å, O-H...O-P, 112°) and one between the secondary alcohol and the γ -phosphate (1.97 Å, O-H...O-P, 103°). Furthermore, the study suggested that PD98059 (Figure 38B) forms two hydrogen bonds with the protein backbone; one between the chromone carbonyl oxygen and NH of Ser212 in the activation loop (2.16 Å, C=O...H-N, 165°) and one between the aniline NH₂ and the carbonyl oxygen of Phe209 (1.99 Å, N-H...O=C, 172°). Additionally, PD98059 does not utilize the hydrophobic tunnel that links to the ATP-binding site (Figure 38B), as shown for PD0325901 (Figure 38A). Nevertheless, the docking study suggested that substituents in the 8-position on the chromone structure could preferably extend toward the ATP-binding site. For example, introduction of an aminopropyl group in the 8-position (e.g. via Pd-mediated cross coupling of a halogenated chromone derivative with an allylamine) could tentatively reach down to the ATP-binding site. According to the docking model the terminal positively charged amino functionality could bind to the γ -phosphate group in ATP (2.07 Å, N-H...O-P, 142°) (Figure 38C). The study also indicated that the amino group could interact via an additional hydrogen bond to the side chain of Asp190 (1.79, N-H...O=C, 162°). Based on these observations, we wanted to explore the use of 3'-bromo-5'-chloro-2'-hydroxyacetophenone as a starting material for the synthesis of 8-substituted PD98059 analogues, due to its commercial availability and low price in comparison with 3'-halogenated 2'-hydroxyacetophenones. However, this must require that a chlorine atom in the 6-position of the chromone structure does not affect the activity or the binding negatively. The chlorine atom in the 6-position, as in **81** or **85**, did not seem to affect the docking or binding mode into the allosteric pocket (Figure 38C). In fact, the chlorine atom could possibly act as a handle (e.g. Pd-mediated coupling reactions) for further modifications since the allosteric pocket extends in the corresponding direction. We also observed that the methoxy group in the 3'-position of PD98059 could be replaced with an ethoxy group, which could utilize the area more efficiently (**80**, Figure 38D). Based on the modeling study we decided to synthesize a few PD98059 analogs and evaluate their biological activity toward MEK1.

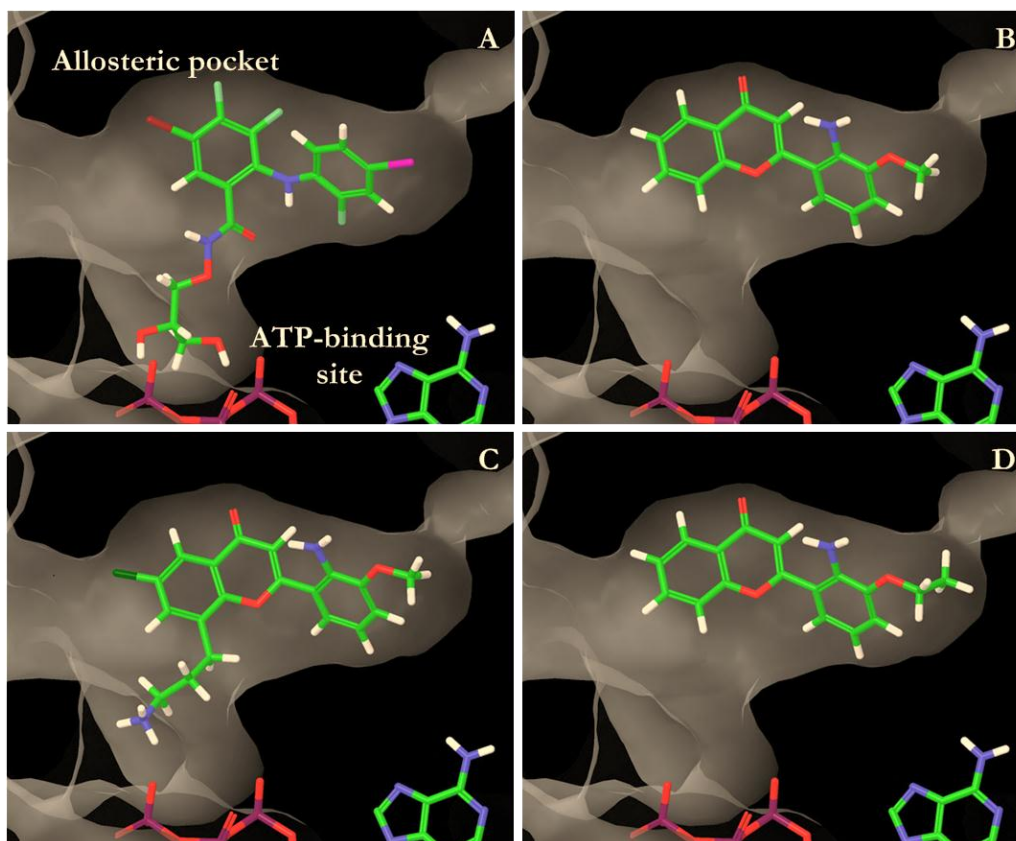


Figure 38. Docking of PD0325901 (A), PD98059 (B) **85** (C) and **80** (D) into the allosteric pocket of MEK1. The adjacent ATP-binding site is located below the allosteric pocket in the figure, thus a part of the ATP molecule can be depicted at the bottom of the panels.

5.3.2 Synthesis of PD98059 analogs

The two-step synthesis of PD98059, 2'-amino-3'-methoxyflavone (Figure 32) has previously been reported starting from 2-pivaloylamino-3-methoxyacetophenone and methyl 2-[(*tert*-butyl-dimethylsilyl)oxy]-benzoate (Figure 39).²⁵⁶ Interestingly, this procedure is, to our knowledge, the only available synthetic protocol for PD98059. However, we wanted to use the same synthetic route as we used for the synthesis of the chromone-based p38 α inhibitors, i.e. via the Baker-Venkataraman rearrangement, starting from 2'-hydroxyacetophenones (Section 5.2.3).

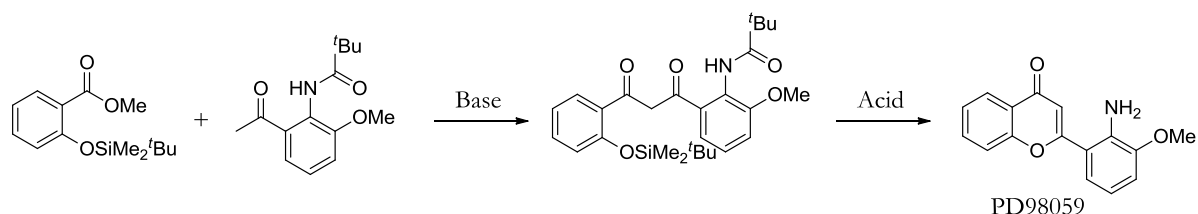
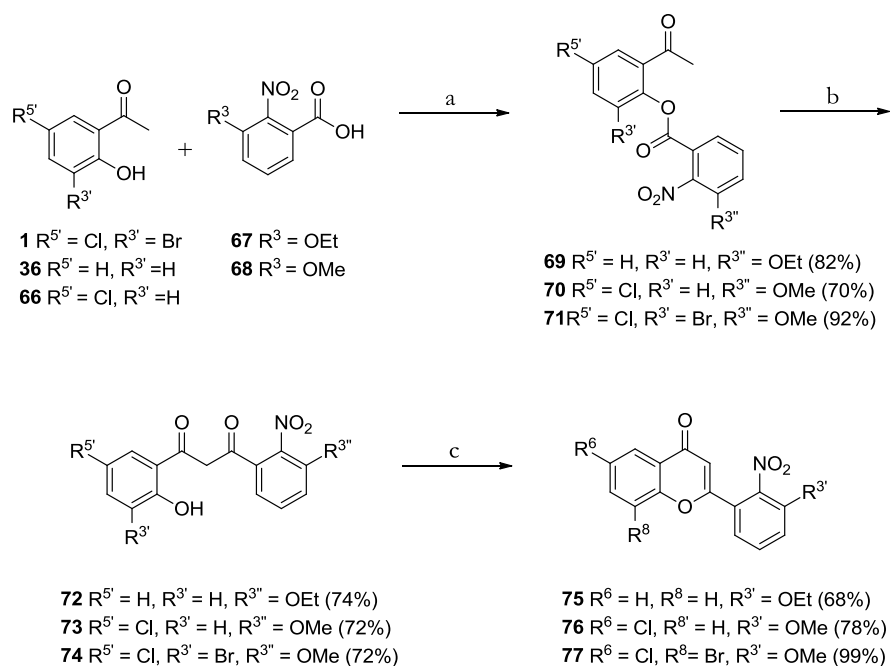


Figure 39. Synthetic protocol of PD98059 from the literature via base-promoted condensation (LiHMDS, THF, -78 °C \rightarrow rt, 43 h) of 2-pivaloylamino-3-methoxyacetophenone and methyl 2-[(*tert*-butyl-dimethylsilyl)oxy]benzoate followed by acid-catalyzed cyclization (H₂SO₄, acetic acid, 100 °C, 3 h).²⁵⁶

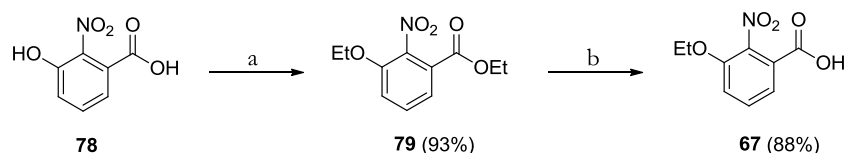
5.3.2.1 Synthesis of flavones 75-77

Esters **69-71** were successfully obtained in 70-92% yield from 2'-hydroxyacetophenones (**1**, **36** or **66**) and the appropriate acid chlorides, which were prepared in situ from the corresponding carboxylic acids, **67-68**, using oxalyl chloride or thionyl chloride as chlorinating agents (Scheme 11).^{218, 257} The 2-nitrobenzoic acids **67-68** were used with the aim to later convert the nitro group to the corresponding amine under reductive reaction conditions.



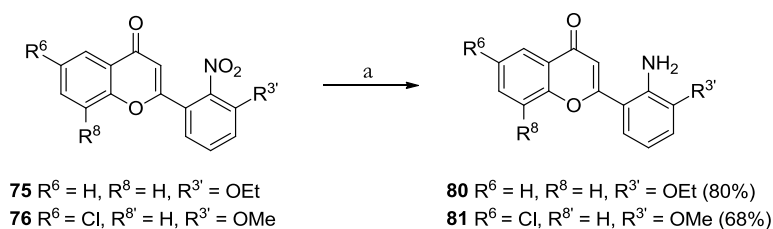
Scheme 11. Synthesis of flavones **75-77**. Reagents and conditions: (a) (i) oxalyl chloride, DMF, dichloromethane, rt, 2 h or SOCl₂, toluene, reflux, 20 h; (ii) pyridine, 0 °C → rt, 1-2.5 h. (b) KOH, pyridine, 50 °C, 30 min, conventional heating or 100 °C, 30 min, microwave heating. (c) H₂SO₄, acetic acid, reflux, 45 min or H₂SO₄, EtOH, 100 °C, 30 min, microwave heating.

Notably, one of the carboxylic acids **67** was synthesized, in two steps from 3-hydroxy-2-nitrobenzoic acid **78** (Scheme 12). Accordingly, **78** was *O*-alkylated to give **79** in 93% yield using ethyl iodide and K₂CO₃ in DMF.²⁵⁸ Thereafter, the simultaneously generated ethyl ester was hydrolyzed using 0.1 M NaOH in order to provide **67** in 88% yield. Base-promoted rearrangement of **69-71** to obtain diketones **72-74** was carried out in pyridine using conventional heating at 50 °C or microwave heating at 100 °C for 30 min (Scheme 11).^{90, 99} Subsequently, acid-promoted cyclization gave the flavones **75-77** in high yields (68-99%).



Scheme 12. Synthesis of 3-ethoxy-2-nitrobenzoic acid **67**. Reagents and conditions: (a) ethyl iodide, K_2CO_3 , DMF, $60\text{ }^\circ\text{C}$, 2 h. (b) 0.1 M NaOH, reflux, 1 h.

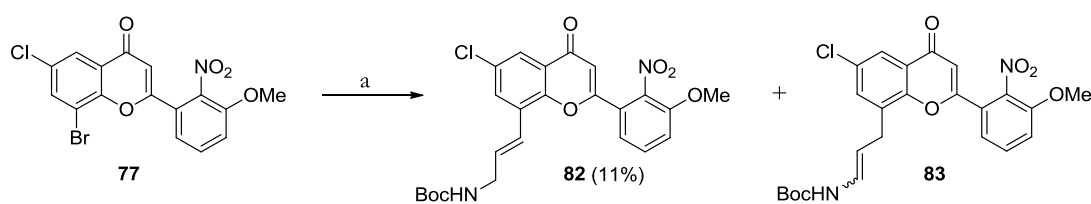
The nitro functionality in **75-76** was successfully converted to the corresponding amine under acidic conditions using tin as a reducing agent in ethanol to afford **80-81** in 80% and 68% yield, respectively (Scheme 13).³⁶



Scheme 13. Reduction of the nitro functionality in **75-76**. Reagents and conditions: (a) Sn powder, conc. HCl, EtOH, reflux, 1 h.

5.3.2.2 Synthesis of **85** via the Heck reaction

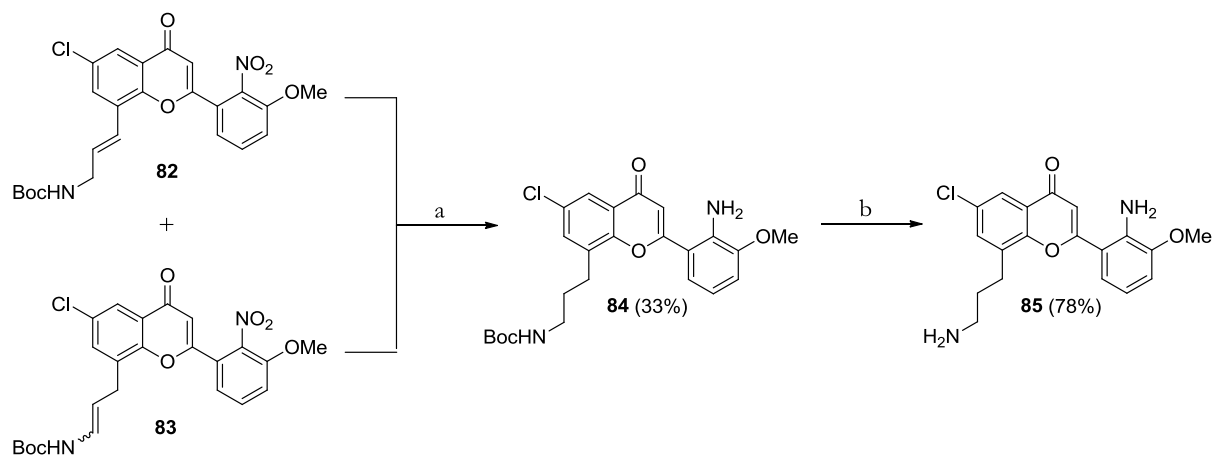
Regioselective introduction of *N*-Boc-protected allylamine in the 8-position of the dihalogenated flavone **77** was achieved using the Heck reaction under inert conditions (Scheme 14). Compound **77** was treated with *N*-Boc-allylamine, $\text{PdCl}_2[\text{P}(o\text{-Tol})_3]_2$ and triethylamine in acetonitrile at $75\text{ }^\circ\text{C}$ overnight to give the pure product **82** in low yield (11%).²⁵⁹ In addition, fractions of a mixture of the target compound **82** and the enamine product **83**, as a mixture of *E/Z* isomers (1:1), was obtained in 34% yield.



Scheme 14. Introduction of *N*-Boc-protected allylamine in the 8-position via the Heck reaction. Reagents and conditions: (a) *N*-Boc-allylamine, $\text{PdCl}_2[\text{P}(o\text{-Tol})_3]_2$, Et_3N , acetonitrile, $75\text{ }^\circ\text{C}$, overnight.

Reduction of the nitro group to the corresponding amine and reduction of the olefin in a mixture of **82** and **83** was performed simultaneously by catalytic hydrogenation over Pd/C (10%) using an H-Cube® Continuous-flow Hydrogenation Reactor (Scheme 15). The product **84** was obtained in low yields (33%), which could be explained by the observation of the formation of at least two byproducts; dehalogenated product together with a product where the olefin had been reduced but not the nitro group. Subsequent

acid-promoted deprotection of the Boc-group in **84** using TFA in dichloromethane gave the target compound **85** in 78%.



Scheme 15. Synthesis of the target compound **85**. Reagents and conditions: (a) H₂ (H-cube®), Pd/C (10%), THF, 20 °C, 30 bar. (b) trifluoroacetic acid, dichloromethane, room temperature, overnight.

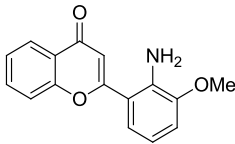
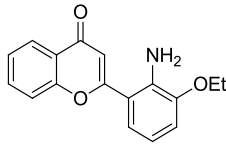
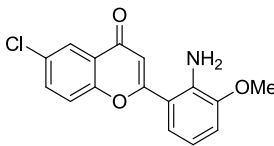
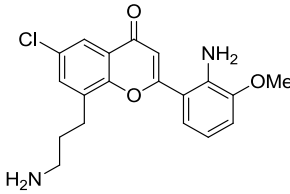
5.3.3 Biological evaluation of compounds **80**, **81** and **85** as MEK1 modulators

The enzymatic activity of MEK1 in the presence of **80**, **81**, or **85**, was evaluated by measuring its ability to increase myelin basic protein (MBP) kinase activity of ERK2 *in vitro*. The study was performed by co-workers at Université de Montréal, Canada. The results show that the synthesized compounds **80**, **81** and **85** inhibit Raf-1 induced activation of MEK1 with similar activities (IC₅₀ 1.9-6.4 μM) as for PD98059 (IC₅₀ 10 μM),²⁰⁴ with the highest activity for **80** (IC₅₀ 1.9 μM) (Table 7). Interestingly, the replacement of the methoxy group in the 3'-position (PD98059) on the chromone structure for an ethoxy group, as in **80**, gave a five-fold increase of the activity (IC₅₀ 10.0 vs. 1.9 μM). Furthermore, introduction of a propylamine in the 8-position, as in **85**, did not increase the activity as much as anticipated. However, going back to the modeling study, this could be explained by the positioning of the carbonyl and aniline amine of **85** in the allosteric pocket. The structure is placed somewhat further down towards the ATP-binding site, which prevents the interaction between the chromone carbonyl and Ser212. According to this observation, it would be interesting to extend the propyl chain in the 8-position by one carbon, to a butylamine. This strategy could possibly give interactions between the amino group to ATP and Asp190 at the same time as the distance between the chromone carbonyl and Ser212 would be optimized for hydrogen bonding. Although **81** showed the lowest activity of the three synthesized compounds (IC₅₀ 6.4 μM), it seems that the chloride in the 6-position does not affect the activity (PD98059 vs. **81**, IC₅₀ 10.0 and 6.4, respectively). However, in order to optimize the potency for a second generation of chromone-based MEK1 modulators it would be preferable without a substituent in the 6-position. Nevertheless, it does not necessarily exclude the use of 3'-bromo-5'-chloro-2'-hydroxyacetophenone as a starting material. The chloride could be removed under the

catalytic hydrogenation step in the synthesis, since the dehalogenated derivative was observed as a byproduct in that particular step during the synthesis.

Preliminary in vivo experiments (not shown) with **80** in IEC-6 and NIH 3T3-cells (rat epithelial and mouse fibroblasts cell lines, respectively) showed reduced phosphorylation of ERK1/ERK2, as monitored with phospho-specific antibody to the activation loop of ERK1/2. Interestingly, the results also demonstrated that **80** displays a slightly less active profile in comparison with the nanomolar modulator CI-1040 (PD184352) (Figure 32).

Table 7. In vitro activity of PD98059,²⁰⁴ **80**, **81** and **85** toward MEK1.

Compound	Structure	IC ₅₀ (μM) MEK1
PD98059		10.0
80		1.9
81		6.4
85		3.6

5.4 CONCLUSIONS

In summary, this chapter describes the design and synthesis of chromone-based ATP-competitive p38α inhibitors and allosteric non-ATP-competitive MEK1 modulators. Molecular docking was used for the design in order to explore suitable substitution patterns on the chromone scaffold to obtain selective and highly active inhibitors or modulators against p38α and MEK1. The biological evaluation revealed that several of the synthesized p38α inhibitors exhibit a strong inhibitory activity toward the p38α MAP kinase (e.g., **59**, IC₅₀ 17 nM). Among them, **59** and **63** were shown to be selective inhibitors of the p38α and p38β isoforms, and it was also revealed that **63** inhibits p38

kinase signaling in human cancer cells. Furthermore, the synthesized allosteric MEK1 modulators showed moderate activities with IC_{50} values in the micromolar range (IC_{50} 1.9-6.4 μ M), which are comparable with the known allosteric MEK1 modulator PD98059 (IC_{50} 10 μ M). The modeling study suggested that substituents in the 8-position on the chromone structure could fit into a hydrophobic cavity in MEK1 that connects the allosteric pocket with the ATP-binding site. Moreover, an ethoxy group in the 3'-position could utilize the area in the allosteric pocket more efficiently than a methoxy group. However, more studies around the structure-activity relationship need to be done. This could e.g. include the synthesis of a second generation of chromone-based allosteric MEK1 modulators with various substituents in the 8-position. However, if this should be done we need to optimize the yields in some of the reaction steps.

6. Concluding Remarks and Future Perspectives

This thesis describes the usefulness of chalcone and chromone derivatives as valuable agents for various applications in the field of medicinal chemistry. The studies show that they are particularly useful as small molecular inhibitors targeting proteins associated with cancer pathogenesis and as fluorophores for live-cell imaging. Through efficient synthetic methods based on scaffold methodology we have prepared several series of differently functionalized chromone derivatives that can be modified to generate compounds that possess different biological activities. However, there are still interesting aspects to explore within the various projects described in this thesis, and some of these aspects are outlined below.

- Further studies of 3-hydroxychromones as potential fluorophores for live-cell imaging could involve covalent probing of biological active compounds such as proteins or small molecule inhibitors. The labeled conjugates could further be used as biological tools in fluorescent microscopy of living cells for the investigation of cellular pathways, uptake, and distribution. Moreover, tuning the fluorescence properties via structural modifications on the chromone scaffold could optimize the absorption and emission toward longer wavelengths, preferable for cell viability.
- In order to further establish the structure-activity relationship for chalcones and related dienones that interfere with tubulin assembly, larger series of structurally diverse derivatives needs to be synthesized. This could also include investigations around what kind of structural modifications that are responsible for the generation of stabilizing vs. destabilizing activities.
- Our development towards chromone-based kinase inhibitors/modulators could be extended with larger series of derivatives in order to understand the structure-activity relationship and to improve the inhibitory activities. However, extensive optimization of several reaction steps for the synthesis of the chromone-based MEK1 modulators needs to be done before such a study can begin. Future investigations could also involve attempts to develop isoform-specific p38 α or MEK1 inhibitors/modulators or the design of MEK1 inhibitors that utilize both the allosteric pocket and the ATP-binding site.

- Since this thesis present chromone derivatives with fluorescence or bioactive properties in would be interesting to combine these features. For example to design fluorescent chromone-based kinase inhibitors and follow their uptake and accumulation in living cells by using fluorescence microscopy. Such studies could provide valuable information of cancer-specific pathways in living organisms.

Acknowledgements

Ett stort tack till alla som har bidragit med ett eller annat (mycket eller litet) under mina fem år som doktorand på GU. Ett speciellt tack riktas till...

Docent **Morten Grøtli**, min handledare. Tack för din obotliga entusiasm och för att du har stått ut med min envishet och mina knasiga idéer.

Professor **Kristina Luthman**, min biträdande handledare. Inga ord kan beskriva hur tacksam jag är för all feedback jag har fått av dig under åren och för alla trevliga samtal vid dörröppningen till ditt kontor. Du är fantastisk!

Mina ambitiösa examensarbetare, **Linda Nilsson Möllers** och **Linda Karlsson Kjäll**. Tack för ert hårda slit med kromonerna och för alla roliga stunder (med barnslig humor) i labbet.

Alla medförfattare (organkemister, fysikalkemister, fysiker och biologer) för lysande samarbeten i spännande projekt. Främst tack till **Karl Börjesson**, **Marcus Wilhelmsson** och **Maria Smedh** som har upplyst mig i en djungel av fluorescence och cellulär imaging.

Mina kära kollegor i läkemedelsgruppen men även alla andra på våning 8 och 9. Främst tack till **KB** för sena kvällar, slitsamma NMR-labbar och trevliga stunder till skogs. **Maria** min kromonpartner och rumskamrat i vått och torrt. **Itedale**, ”Habba Habba”, lycka till med slutspurten. **Anna Said** (din galna skånska chalmerist) för att du orkar ta dig ner en trapp och förgylla både lunch och fikapausen. Dr **Peter** (”motorprinsen”) **Dinér** för alla pratstunder om kemi, kinaser och antirojalism samt den kontinuerliga uppdateringen av diverse skvaller. Dr **Thanos** (”Peanuts”) Galanis for crazy laughs including fireworks, talks about the karate guy and fishing competitions. **Carlos** för lysande syntesarbete i MEK-projektet. **Jonatan** för att du har orkat lyssna på mina rövarhistorier och för psykologiskt stöd inför avhandlingstryck, disputation och fest. Professor **Per-Ola Norrby** för din vilja att diskutera kemi, för trevligt sällskap i fikarummet och för att du gärna tar dig tid för feedback. Dr **Erik Wallén** och **Fariba Jam** som gjorde den första tiden i regniga Göteborg mer inbjudande för en förvirrad liten östgöte med hemlängtan.

Apotekarsocieteten och Göteborgs Universitet för finansiering av internationellt konferensdeltagande.

Min älskade lilla familj: **Gibson**, **Bäckis** och **Kisse**.

References and Notes

1. Di Carlo, G.; Mascolo, N.; Izzo, A. A.; Capasso, F., Flavonoids: Old and new aspects of a class of natural therapeutic drugs. *Life Sci.* **1999**, *65*, 337-353.
2. Rackova, L.; Firakova, S.; Kostalova, D.; Stefek, M.; Sturdik, E.; Majekova, M., Oxidation of liposomal membrane suppressed by flavonoids: Quantitative structure-activity relationship. *Bioorg. Med. Chem.* **2005**, *13*, 6477-6484.
3. Middleton, E.; Kandaswami, C.; Theoharides, T. C., The effects of plant flavonoids on mammalian cells: Implications for inflammation, heart disease, and cancer. *Pharmacol. Rev.* **2000**, *52*, 673-751.
4. Nijveldt, R. J.; van Nood, E.; van Hoorn, D. E. C.; Boelens, P. G.; van Norren, K.; van Leeuwen, P. A. M., Flavonoids: a review of probable mechanisms of action and potential applications. *Am. J. Clin. Nutr.* **2001**, *74*, 418-425.
5. Harborne, J. B.; Williams, C. A., Advances in flavonoid research since 1992. *Phytochemistry* **2000**, *55*, 481-504.
6. Torssell, K. B. G., *Natural Product Chemistry*. Apotekarsociteten-Swedish Pharmaceutical Society, Swedish Pharmaceutical Press: Stockholm, 1997.
7. Pick, A.; Muller, H.; Mayer, R.; Haenisch, B.; Pajeva, I. K.; Weigt, M.; Bonisch, H.; Muller, C. E.; Wiese, M., Structure-activity relationships of flavonoids as inhibitors of breast cancer resistance protein (BCRP). *Bioorg. Med. Chem.* **2011**, *19*, 2090-2102.
8. Amaral, S.; Mira, L.; Nogueira, J. M. F.; da Silva, A. P.; Florencio, M. H., Plant extracts with anti-inflammatory properties-A new approach for characterization of their bioactive compounds and establishment of structure-antioxidant activity relationships. *Bioorg. Med. Chem.* **2009**, *17*, 1876-1883.
9. Mastuda, H.; Morikawa, T.; Ueda, K.; Managi, H.; Yoshikawa, M., Structural requirements of flavonoids for inhibition of antigen-induced degranulation, TNF-alpha and IL-4 production from RBL-2H3 cells. *Bioorg. Med. Chem.* **2002**, *10*, 3123-3128.
10. Ferrali, M.; Donati, D.; Bambagioni, S.; Fontani, M.; Giorgi, G.; Pietrangelo, A., 3-hydroxy-(4H)-benzopyran-4-ones as potential iron chelating agents in vivo. *Bioorg. Med. Chem.* **2001**, *9*, 3041-3047.
11. Gong, J. X.; Huang, K. X.; Wang, F.; Yang, L. X.; Feng, Y. B.; Li, H. B.; Li, X. K.; Zeng, S.; Wu, X. M.; Stoeckigt, J.; Zhao, Y.; Qu, J., Preparation of two sets of 5,6,7-trioxygenated dihydroflavonol derivatives as free radical scavengers and neuronal cell protectors to oxidative damage. *Bioorg. Med. Chem.* **2009**, *17*, 3414-3425.
12. Burda, S.; Oleszek, W., Antioxidant and antiradical activities of flavonoids. *J. Agric. Food Chem.* **2001**, *49*, 2774-2779.
13. Ollis, W. D., Neoflavanoids a New Class of Natural Products. *Experientia* **1966**, *22*, 777-783.
14. Nowakowska, Z., A review of anti-infective and anti-inflammatory chalcones. *Eur. J. Med. Chem.* **2007**, *42*, 125-137.
15. Burlando, B.; Verotta, L.; Cornara, L.; Bottini-Massa, E., *Herbal Principles in Cosmetics: Properties and Mechanisms of Action* CRC Press, Taylor & Francis Group: Boca Raton, FL, USA, 2010.
16. Dimmock, J. R.; Elias, D. W.; Beazely, M. A.; Kandepu, N. M., Bioactivities of chalcones. *Curr. Med. Chem.* **1999**, *6*, 1125-1149.
17. Hadfield, J. A.; Ducki, S.; Hirst, N.; McGown, A. T., *Progress in Cell Cycle Research*. Editions Life in Progress: New York, 2003; Vol. 5, p 309-325.

18. Bandgar, B. P.; Gawande, S. S.; Bodade, R. G.; Totre, J. V.; Khobragade, C. N., Synthesis and biological evaluation of simple methoxylated chalcones as anticancer, anti-inflammatory and antioxidant agents. *Bioorg. Med. Chem.* **2010**, *18*, 1364-1370.
19. Patil, C. B.; Mahajan, S. K.; Katti, S. A., Chalcone: A Versatile Molecule. *J. Pharm. Sci. Res.* **2009**, *1*, 11-22.
20. Claisen, L.; Claparède, A., Condensationen von Ketonen mit Aldehyden. *Chem. Ber.* **1881**, *14*, 2460-2468.
21. Schmidt, J. G., Ueber die Einwirkung von Aceton auf Furfurol und auf Bittermandelöl bei Gegenwart von Alkalilauge. *Chem. Ber.* **1881**, *14*, 1459-1461.
22. Eddarir, S.; Cotelte, N.; Bakkour, Y.; Rolando, C., An efficient synthesis of chalcones based on the Suzuki reaction. *Tetrahedron Lett.* **2003**, *44*, 5359-5363.
23. Wu, X. F.; Neumann, H.; Spannenberg, A.; Schulz, T.; Jiao, H. J.; Beller, M., Development of a General Palladium-Catalyzed Carbonylative Heck Reaction of Aryl Halides. *J. Am. Chem. Soc.* **2010**, *132*, 14596-14602.
24. Joule, J. A.; Mills, K., *Heterocyclic Chemistry*. 5th ed.; Chichester, United Kingdom, 2010.
25. Horton, D. A.; Bourne, G. T.; Smythe, M. L., The combinatorial synthesis of bicyclic privileged structures or privileged substructures. *Chem. Rev.* **2003**, *103*, 893-930.
26. Evans, B. E.; Rittle, K. E.; Bock, M. G.; Dipardo, R. M.; Freidinger, R. M.; Whitter, W. L.; Lundell, G. F.; Veber, D. F.; Anderson, P. S.; Chang, R. S. L.; Lotti, V. J.; Cerino, D. J.; Chen, T. B.; Kling, P. J.; Kunkel, K. A.; Springer, J. P.; Hirshfield, J., Methods for Drug Discovery - Development of Potent, Selective, Orally Effective Cholecystokinin Antagonists. *J. Med. Chem.* **1988**, *31*, 2235-2246.
27. Bhatnagar, S.; Sahi, S.; Kackar, P.; Kaushik, S.; Dave, M. K.; Shukla, A.; Goel, A., Synthesis and docking studies on styryl chromones exhibiting cytotoxicity in human breast cancer cell line. *Bioorg. Med. Chem. Lett.* **2010**, *20*, 4945-4950.
28. Alves, C. N.; Pinheiro, J. C.; Camargo, A. J.; de Souza, A. J.; Carvalho, R. B.; da Silva, A. B. F., A quantum chemical and statistical study of flavonoid compounds with anti-HIV activity. *J. Mol. Struct. (Theochem)* **1999**, *491*, 123-131.
29. Ungwitayatorn, H.; Samee, W.; Pimthon, J., 3D-QSAR studies on chromone derivatives as HIV-1 protease inhibitors. *J. Mol. Struct.* **2004**, *689*, 99-106.
30. Göker, H.; Ozden, S.; Yildiz, S.; Boykin, D. W., Synthesis and potent antibacterial activity against MRSA of some novel 1,2-disubstituted-1H-benzimidazole-N-alkylated-5-carboxamides. *Eur. J. Med. Chem.* **2005**, *40*, 1062-1069.
31. Liu, G. B.; Xu, J. L.; Geng, M.; Xu, R.; Hui, R. R.; Zhao, J. W.; Xu, Q.; Xu, H. X.; Li, J. X., Synthesis of a novel series of diphenolic chromone derivatives as inhibitors of NO production in LPS-activated RAW264.7 macrophages. *Bioorg. Med. Chem.* **2010**, *18*, 2864-2871.
32. Parmar, V. S.; Bracke, M. E.; Philippe, J.; Wengel, J.; Jain, S. C.; Olsen, C. E.; Bisht, K. S.; Sharma, N. K.; Courtens, A.; Sharma, S. K.; Vennekens, K.; VanMarck, V.; Singh, S. K.; Kumar, N.; Kumar, A.; Malhotra, S.; Kumar, R.; Rajwanshi, V. K.; Jain, R.; Mareel, M. M., Anti-invasive activity of alkaloids and polyphenolics in vitro. *Bioorg. Med. Chem.* **1997**, *5*, 1609-1619.
33. Yu, D. L.; Chen, C. H.; Brossi, A.; Lee, K. H., Anti-AIDS agents. 60.(dagger) substituted 3' R,4' R-Di-O(-)-camphanoyl-2',2'-dimethyldihydropyrano[2,3-f]chromone (DCP) analogues as potent anti-HIV agents. *J. Med. Chem.* **2004**, *47*, 4072-4082.
34. Hutter, J. A.; Salman, M.; Stavinoha, W. B.; Satsangi, N.; Williams, R. F.; Streeper, R. T.; Weintraub, S. T., Antiinflammatory C-glucosyl chromone from *Aloe barbadensis*. *J. Nat. Prod.* **1996**, *59*, 541-543.
35. Ahn, Y. M.; Vogeti, L.; Liu, C. J.; Santhapuram, H. K. R.; White, J. M.; Vasandani, V.; Mitscher, L. A.; Lushington, G. H.; Hanson, P. R.; Powell, D. R.; Himes, R. H.; Roby, K. F.; Ye, Q. Z.;

- Georg, G. I., Design, synthesis, and antiproliferative and CDK2-cyclin A inhibitory activity of novel flavopiridol analogues. *Bioorg. Med. Chem.* **2007**, *15*, 702-713.
36. Kahnberg, P.; Lager, E.; Rosenberg, C.; Schougaard, J.; Camet, L.; Sterner, O.; Nielsen, E. O.; Nielsen, M.; Liljefors, T., Refinement and evaluation of a pharmacophore model for flavone derivatives binding to the benzodiazepine site of the GABA(A) receptor. *J. Med. Chem.* **2002**, *45*, 4188-4201.
 37. Niisato, N.; Nishino, H.; Nishio, K.; Marunaka, Y., Cross talk of cAMP and flavone in regulation of cystic fibrosis transmembrane conductance regulator (CFTR) Cl⁻ channel and Na⁺/K⁺/2Cl⁻ cotransporter in renal epithelial A6 cells. *Biochem. Pharmacol.* **2004**, *67*, 795-801.
 38. Edwards, A. M.; Howell, J. B. L., The chromones: history, chemistry and clinical development. A tribute to the work of Dr R. E. C. Altounyan. *Clin. Exp. Allergy* **2000**, *30*, 756-774.
 39. Nordlund, J. J., *The pigmentary system: physiology and pathophysiology* 2th ed.; Blackwell Publishing, Inc.: Malden, Massachusetts, USA, 2006.
 40. de Leeuw, J.; Assen, Y. J.; van der Beek, N.; Bjerring, P.; Neumann, H. A. M., Treatment of vitiligo with khellin liposomes, ultraviolet light and blister roof transplantation. *J. Eur. Acad. Dermatol. Venereol.* **2011**, *25*, 74-81.
 41. Holgate, S. T.; Polosao, R., Treatment strategies for allergy and asthma. *Nat. Rev. Immunol.* **2008**, *8*, 218-230.
 42. <http://www.fass.se>
 43. Frick, R. W., Three treatments for chronic venous insufficiency: Escin, hydroxyethylrutoside, and Daflon. *Angiology* **2000**, *51*, 197-205.
 44. Ruffmann, R., A Review of Flavoxate Hydrochloride in the Treatment of Urge Incontinence. *J. Int. Med. Res.* **1988**, *16*, 317-330.
 45. <http://www.drugs.com/pro/flavoxate.html>
 46. Klymchenko, A. S.; Shynkar, V. V.; Piemont, E.; Demchenko, A. P.; Mely, Y., Dynamics of intermolecular hydrogen bonds in the excited states of 4'-dialkylamino-3-hydroxyflavones. On the pathway to an ideal fluorescent hydrogen bonding sensor. *J. Phys. Chem. A* **2004**, *108*, 8151-8159.
 47. Klymchenko, A. S.; Shvadchak, V. V.; Yushchenko, D. A.; Jain, N.; Mely, Y., Excited-state intramolecular proton transfer distinguishes microenvironments in single- and double-stranded DNA. *J. Phys. Chem. B* **2008**, *112*, 12050-12055.
 48. Wang, J.; Yi, X. Y.; Wang, B. D.; Yang, Z. Y., DNA-binding properties studies and spectra of a novel fluorescent Zn(II) complex with a new chromone derivative. *J. Photochem. Photobiol., A* **2009**, *201*, 183-190.
 49. Torkin, R.; Lavoie, J. F.; Kaplan, D. R.; Yeger, H., Induction of caspase-dependent, p53-mediated apoptosis by apigenin in human neuroblastoma. *Mol. Cancer Ther.* **2005**, *4*, 1-11.
 50. Baker, W., Molecular Rearrangement of some o-Acyloxyacetophenones and the mechanism of the Production of 3-Acylchromones. *J. Chem. Soc.* **1933**, 1381-1389.
 51. Baker, W., Attempts to synthesise 5 : 6-dihydroxyflavone (primetin). *J. Chem. Soc.* **1934**, 1953-1954.
 52. Mahal, H. S.; Venkataraman, K., Synthetical Experiments in the Chromone Group. Part XIV. The Action of Sodamide on 1-Acyloxy-2-acetophenones. *J. Chem. Soc.* **1934**, 1767-1769.
 53. Bhalla, D. C.; Mahal, H. S.; Venkataraman, K., Synthetical experiments in the chromone group. Part XVII. Further observations on the action of sodamide on o-acyloxyacetophenones. *J. Chem. Soc.* **1935**, 868-870.
 54. Algar, J.; Flynn, J. P. *Proc. R. Ir. Acad.* **1934**, *42B*, 1-8.
 55. Oyamada, B. *J. Chem. Soc. Japan* **1934**, *55*, 1256.
 56. Zhou, C. X.; Dubrovsky, A. V.; Larock, R. C., Diversity-oriented synthesis of 3-iodochromones and heteroatom analogues via ICl-induced cyclization. *J. Org. Chem.* **2006**, *71*, 1626-1632.

57. Torii, S.; Okumoto, H.; Xu, L. H.; Sadakane, M.; Shostakovskiy, M. V.; Ponomaryov, A. B.; Kalinin, V. N., Syntheses of Chromones and Quinolones Via Pd-Catalyzed Carbonylation of O-Iodophenols and Anilines in the Presence of Acetylenes. *Tetrahedron* **1993**, *49*, 6773-6784.
58. Hartwig, J. F., *Organotransition Metal Chemistry: From Bonding to Catalysis*. University Science Books: Sausalito, CA, 2010.
59. Clayden, J.; Greeves, N.; Warren, S.; Wothers, P., *Organic Chemistry*. Oxford University Press: New York, 2001.
60. Nicolaou, K. C.; Bulger, P. G.; Sarlah, D., Palladium-catalyzed cross-coupling reactions in total synthesis. *Angew. Chem., Int. Ed.* **2005**, *44*, 4442-4489.
61. <http://www.nobelprize.org/>
62. Heck, R. F., Arylation Methylation and Carboxyalkylation of Olefins by Group 8 Metal Derivatives. *J. Am. Chem. Soc.* **1968**, *90*, 5518-5526.
63. Mizoroki, T.; Mori, K.; Ozaki, A., Arylation of Olefin with Aryl Iodide Catalyzed by Palladium. *Bull. Chem. Soc. Jpn.* **1971**, *44*, 581.
64. Heck, R. F.; Nolley, J. P., Palladium-Catalyzed Vinylic Hydrogen Substitution Reactions with Aryl, Benzyl, and Styryl Halides. *J. Org. Chem.* **1972**, *37*, 2320-2322.
65. Dieck, H. A.; Heck, R. F., Organophosphinepalladium Complexes as Catalysts for Vinylic Hydrogen Substitution-Reactions. *J. Am. Chem. Soc.* **1974**, *96*, 1133-1136.
66. Höltle, H.-D.; Sippl, W.; Rognan, D.; Folkers, G., *Molecular Modeling, Basic Principles and Applications*. 2th ed.; WILEY-VCH Verlag GmbH & Co.: Weinheim, 2003.
67. Jhoti, H.; Leach, A. R., *Structure-Based Drug Discovery*. Springer: Berlin, 2007.
68. Nadendla, R. R., Molecular modeling: A powerful tool for drug design and molecular docking. *Resonance* **2004**, *9*, 51-60.
69. Osman, G., *Pharmacophore Perception, Development and Use in Drug Design*. International University Line: La Jolla, CA, 2000.
70. Lakowicz, J. R., *Principles of Fluorescence Spectroscopy*. 3th edition ed.; Springer Science and Business Media, LLC: Baltimore, 2006.
71. Atkins, P.; de Paula, J., *Physical chemistry*. 7th ed.; Oxford University Press Inc.: New York, 2002.
72. Haugland, R. P., *The handbook. A guide to fluorescent probes and labeling technologies*. Invitrogen corp.: USA, 2005.
73. Weber, G.; Teale, F. W. J., Determination of the Absolute Quantum Yield of Fluorescent Solutions. *Trans. Faraday Soc.* **1957**, *53*, 646-655.
74. Melhuish, W. H., Quantum Efficiencies of Fluorescence of Organic Substances - Effect of Solvent and Concentration of Fluorescent Solute. *J. Phys. Chem.* **1961**, *65*, 229-235.
75. Diaspro, A.; Chirico, G.; Collini, M., Two-photon fluorescence excitation and related techniques in biological microscopy. *Q. Rev. Biophys.* **2005**, *38*, 97-166.
76. Sengupta, P. K.; Kasha, M., Excited-State Proton-Transfer Spectroscopy of 3-Hydroxyflavone and Quercetin. *Chem. Phys. Lett.* **1979**, *68*, 382-385.
77. Itoh, M.; Tanimoto, Y.; Tokumura, K., Transient Absorption Study of the Intramolecular Excited-State and Ground-State Proton-Transfer in 3-Hydroxyflavone and 3-Hydroxychromone. *J. Am. Chem. Soc.* **1983**, *105*, 3339-3340.
78. Itoh, M.; Fujiwara, Y.; Sumitani, M.; Yoshihara, K., Mechanism of Intramolecular Excited-State Proton-Transfer and Relaxation Processes in the Ground and Excited-States of 3-Hydroxyflavone and Related-Compounds. *J. Phys. Chem.* **1986**, *90*, 5672-5678.
79. Enander, K.; Choulier, L.; Olsson, A. L.; Yushchenko, D. A.; Kanmert, D.; Klymchenko, A. S.; Demchenko, A. P.; Mely, Y.; Altschuh, D., A peptide-based, ratiometric biosensor construct for direct fluorescence detection of a protein analyte. *Bioconjugate Chem.* **2008**, *19*, 1864-1870.
80. Shynkar, V. V.; Klymchenko, A. S.; Piemont, E.; Demchenko, A. P.; Mely, Y., Dynamics of intermolecular hydrogen bonds in the excited states of 4'-dialkylamino-3-hydroxyflavones. On

- the pathway to an ideal fluorescent hydrogen bonding sensor. *J. Phys. Chem. A* **2004**, *108*, 8151-8159.
81. Klymchenko, A. S.; Duportail, G.; Mely, Y.; Demchenko, A. P., Ultrasensitive two-color fluorescence probes for dipole potential in phospholipid membranes. *Proc. Natl. Acad. Sci. U. S. A.* **2003**, *100*, 11219-11224.
 82. Klymchenko, A. S.; Duportail, G.; Ozturk, T.; Pivovarenko, V. G.; Mely, Y.; Demchenko, A. P., Novel two-band ratiometric fluorescence probes with different location and orientation in phospholipid membranes. *Chem. Biol.* **2002**, *9*, 1199-1208.
 83. M'Baye, G.; Shynkar, V. V.; Klymchenko, A. S.; Mely, Y.; Duportail, G., Membrane dipole potential as measured by ratiometric 3-hydroxyflavone fluorescence probes: Accounting for hydration effects. *J. Fluoresc.* **2006**, *16*, 35-42.
 84. Duportail, G.; Klymchenko, A.; Mely, Y.; Demchenko, A., Neutral fluorescence probe with strong ratiometric response to surface charge of phospholipid membranes. *FEBS Lett.* **2001**, *508*, 196-200.
 85. Shynkar, V. V.; Klymchenko, A. S.; Duportail, G.; Demchenko, A. P.; Mely, Y., Two-color fluorescent probes for imaging the dipole potential of cell plasma membranes. *Biochimica et Biophysica Acta-Biomembranes* **2005**, *1712*, 128-136.
 86. Avilov, S. V.; Bode, C.; Tolgyesi, F. G.; Klymchenko, A. S.; Fidy, J.; Demchenko, A. R., Heat perturbation of bovine eye lens alpha-crystallin probed by covalently attached ratiometric fluorescent dye 4'-diethylamino-3-hydroxyflavone. *Biopolymers* **2005**, *78*, 340-348.
 87. Ercelen, S.; Klymchenko, A. S.; Demchenko, A. P., Novel two-color fluorescence probe with extreme specificity to bovine serum albumin. *FEBS Lett.* **2003**, *538*, 25-28.
 88. Shynkar, V. V.; Klymchenko, A. S.; Kunzelmann, C.; Duportail, G.; Muller, C. D.; Demchenko, A. P.; Freyssinet, J. M.; Mely, Y., Fluorescent biomembrane probe for ratiometric detection of apoptosis. *J. Am. Chem. Soc.* **2007**, *129*, 2187-2193.
 89. Chou, P. T.; Martinez, M. L.; Clements, J. H., Reversal of Excitation Behavior of Proton-Transfer Vs Charge-Transfer by Dielectric Perturbation of Electronic Manifolds. *J. Phys. Chem.* **1993**, *97*, 2618-2622.
 90. Dahlen, K.; Wallen, E. A. A.; Grotli, M.; Luthman, K., Synthesis of 2,3,6,8-tetrasubstituted chromone scaffolds. *J. Org. Chem.* **2006**, *71*, 6863-6871.
 91. Dahlén, K.; Grötli, M.; Luthman, K., A scaffold approach to 3,6,8-trisubstituted flavones. *Synlett* **2006**, *6*, 897-900.
 92. Desideri, N.; Conti, C.; Mastromarino, P.; Mastropaolo, F., Synthesis and anti-rhinovirus activity of 2-styrylchromones. *Antiviral Chem. Chemother.* **2000**, *11*, 373-381.
 93. Klymchenko, A. S.; Ozturk, T.; Demchenko, A. P., Synthesis of furanochromones: a new step in improvement of fluorescence properties. *Tetrahedron Lett.* **2002**, *43*, 7079-7082.
 94. It should be noted that the acetylation of **18** was successfully conducted from the crude starting material. However, the low yield presented in Scheme 2 refers to the yield over three steps, starting from compound **1** (Scheme 1).
 95. Sonogashira, K.; Tohda, Y.; Hagihara, N., Convenient Synthesis of Acetylenes - Catalytic Substitutions of Acetylenic Hydrogen with Bromoalkenes, Iodoarenes, and Bromopyridines. *Tetrahedron Lett.* **1975**, 4467-4470.
 96. Chinchilla, R.; Najera, C., The sonogashira reaction: A booming methodology in synthetic organic chemistry. *Chem. Rev.* **2007**, *107*, 874-922.
 97. Larhed, M.; Moberg, C.; Hallberg, A., Microwave-accelerated homogeneous catalysis in organic chemistry. *Acc. Chem. Res.* **2002**, *35*, 717-727.
 98. Kappe, C. O., Controlled microwave heating in modern organic synthesis. *Angew. Chem., Int. Ed.* **2004**, *43*, 6250-6284.

99. Dahlen, K.; Grotli, M.; Luthman, K., A scaffold approach to 3,6,8-trisubstituted flavones. *Synlett* **2006**, 897-900.
100. Wallen, E. A. A.; Dahlen, K.; Grotli, M.; Luthman, K., Synthesis of 3-aminomethyl-2-aryl-8-bromo-6-chlorochromones. *Org. Lett.* **2007**, *9*, 389-391.
101. Klymchenko, A. S.; Pivovarenko, V. G.; Ozturk, T.; Demchenko, A. P., Modulation of the solvent-dependent dual emission in 3-hydroxychromones by substituents. *New J. Chem.* **2003**, *27*, 1336-1343.
102. Davis, M. M.; Hetzer, H. B., Titrimetric and Equilibrium Studies Using Indicators Related to Nile Blue A. *Anal. Chem.* **1966**, *38*, 451-461.
103. Sackett, D. L.; Wolff, J., Nile Red as a Polarity-Sensitive Fluorescent-Probe of Hydrophobic Protein Surfaces. *Anal. Biochem.* **1987**, *167*, 228-234.
104. Klymchenko, A. S.; Mely, Y., 7-(2-methoxycarbonylvinyl)-3-hydroxychromones: new dyes with red shifted dual emission. *Tetrahedron Lett.* **2004**, *45*, 8391-8394.
105. Duportail, G.; Klymchenko, A.; Mely, Y.; Demchenko, A. P., On the coupling between surface charge and hydration in biomembranes: Experiments with 3-hydroxyflavone probes. *J. Fluoresc.* **2002**, *12*, 181-185.
106. Klymchenko, A. S.; Demchenko, A. P., 3-Hydroxychromone dyes exhibiting excited-state intramolecular proton transfer in water with efficient two-band fluorescence. *New J. Chem.* **2004**, *28*, 687-692.
107. Shynkar, V. V.; Klymchenko, A. S.; Duportail, G.; Demchenko, A. P.; Mely, Y., Ratiometric fluorescence measurements and imaging of the dipole potential in cell plasma membranes. *Biophotonics Micro-and Nano-Imaging* **2004**, *5462*, 118-130.
108. The optimal two-photon excitation (2PE) was measured for each compound prior to the live-cell imaging (Supporting information, Paper I, Figure S3).
109. Goldenthal, K. L.; Pastan, I.; Willingham, M. C., Initial Steps in Receptor-Mediated Endocytosis - the Influence of Temperature on the Shape and Distribution of Plasma-Membrane Clathrin-Coated Pits in Cultured Mammalian-Cells. *Exp. Cell Res.* **1984**, *152*, 558-564.
110. $1 \text{ GM} = 10^{50} \text{ cm}^4 \text{ s photon}^{-1} \text{ molecule}^{-1}$. For further information regarding the calculations, see paper I, supporting information.
111. Jordan, M. A.; Wilson, L., Microtubules as a target for anticancer drugs. *Nat. Rev. Cancer* **2004**, *4*, 253-265.
112. Kavallaris, M., Microtubules and resistance to tubulin-binding agents. *Nat. Rev. Cancer* **2010**, *10*, 194-204.
113. Mandelkow, E.; Mandelkow, E. M., Microtubule Structure. *Curr. Opin. Struct. Biol.* **1994**, *4*, 171-179.
114. Lowe, J.; Li, H.; Downing, K. H.; Nogales, E., Refined structure of alpha beta-tubulin at 3.5 Å resolution. *Journal of Molecular Biology* **2001**, *313*, 1045-1057.
115. Arnal, I.; Wade, R. H., How Does Taxol Stabilize Microtubules. *Curr. Biol.* **1995**, *5*, 900-908.
116. Pellegrini, F.; Budman, D. R., Review: Tubulin function, action of antitubulin drugs, and new drug development. *Cancer Invest.* **2005**, *23*, 264-273.
117. Kerr, D. J.; Hamel, E.; Jung, M. K.; Flynn, B. L., The concise synthesis of chalcone, indanone and indenone analogues of combretastatin A4. *Bioorg. Med. Chem.* **2007**, *15*, 3290-3298.
118. The illustration was made from three different X-ray structures (PDB: 1SA1, 1JFF, and 1Z2B).
119. Nicolaou, K. C.; Sorensen, E. J., *Classics in Total Synthesis: Targets, Strategies, Methods*. VCH Verlagsgesellschaft mbH: Weinheim, Germany, 1996.
120. Nicolaou, K. C.; Snyder, S. A., *Classics in Total Synthesis II. More targets, strategies, methods*. WILEY-VCH Verlag GmbH & Co. KGaA: Weinheim, Germany, 2003.
121. Edwards, M. L.; Stemerick, D. M.; Sunkara, P. S., Chalcones - a New Class of Antimitotic Agents. *J. Med. Chem.* **1990**, *33*, 1948-1954.

122. Ducki, S., Antimitotic Chalcones and Related Compounds as Inhibitors of Tubulin Assembly. *Anticancer Agents Med. Chem.* **2009**, *9*, 336-347.
123. Peyrot, V.; Leynadier, D.; Sarrazin, M.; Briand, C.; Rodriguez, A.; Nieto, J. M.; Andreu, J. M., Interaction of Tubulin and Cellular Microtubules with the New Antitumor Drug Mdl 27048 - a Powerful and Reversible Microtubule Inhibitor. *J. Biol. Chem.* **1989**, *264*, 21296-21301.
124. Peyrot, V.; Leynadier, D.; Sarrazin, M.; Briand, C.; Menendez, M.; Laynez, J.; Andreu, J. M., Mechanism of Binding of the New Antimitotic Drug Mdl-27048 to the Colchicine Site of Tubulin - Equilibrium Studies. *Biochemistry* **1992**, *31*, 11125-11132.
125. Ducki, S.; Rennison, D.; Woo, M.; Kendall, A.; Chabert, J. F. D.; McGown, A. T.; Lawrence, N. J., Combretastatin-like chalcones as inhibitors of microtubule polymerization. Part 1: Synthesis and biological evaluation of antivasular activity. *Bioorg. Med. Chem.* **2009**, *17*, 7698-7710.
126. Go, M. L.; Wu, X.; Liu, X. L., Chalcones: An update on cytotoxic and chemoprotective properties. *Curr. Med. Chem.* **2005**, *12*, 483-499.
127. Boumendjel, A.; Boccard, J.; Carrupt, P. A.; Nicolle, E.; Blanc, M.; Geze, A.; Choisnard, L.; Wouessidjewe, D.; Matera, E. L.; Dumontet, C., Antimitotic and antiproliferative activities of chalcones: Forward structure-activity relationship. *J. Med. Chem.* **2008**, *51*, 2307-2310.
128. Srinivasan, B.; Johnson, T. E.; Lad, R.; Xing, C. G., Structure-Activity Relationship Studies of Chalcone Leading to 3-Hydroxy-4,3',4',5'-tetramethoxychalcone and Its Analogues as Potent Nuclear Factor kappa B Inhibitors and Their Anticancer Activities. *J. Med. Chem.* **2009**, *52*, 7228-7235.
129. Ducki, S.; Forrest, R.; Hadfield, J. A.; Kendall, A.; Lawrence, N. J.; McGown, A. T.; Rennison, D., Potent antimitotic and cell growth inhibitory properties of substituted chalcones. *Bioorg. Med. Chem. Lett.* **1998**, *8*, 1051-1056.
130. Ducki, S.; Mackenzie, G.; Greedy, B.; Armitage, S.; Chabert, J. F. D.; Bennett, E.; Nettles, J.; Snyder, J. P.; Lawrence, N. J., Combretastatin-like chalcones as inhibitors of microtubule polymerisation. Part 2: Structure-based discovery of alpha-aryl chalcones. *Bioorg. Med. Chem.* **2009**, *17*, 7711-7722.
131. Pettit, G. R.; Singh, S. B.; Hamel, E.; Lin, C. M.; Alberts, D. S.; Garciakendall, D., Antineoplastic Agents .145. Isolation and Structure of the Strong Cell-Growth and Tubulin Inhibitor Combretastatin-a-4. *Experientia* **1989**, *45*, 209-211.
132. Lin, C. M.; Singh, S. B.; Chu, P. S.; Dempcy, R. O.; Schmidt, J. M.; Pettit, G. R.; Hamel, E., Interactions of Tubulin with Potent Natural and Synthetic Analogs of the Antimitotic Agent Combretastatin - a Structure-Activity Study. *Mol. Pharmacol.* **1988**, *34*, 200-208.
133. Lin, C. M.; Ho, H. H.; Pettit, G. R.; Hamel, E., Antimitotic Natural-Products Combretastatin-a-4 and Combretastatin-a-2 - Studies on the Mechanism of Their Inhibition of the Binding of Colchicine to Tubulin. *Biochemistry* **1989**, *28*, 6984-6991.
134. Katsori, A. M.; Hadjipavlou-Litina, D., Chalcones in Cancer: Understanding their Role in Terms of QSAR. *Curr. Med. Chem.* **2009**, *16*, 1062-1081.
135. Doria, G.; Romeo, C.; Forgione, A.; Sberze, P.; Tibolla, N.; Corno, M. L.; Cruzzola, G.; Cadelli, G., Anti-Allergic Agents .3. Substituted Trans-2-Ethenyl-4 Oxo-4h-1-Benzopyran-6-Carboxylic Acids. *Eur. J. Med. Chem.* **1979**, *14*, 347-351.
136. NMR spectroscopy reveals that compound **34** exists as an enol tautomer.
137. Larsson, R.; Nygren, P., A Rapid Fluorometric Method for Semiautomated Determination of Cyto-Toxicity and Cellular Proliferation of Human-Tumor Cell-Lines in Microculture. *Anticancer Res.* **1989**, *9*, 1111-1119.
138. Lindhagen, E.; Nygren, P.; Larsson, R., The fluorometric microculture cytotoxicity assay. *Nat. Protoc.* **2008**, *3*, 1364-1369.

139. Dhar, S.; Nygren, P.; Csoka, K.; Botling, J.; Nilsson, K.; Larsson, R., Anti-cancer drug characterisation using a human cell line panel representing defined types of drug resistance. *Br. J. Cancer* **1996**, *74*, 888-896.
140. Sullivan, C. M.; Smith, D. M.; Matsui, N. M.; Andrews, L. E.; Clauser, K. R.; Chapeaurouge, A.; Burlingame, A. L.; Epstein, L. B., Identification of constitutive and gamma-interferon- and interleukin 4 regulated proteins in the human renal carcinoma cell line ACHN. *Cancer Res.* **1997**, *57*, 1137-1143.
141. <http://www.cytoskeleton.com/products/biochem/bk011.html>.
142. Bonne, D.; Heusele, C.; Simon, C.; Pantaloni, D., 4',6-Diamidino-2-Phenylindole, a Fluorescent-Probe for Tubulin and Microtubules. *J. Biol. Chem.* **1985**, *260*, 2819-2825.
143. Pazdur, R.; Kudelka, A. P.; Kavanagh, J. J.; Cohen, P. R.; Raber, M. N., The Taxoids - Paclitaxel (Taxol(R)) and Docetaxel (Taxotere(R)). *Cancer Treat. Rev.* **1993**, *19*, 351-386.
144. *Maestro [9.0]*, Schrödinger, LLC, Portland, **2009**; *Glide [2.1]*, Schrödinger, LLC, Portland, **2009**
145. <http://www.pdb.org>.
146. Ravelli, R. B. G.; Gigant, B.; Curmi, P. A.; Jourdain, I.; Lachkar, S.; Sobel, A.; Knossow, M., Insight into tubulin regulation from a complex with colchicine and a stathmin-like domain. *Nature* **2004**, *428*, 198-202.
147. Kim, D. Y.; Kim, K. H.; Kim, N. D.; Lee, K. Y.; Han, C. K.; Yoon, J. H.; Moon, S. K.; Lee, S. S.; Seong, B. L., Design and biological evaluation of novel tubulin inhibitors as antimetabolic agents using a pharmacophore binding model with tubulin. *J. Med. Chem.* **2006**, *49*, 5664-5670.
148. Dimmock, J. R.; Kandepu, N. M.; Hetherington, M.; Quail, J. W.; Pugazhenthii, U.; Sudom, A. M.; Chamankhah, M.; Rose, P.; Pass, E.; Allen, T. M.; Halleran, S.; Szydlowski, J.; Mutus, B.; Tannous, M.; Manavathu, E. K.; Myers, T. G.; De Clercq, E.; Balzarini, J., Cytotoxic activities of Mannich bases of chalcones and related compounds. *J. Med. Chem.* **1998**, *41*, 1014-1026.
149. Reduced glutathione (19 mg, 0.06 mmol) was added to a solution of chalcone **10** (25 mg, 0.06 mmol) in THF (4 mL). The mixture was heated to 37 °C and stirred for 2 hours. Additionally, it should be noted that the reaction was initially performed in phosphate buffer at pH 7. However, THF were used instead due to solubility problems.
150. Manning, G.; Whyte, D. B.; Martinez, R.; Hunter, T.; Sudarsanam, S., The protein kinase complement of the human genome. *Science* **2002**, *298*, 1912-1943.
151. Hanks, S. K.; Quinn, A. M.; Hunter, T., The Protein-Kinase Family - Conserved Features and Deduced Phylogeny of the Catalytic Domains. *Science* **1988**, *241*, 42-52.
152. Fischer, P. M., The design of drug candidate molecules as selective inhibitors of therapeutically relevant protein kinases. *Curr. Med. Chem.* **2004**, *11*, 1563-1583.
153. Ubersax, J. A.; Ferrell, J. E., Mechanisms of specificity in protein phosphorylation. *Nat. Rev. Mol. Cell Biol.* **2007**, *8*, 530-541.
154. Lawrence, D. S., Chemical probes of signal-transducing proteins. *Acc. Chem. Res.* **2003**, *36*, 401-409.
155. Dhanasekaran, N.; Reddy, E. P., Signaling by dual specificity kinases. *Oncogene* **1998**, *17*, 1447-1455.
156. Wolanin, P. M.; Thomason, P. A.; Stock, J. B., Histidine protein kinases: key signal transducers outside the animal kingdom. *Genome Biol.* **2002**, *3*.
157. Besant, P. G.; Attwood, P. V., Mammalian histidine kinases. *Bba-Proteins Proteom.* **2005**, *1754*, 281-290.
158. Fischer, E. H.; Krebs, E. G., Conversion of Phosphorylase-B to Phosphorylase-a in Muscle Extracts. *J. Biol. Chem.* **1955**, *216*, 121-132.
159. Liao, J. J. L., Molecular recognition of protein kinase binding pockets for design of potent and selective kinase inhibitors. *J. Med. Chem.* **2007**, *50*, 409-424.
160. Hunter, T., Signaling - 2000 and beyond. *Cell* **2000**, *100*, 113-127.

161. Johnson, L. N., Protein kinase inhibitors: contributions from structure to clinical compounds. *Q. Rev. Biophys.* **2009**, *42*, 1-40.
162. Zhang, J. M.; Yang, P. L.; Gray, N. S., Targeting cancer with small molecule kinase inhibitors. *Nat. Rev. Cancer* **2009**, *9*, 28-39.
163. Huse, M.; Kuriyan, J., The conformational plasticity of protein kinases. *Cell* **2002**, *109*, 275-282.
164. Liu, Y.; Gray, N. S., Rational design of inhibitors that bind to inactive kinase conformations. *Nat. Chem. Biol.* **2006**, *2*, 358-364.
165. Zuccotto, F.; Ardini, E.; Casale, E.; Angiolini, M., Through the "Gatekeeper Door": Exploiting the Active Kinase Conformation. *J. Med. Chem.* **2010**, *53*, 2681-2694.
166. Kornev, A. P.; Haste, N. M.; Taylor, S. S.; Ten Eyck, L. F., Surface comparison of active and inactive protein kinases identifies a conserved activation mechanism. *Proc. Natl. Acad. Sci. U. S. A.* **2006**, *103*, 17783-17788.
167. Laufer, S. A.; Domeyer, D. M.; Scior, T. R. F.; Albrecht, W.; Hauser, D. R. J., Synthesis and biological testing of purine derivatives as potential ATP-competitive kinase inhibitors. *J. Med. Chem.* **2005**, *48*, 710-722.
168. Pearson, G.; Robinson, F.; Gibson, T. B.; Xu, B. E.; Karandikar, M.; Berman, K.; Cobb, M. H., Mitogen-activated protein (MAP) kinase pathways: Regulation and physiological functions. *Endocr. Rev.* **2001**, *22*, 153-183.
169. Chen, Z.; Gibson, T. B.; Robinson, F.; Silvestro, L.; Pearson, G.; Xu, B. E.; Wright, A.; Vanderbilt, C.; Cobb, M. H., MAP kinases. *Chem. Rev.* **2001**, *101*, 2449-2476.
170. Kyriakis, J. M.; Avruch, J., Mammalian mitogen-activated protein kinase signal transduction pathways activated by stress and inflammation. *Physiol. Rev.* **2001**, *81*, 807-869.
171. Akella, R.; Moon, T. M.; Goldsmith, E. J., Unique MAP kinase binding sites. *Bba-Proteins Proteom.* **2008**, *1784*, 48-55.
172. Krishna, M.; Narang, H., The complexity of mitogen-activated protein kinases (MAPKs) made simple. *Cell. Mol. Life Sci.* **2008**, *65*, 3525-3544.
173. Johnson, G. L.; Lapadat, R., Mitogen-activated protein kinase pathways mediated by ERK, JNK, and p38 protein kinases. *Science* **2002**, *298*, 1911-1912.
174. Pierce, K. L.; Premont, R. T.; Lefkowitz, R. J., Seven-transmembrane receptors. *Nat. Rev. Mol. Cell Biol.* **2002**, *3*, 639-650.
175. http://www.cellsignal.com/reference/pathway/MAPK_Cascades.html
176. Noble, M. E. M.; Endicott, J. A.; Johnson, L. N., Protein kinase inhibitors: Insights into drug design from structure. *Science* **2004**, *303*, 1800-1805.
177. Cohen, P., Protein kinases - the major drug targets of the twenty-first century? *Nat. Rev. Drug Discov.* **2002**, *1*, 309-315.
178. Hanks, S. K.; Hunter, T., Protein Kinases .6. The Eukaryotic Protein-Kinase Superfamily - Kinase (Catalytic) Domain-Structure and Classification. *FASEB J.* **1995**, *9*, 576-596.
179. Garuti, L.; Roberti, M.; Bottegoni, G., Non-ATP Competitive Protein Kinase Inhibitors. *Curr. Med. Chem.* **2010**, *17*, 2804-2821.
180. Beis, I.; Newsholme, E. A., Contents of Adenine-Nucleotides, Phosphagens and Some Glycolytic Intermediates in Resting Muscles from Vertebrates and Invertebrates. *Biochem. J.* **1975**, *152*, 23-32.
181. McInnes, C.; Fischer, P. M., Strategies for the design of potent and selective kinase inhibitors. *Curr. Pharm. Des.* **2005**, *11*, 1845-1863.
182. Sawa, M., Strategies for the Design of Selective Protein Kinase Inhibitors. *Mini-Rev. Med. Chem.* **2008**, *8*, 1291-1297.
183. Alaimo, P. J.; Knight, Z. A.; Shokat, K. M., Targeting the gatekeeper residue in phosphoinositide 3-kinases. *Bioorg. Med. Chem.* **2005**, *13*, 2825-2836.

184. Pargellis, C.; Tong, L.; Churchill, L.; Cirillo, P. F.; Gilmore, T.; Graham, A. G.; Grob, P. M.; Hickey, E. R.; Moss, N.; Pav, S.; Regan, J., Inhibition of p38 MAP kinase by utilizing a novel allosteric binding site. *Nat. Struct. Biol.* **2002**, *9*, 268-272.
185. Lee, J. C.; Laydon, J. T.; McDonnell, P. C.; Gallagher, T. F.; Kumar, S.; Green, D.; McNulty, D.; Blumenthal, M. J.; Heys, J. R.; Landvatter, S. W.; Strickler, J. E.; Mclaughlin, M. M.; Siemens, I. R.; Fisher, S. M.; Livi, G. P.; White, J. R.; Adams, J. L.; Young, P. R., A Protein-Kinase Involved in the Regulation of Inflammatory Cytokine Biosynthesis. *Nature* **1994**, *372*, 739-746.
186. Kumar, S.; Boehm, J.; Lee, J. C., p38 map kinases: Key signalling molecules as therapeutic targets for inflammatory diseases. *Nat. Rev. Drug Discov.* **2003**, *2*, 717-726.
187. Cuenda, A.; Rousseau, S., P38 MAP-Kinases pathway regulation, function and role in human diseases. *Bba-Mol. Cell Res.* **2007**, *1773*, 1358-1375.
188. Zhang, J. Y.; Shen, B. F.; Lin, A. N., Novel strategies for inhibition of the p38 MAPK pathway. *Trends Pharmacol. Sci.* **2007**, *28*, 286-295.
189. Dominguez, C.; Tamayo, N.; Zhang, D. W., P38 Inhibitors: beyond pyridinylimidazoles. *Expert Opin. Ther. Pat.* **2005**, *15*, 801-816.
190. Wagner, E. F.; Nebreda, A. R., Signal integration by JNK and p38 MAPK pathways in cancer development. *Nat. Rev. Cancer* **2009**, *9*, 537-549.
191. Bradham, C.; McClay, D. R., p38 MAPK in development and cancer. *Cell Cycle* **2006**, *5*, 824-828.
192. Chen, L.; Mayer, J. A.; Krisko, T. I.; Speers, C. W.; Wang, T.; Hilsenbeck, S. G.; Brown, P. H., Inhibition of the p38 Kinase Suppresses the Proliferation of Human ER-Negative Breast Cancer Cells. *Cancer Res.* **2009**, *69*, 8853-8861.
193. Cuenda, A.; Rouse, J.; Doza, Y. N.; Meier, R.; Cohen, P.; Gallagher, T. F.; Young, P. R.; Lee, J. C., Sb-203580 Is a Specific Inhibitor of a Map Kinase Homolog Which Is Stimulated by Cellular Stresses and Interleukin-1. *FEBS Lett.* **1995**, *364*, 229-233.
194. Tong, L.; Pav, S.; White, D. M.; Rogers, S.; Crane, K. M.; Cywin, C. L.; Brown, M. L.; Pargellis, C. A., A highly specific inhibitor of human p38 MAP kinase binds in the ATP pocket. *Nat. Struct. Biol.* **1997**, *4*, 311-316.
195. Wang, Z. L.; Canagarajah, B. J.; Boehm, J. C.; Kassisa, S.; Cobb, M. H.; Young, P. R.; Abdel-Meguid, S.; Adams, J. L.; Goldsmith, E. J., Structural basis of inhibitor selectivity in MAP kinases. *Structure with Folding & Design* **1998**, *6*, 1117-1128.
196. Boehm, J. C.; Adams, J. L., New inhibitors of p38 kinase. *Expert Opin. Ther. Pat.* **2000**, *10*, 25-37.
197. Young, P. R.; McLaughlin, M. M.; Kumar, S.; Kassis, S.; Doyle, M. L.; McNulty, D.; Gallagher, T. F.; Fisher, S.; McDonnell, P. C.; Carr, S. A.; Huddleston, M. J.; Seibel, G.; Porter, T. G.; Livi, G. P.; Adams, J. L.; Lee, J. C., Pyridinyl imidazole inhibitors of p38 mitogen-activated protein kinase bind in the ATP site. *J. Biol. Chem.* **1997**, *272*, 12116-12121.
198. Buijsman, R., *Chemogenomics in drug discovery: A medicinal chemistry perspective*. WILEY-VCH Verlag GmbH & Co. KGaA: Weinheim, 2004.
199. Natarajan, S. R.; Wisnoski, D. D.; Singh, S. B.; Stelmach, J. E.; O'Neill, E. A.; Schwartz, C. D.; Thompson, C. M.; Fitzgerald, C. E.; O'Keefe, S. J.; Kumar, S.; Hop, C. E. C. A.; Zaller, D. M.; Schmatz, D. M.; Doherty, J. B., p38 MAP kinase inhibitors. Part 1: Design and development of a new class of potent and highly selective inhibitors based on 3,4-dihydropyrido[3,2-d]pyrimidone scaffold. *Bioorg. Med. Chem. Lett.* **2003**, *13*, 273-276.
200. Hunt, J. A.; Kallashi, F.; Ruzek, R. D.; Sinclair, P. J.; Ita, I.; McCormick, S. X.; Pivnichny, J. V.; Hop, C. E. C. A.; Kumar, S.; Wang, Z.; O'Keefe, S. J.; O'Neill, E. A.; Porter, G.; Thompson, J. E.; Woods, A.; Zaller, D. M.; Doherty, J. B., p38 inhibitors: Piperidine- and 4-aminopiperidine-substituted naphthyridinones, quinolinones, and dihydroquinazolinones. *Bioorg. Med. Chem. Lett.* **2003**, *13*, 467-470.
201. Stelmach, J. E.; Liu, L. P.; Patela, S. B.; Pivnichny, J. V.; Scapin, G.; Singh, S.; Hop, C. E. C. A.; Wang, Z.; Strauss, J. R.; Cameron, P. M.; Nichols, E. A.; O'Keefe, S. J.; O'Neill, E. A.; Schmatz,

- D. M.; Schwartz, C. D.; Thompson, C. M.; Zaller, D. M.; Doherty, J. B., Design and synthesis of potent, orally bioavailable dihydroquinazolinone inhibitors of p38 MAP kinase. *Bioorg. Med. Chem. Lett.* **2003**, *13*, 277-280.
202. Fitzgerald, C. E.; Patel, S. B.; Becker, J. W.; Cameron, P. M.; Zaller, D.; Pikounis, V. B.; O'Keefe, S. J.; Scapin, G., Structural basis for p38 alpha MAP kinase quinazolinone and pyridol-pyrimidine inhibitor specificity. *Nat. Struct. Biol.* **2003**, *10*, 764-769.
203. Regan, J.; Breifelder, S.; Cirillo, P.; Gilmore, T.; Graham, A. G.; Hickey, E.; Klaus, B.; Madwed, J.; Moriak, M.; Moss, N.; Pargellis, C.; Pav, S.; Proto, A.; Swinamer, A.; Tong, L.; Torcellini, C., Pyrazole urea-based inhibitors of p38 MAP kinase: From lead compound to clinical candidate. *J. Med. Chem.* **2002**, *45*, 2994-3008.
204. Yap, J. L.; Worlikar, S.; MacKerell, A. D.; Shapiro, P.; Fletcher, S., Small-Molecule Inhibitors of the ERK Signaling Pathway: Towards Novel Anticancer Therapeutics. *ChemMedChem* **2011**, *6*, 38-48.
205. Zheng, C. F.; Guan, K. L., Cloning and Characterization of 2 Distinct Human Extracellular Signal-Regulated Kinase Activator Kinases, Mek1 and Mek2. *J. Biol. Chem.* **1993**, *268*, 11435-11439.
206. Fremin, C.; Meloche, S., From basic research to clinical development of MEK1/2 inhibitors for cancer therapy. *J. Hematol. Oncol.* **2010**, *3*, 1-11.
207. English, J. M.; Cobb, M. H., Pharmacological inhibitors of MAPK pathways. *Trends Pharmacol. Sci.* **2002**, *23*, 40-45.
208. Spicer, J. A.; Rewcastle, G. W.; Kaufman, M. D.; Black, S. L.; Plummer, M. S.; Denny, W. A.; Quin, J.; Shahripour, A. B.; Barrett, S. D.; Whitehead, C. E.; Milbank, J. B. J.; Ohren, J. F.; Gowan, R. C.; Omer, C.; Camp, H. S.; Esmail, N.; Moore, K.; Sebolt-Leopold, J. S.; Pryzbranowski, S.; Merriman, R. L.; Ortwine, D. F.; Warmus, J. S.; Flamme, C. M.; Pavlovsky, A. G.; Teclé, H., 4-anilino-5-carboxamido-2-pyridone derivatives as noncompetitive inhibitors of mitogen-activated protein kinase kinase. *J. Med. Chem.* **2007**, *50*, 5090-5102.
209. Duncia, J. V.; Santella, J. B.; Higley, C. A.; Pitts, W. J.; Wityak, J.; Frieze, W. E.; Rankin, F. W.; Sun, J. H.; Earl, R. A.; Tabaka, A. C.; Teleha, C. A.; Blom, K. F.; Favata, M. F.; Manos, E. J.; Daulerio, A. J.; Stradley, D. A.; Horiuchi, K.; Copeland, R. A.; Scherle, P. A.; Trzaskos, J. M.; Magolda, R. L.; Trainor, G. L.; Wexler, R. R.; Hobbs, F. W.; Olson, R. E., MEK inhibitors: The chemistry and biological activity of U0126, its analogs, and cyclization products. *Bioorg. Med. Chem. Lett.* **1998**, *8*, 2839-2844.
210. Kataoka, T.; Watanabe, S.; Mori, E.; Kadomoto, R.; Tanimura, S.; Kohno, M., Synthesis and structure-activity relationships of thioflavone derivatives as specific inhibitors of the ERK-MAP kinase signaling pathway. *Bioorg. Med. Chem.* **2004**, *12*, 2397-2407.
211. Larroque-Lombard, A. L.; Todorova, M.; Qiu, Q. Y.; Jean-Claude, B., Synthesis and Studies on Three-Compartment Flavone-Containing Combi-Molecules Designed to Target EGFR, DNA, and MEK. *Chem. Biol. Drug Des.* **2011**, *77*, 309-318.
212. Laufer, S. A.; Hauser, D. R. J.; Domeyer, D. M.; Kinkel, K.; Liedtke, A. J., Design, synthesis, and biological evaluation of novel tri- and tetrasubstituted imidazoles as highly potent and specific ATP-mimetic inhibitors of p38 MAP kinase: Focus on optimized interactions with the enzyme's surface-exposed front region. *J. Med. Chem.* **2008**, *51*, 4122-4149.
213. Koch, P.; Laufer, S., Unexpected Reaction of 2-Alkylsulfanylimidazoles to Imidazol-2-ones: Pyridinylimidazol-2-ones as Novel Potent p38 alpha Mitogen-Activated Protein Kinase Inhibitors. *J. Med. Chem.* **2010**, *53*, 4798-4802.
214. Laufer, S. A.; Wagner, G. K.; Kotschenreuther, D. A.; Albrecht, W., Novel substituted pyridinyl imidazoles as potent anticytokine agents with low activity against hepatic cytochrome P450 enzymes. *J. Med. Chem.* **2003**, *46*, 3230-3244.

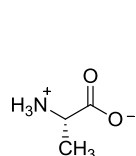
215. Koch, P.; Bauerlein, C.; Jank, H.; Laufer, S., Targeting the ribose and phosphate binding site of p38 mitogen-activated protein (MAP) kinase: Synthesis and biological testing of 2-alkylsulfanyl-, 4(5)-aryl-, 5(4)-heteroaryl-substituted imidazoles. *J. Med. Chem.* **2008**, *51*, 5630-5640.
216. Koch, P.; Jahns, H.; Schattel, V.; Goettert, M.; Laufer, S., Pyridinylquinoxalines and Pyridinylpyridopyrazines as Lead Compounds for Novel p38 alpha Mitogen-Activated Protein Kinase Inhibitors. *J. Med. Chem.* **2010**, *53*, 1128-1137.
217. Chen, C. L.; Lin, C. W.; Hsieh, C. C.; Lai, C. H.; Lee, G. H.; Wang, C. C.; Chou, P. T., Dual Excited-State Intramolecular Proton Transfer Reaction in 3-Hydroxy-2-(pyridin-2-yl)-4H-chromen-4-one. *J. Phys. Chem. A* **2009**, *113*, 205-214.
218. Anderson, W. K.; Dean, D. C.; Endo, T., Synthesis, Chemistry, and Antineoplastic Activity of Alpha-Halopyridinium Salts - Potential Pyridone Prodrugs of Acylated Vinylogous Carbinolamine Tumor Inhibitors. *J. Med. Chem.* **1990**, *33*, 1667-1675.
219. Ono, M.; Watanabe, R.; Kawashima, H.; Kawai, T.; Watanabe, H.; Haratake, M.; Saji, H.; Nakayama, M., (18)F-labeled flavones for in vivo imaging of beta-amyloid plaques in Alzheimer's brains. *Bioorg. Med. Chem.* **2009**, *17*, 2069-2076.
220. Ghani, S. B. A.; Weaver, L.; Zidan, Z. H.; Ali, H. M.; Keevil, C. W.; Brown, R. C. D., Microwave-assisted synthesis and antimicrobial activities of flavonoid derivatives. *Bioorg. Med. Chem. Lett.* **2008**, *18*, 518-522.
221. Minassi, A.; Giana, A.; Ech-Chahad, A.; Appendino, G., A regiodivergent synthesis of ring a C-prenylflavones. *Org. Lett.* **2008**, *10*, 2267-2270.
222. Valla, C.; Baeza, A.; Menges, F.; Pfaltz, A., Enantioselective Synthesis of Chromanes by Iridium-Catalyzed Asymmetric Hydrogenation of 4H-Chromenes. *Synlett* **2008**, 3167-3171.
223. Dao, T. T.; Chi, Y. S.; Kim, J. S.; Kim, H. P.; Kim, S. H.; Park, H., Synthesis and inhibitory activity against COX-2 catalyzed prostaglandin production of chrysin derivatives. *Bioorg. Med. Chem. Lett.* **2004**, *14*, 1165-1167.
224. Fitzmaurice, R. J.; Etheridge, Z. C.; Jumel, E.; Woolfson, D. N.; Caddick, S., Microwave enhanced palladium catalysed coupling reactions: A diversity-oriented synthesis approach to functionalised flavones. *Chem. Commun.* **2006**, 4814-4816.
225. Joo, Y. H.; Kim, J. K.; Kang, S. H.; Noh, M. S.; Ha, J. Y.; Choi, J. K.; Lim, K. M.; Lee, C. H.; Chung, S., 2,3-Diarylbenzopyran derivatives as a novel class of selective cyclooxygenase-2 inhibitors. *Bioorg. Med. Chem. Lett.* **2003**, *13*, 413-417.
226. Ding, K.; Wang, S. M., Efficient synthesis of isoflavone analogues via a Suzuki coupling reaction. *Tetrahedron Lett.* **2005**, *46*, 3707-3709.
227. Sy, W. W., Iodination of Methoxyamphetamines with Iodine and Silver Sulfate. *Tetrahedron Lett.* **1993**, *34*, 6223-6224.
228. Horiuchi, C. A.; Ikeda, A.; Kanamori, M.; Hosokawa, H.; Sugiyama, T.; Takahashi, T. T., A new synthesis of trans-iodohydrins using iodine-cerium(IV) salts. *J. Chem. Res. (S)* **1997**, 60-61.
229. Pal, M.; Subramanian, V.; Parasuraman, K.; Yeleswarapu, K. R., Palladium catalyzed reaction in aqueous DMF: synthesis of 3-alkynyl substituted flavones in the presence of prolinol. *Tetrahedron* **2003**, *59*, 9563-9570.
230. Das, B.; Krishnaiah, M.; Venkateswarlu, K.; Reddy, V. S., A mild and simple regioselective iodination of activated aromatics with iodine and catalytic ceric ammonium nitrate *Tetrahedron Lett.* **2007**, *48*, 81-83.
231. Nair, V.; Deepthi, A., Cerium(IV) ammonium nitrate - A versatile single-electron oxidant. *Chem. Rev.* **2007**, *107*, 1862-1891.
232. Cardenas, M.; Marder, M.; Blank, V. C.; Roguin, L. P., Antitumor activity of some natural flavonoids and synthetic derivatives on various human and murine cancer cell lines. *Bioorg. Med. Chem.* **2006**, *14*, 2966-2971.

233. Zhou, Z. Z.; Zhao, P. L.; Huang, W.; Yang, G. F., A selective transformation of flavanones to 3-bromoflavones and flavones under microwave irradiation. *Adv. Synth. Catal.* **2006**, *348*, 63-67.
234. Caballero, E.; Avendano, C.; Menendez, J. C., Steric and stereochemical effects on the free-radical bromination of tetracyclic and hexacyclic fragments of the MDR inhibitor N-acetylardeemin. *Tetrahedron* **1999**, *55*, 14185-14198.
235. Costa, A. M. B. S. R. C. S.; Dean, F. M.; Jones, M. A.; Varma, R. S., Lithiation in Flavones, Chromones, Coumarins, and Benzofuran Derivatives. *J. Chem. Soc., Perkin Trans. 1* **1985**, 799-808.
236. Beryozkina, T.; Appukkuttan, P.; Mont, N.; Van der Eycken, E., Microwave-enhanced synthesis of new (-)-steganacin and (-)-steganone aza analogues. *Org. Lett.* **2006**, *8*, 487-490.
237. Diner, P.; Andersson, T.; Kjellen, J.; Elbing, K.; Hohmann, S.; Grotli, M., Short cut to 1,2,3-triazole-based p38 MAP kinase inhibitors via [3+2]-cycloaddition chemistry. *New J. Chem.* **2009**, *33*, 1010-1016.
238. Diner, P.; Vilg, J. V.; Kjellen, J.; Migdal, I.; Andersson, T.; Gebbia, M.; Giaever, G.; Nislow, C.; Hohmann, S.; Wysocki, R.; Tamas, M. J.; Grotli, M., Design, Synthesis, and Characterization of a Highly Effective Hog1 Inhibitor: A Powerful Tool for Analyzing MAP Kinase Signaling in Yeast. *PLoS ONE* **2011**, *6*.
239. Felpin, F. X., Practical and efficient Suzuki-Miyaura cross-coupling of 2-iodocycloenones with arylboronic acids catalyzed by recyclable Pd(0)/C. *J. Org. Chem.* **2005**, *70*, 8575-8578.
240. Han, W.; Liu, C.; Jin, Z. L., In situ generation of palladium nanoparticles: A simple and highly active protocol for oxygen-promoted ligand-free suzuki coupling reaction of aryl chlorides. *Org. Lett.* **2007**, *9*, 4005-4007.
241. Corma, A.; Garcia, H.; Leyva, A., Polyethyleneglycol as scaffold and solvent for reusable C-C coupling homogeneous Pd catalysts. *J. Catal.* **2006**, *240*, 87-99.
242. Li, J. H.; Liu, W. J.; Xie, Y. X., Recyclable and reusable Pd(OAc)₂/DABCO/PEG-400 system for Suzuki-Miyaura cross-coupling reaction. *J. Org. Chem.* **2005**, *70*, 5409-5412.
243. Wolfe, J. P.; Tomori, H.; Sadighi, J. P.; Yin, J. J.; Buchwald, S. L., Simple, efficient catalyst system for the palladium-catalyzed amination of aryl chlorides, bromides, and triflates. *J. Org. Chem.* **2000**, *65*, 1158-1174.
244. Li, J. J.; Wang, Z.; Mitchell, L. H., A practical Buchwald-Hartwig amination of 2-bromopyridines with volatile amines. *J. Org. Chem.* **2007**, *72*, 3606-3607.
245. <http://www.millipore.com/>
246. Goettert, M.; Schattel, V.; Koch, P.; Merfort, I.; Laufer, S., Biological Evaluation and Structural Determinants of p38 alpha Mitogen-Activated-Protein Kinase and c-Jun-N-Terminal Kinase 3 Inhibition by Flavonoids. *ChemBioChem* **2010**, *11*, 2579-2588.
247. The cellular experiments were performed by co-workers at the Department of Cell and Molecular Biology, University of Gothenburg.
248. Reinhardt, H. C.; Aslanian, A. S.; Lees, J. A.; Yaffe, M. B., p53-deficient cells rely on ATM- and ATR-mediated checkpoint signaling through the p38MAPK/MK2 pathway for survival after DNA damage. *Cancer Cell* **2007**, *11*, 175-189.
249. Gould, G. W.; Cuenda, A.; Thomson, F. J.; Cohen, P., The Activation of Distinct Mitogen-Activated Protein-Kinase Cascades Is Required for the Stimulation of 2-Deoxyglucose Uptake by Interleukin-1 and Insulin-Like Growth-Factor-I in Kb Cells. *Biochem. J.* **1995**, *311*, 735-738.
250. Alessi, D. R.; Cuenda, A.; Cohen, P.; Dudley, D. T.; Saltiel, A. R., Pd-098059 Is a Specific Inhibitor of the Activation of Mitogen-Activated Protein-Kinase Kinase in-Vitro and in-Vivo. *J. Biol. Chem.* **1995**, *270*, 27489-27494.
251. Dudley, D. T.; Pang, L.; Decker, S. J.; Bridges, A. J.; Saltiel, A. R., A Synthetic Inhibitor of the Mitogen-Activated Protein-Kinase Cascade. *Proc. Natl. Acad. Sci. U. S. A.* **1995**, *92*, 7686-7689.

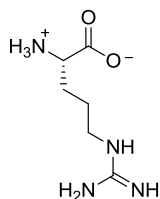
252. Moon, D. O.; Park, C.; Heo, M. S.; Park, Y. M.; Choi, Y. H.; Kim, G. Y., PD98059 triggers G1 arrest and apoptosis in human leukemic U937 cells through downregulation of Akt signal pathway. *Int. Immunopharmacol.* **2007**, *7*, 36-45.
253. Davison, Z.; Dutkowski, C.; Gee, J. M. W.; Nicholson, R. I.; Heard, C. M., In vitro effects on MCF-7 breast cancer cells of signal transduction inhibitor/tamoxifen/eicosapentaenoic acid combinations and their simultaneous delivery across skin. *Pharm. Res.* **2008**, *25*, 2516-2525.
254. Zelivianski, S.; Spellman, M.; Kellerman, M.; Kakitelashvili, V.; Zhou, X. W.; Lugo, E.; Lee, M. S.; Taylor, R.; Davis, T. L.; Hauke, R.; Lin, M. F., Erk inhibitor PD98059 enhances docetaxel-induced apoptosis of androgen-independent human prostate cancer cells. *Int. J. Cancer* **2003**, *107*, 478-485.
255. Ohren, J. F.; Chen, H. F.; Pavlovsky, A.; Whitehead, C.; Zhang, E. L.; Kuffa, P.; Yan, C. H.; McConnell, P.; Spessard, C.; Banotai, C.; Mueller, W. T.; Delaney, A.; Omer, C.; Sebolt-Leopold, J.; Dudley, D. T.; Leung, I. K.; Flamme, C.; Warmus, J.; Kaufman, M.; Barrett, S.; Teclé, H.; Hasemann, C. A., Structures of human MAP kinase kinase 1 (MEK1) and MEK2 describe novel noncompetitive kinase inhibition. *Nat. Struct. Mol. Biol.* **2004**, *11*, 1192-1197.
256. Mahboobi, S.; Pongratz, H., Synthesis of 2'-amino-3'-methoxyflavone (PD 98059). *Synth. Commun.* **1999**, *29*, 1645-1652.
257. Ye, B.; Arnaiz, D. O.; Chou, Y. L.; Griedel, B. D.; Karanjawala, R.; Lee, W.; Morrissey, M. M.; Sacchi, K. L.; Sakata, S. T.; Shaw, K. J.; Wu, S. C.; Zhao, Z. C.; Adler, M.; Cheeseman, S.; Dole, W. P.; Ewing, J.; Fitch, R.; Lentz, D.; Liang, A.; Light, D.; Morser, J.; Post, J.; Rumennik, G.; Subramanyam, B.; Sullivan, M. E.; Vergona, R.; Walters, J.; Wang, Y. X.; White, K. A.; Whitlow, M.; Kochanny, M. J., Thiophene-anthranilamides as highly potent and orally available factor Xa inhibitors. *J. Med. Chem.* **2007**, *50*, 2967-2980.
258. Vancaelenbergh, S.; Verlinde, C. L. M. J.; Soenens, J.; Debruyne, A.; Callens, M.; Blaton, N. M.; Peeters, O. M.; Rozenski, J.; Hol, W. G. J.; Herdewijn, P., Synthesis and Structure-Activity-Relationships of Analogs of 2'-Deoxy-2'-(3-Methoxy-benzamido)Adenosine, a Selective Inhibitor of Trypanosomal Glycosomal Glyceraldehyde-3-Phosphate Dehydrogenase. *J. Med. Chem.* **1995**, *38*, 3838-3849.
259. Dong, Y.; Busacca, C. A., Indoles from *O*-haloanilines: Syntheses of tryptamines and tryptophols via regioselective hydroformylation of functionalized anilines. *J. Org. Chem.* **1997**, *62*, 6464-6465.

Appendix

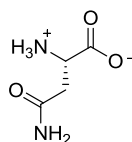
A. ESSENTIAL AMINO ACIDS FOUND IN PROTEINS



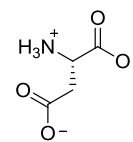
Alanine (Ala, A)



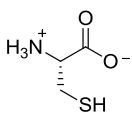
Arginine (Arg, R)



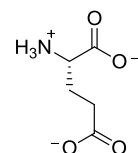
Asparagine (Asn, N)



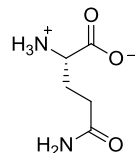
Aspartate (Asp, D)



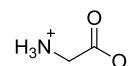
Cysteine (Cys, C)



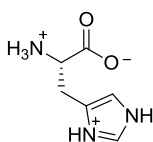
Glutamate (Glu, E)



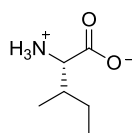
Glutamine (Gln, Q)



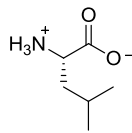
Glycine (Gly, G)



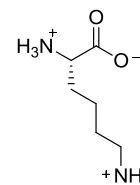
Histidine (His, H)



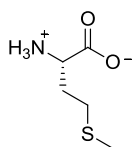
Isoleucine (Ile, I)



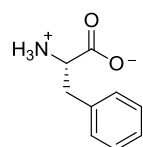
Leucine (Leu, L)



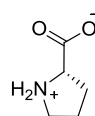
Lysine (Lys, K)



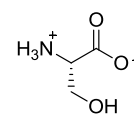
Methionine (Met, M)



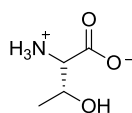
Phenylalanine (Phe, F)



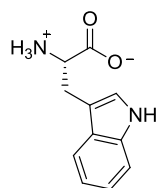
Proline (Pro, P)



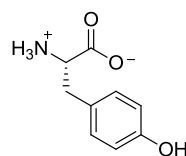
Serine (Ser, S)



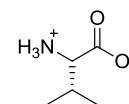
Threonine (Thr, T)



Tryptophan (Trp, W)



Tyrosine (Tyr, Y)

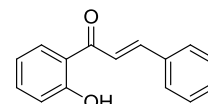


Valine (Val, V)

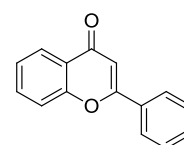
B. EXPERIMENTAL PROCEDURES FOR COMPOUNDS NOT INCLUDED IN PAPERS I-IV

General All reagents and solvents were of analysis or synthesis grade. ^1H NMR-spectra were recorded on a JEOL JNM-EX 400-spectrometer at 400 MHz in CDCl_3 . Chemical shifts are reported in ppm with the solvent residual peak as reference; CDCl_3 (δ_{H} 7.26). The reactions were monitored by thin-layer chromatography (TLC), on silica plated (Silica gel 60 F₂₅₄, E. Merck) aluminum sheets, detecting spots by UV (254 and 365 nm). Flash chromatography was performed using a Biotage SP4 Flash instrument with prepacked columns. Microwave reactions were carried out in a Biotage Initiator instrument with a fixed hold time using capped vials.

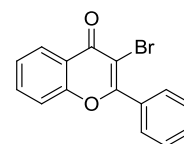
(E)-1-(2-Hydroxyphenyl)-3-phenylprop-2-en-1-one (39). KOH (3.7 g, 66.0 mmol) was added to a stirred solution of 2'-hydroxyacetophenone **36** (3.0 g, 22.0 mmol) and benzaldehyde (2.46 ml, 24.2 mmol) in EtOH (150 mL). The mixture was heated at 50 °C for 3 h and was then stirred at room temperature overnight. The dark red solution was acidified with HCl (aq., 1M) to yield a yellow precipitate, which was filtered off and washed with water. The precipitate was recrystallized from EtOH to afford **39** (1.9 g, 67%) as yellow crystals. ^1H NMR (CDCl_3) δ 6.92-6.99 (m, 1H), 7.04 (dd, $J = 1.1, 8.4$ Hz, 1H), 7.42-7.54 (m, 4H), 7.63-7.69 (m, 3H), 7.93-7.99 (m, 2H), 12.84 (s, 1H).



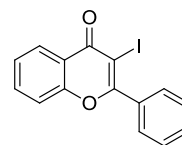
2-Phenylchromone (40). Iodine (226 mg, 0.89 mmol) was added to a solution of **39** (100 mg, 0.45 mmol) in EtOH (5 mL) and the suspension was heated in a microwave cavity at 150 °C for 160 min. The mixture was quenched with saturated $\text{Na}_2\text{S}_2\text{O}_3$ (aq), extracted with dichloromethane (3×10 mL), dried over MgSO_4 and concentrated. The product **40** (99 mg, 99%) was obtained as off-white crystals. ^1H NMR (CDCl_3) δ 6.84 (s, 1H), 7.39-7.46 (m, 1H), 7.50-7.60 (m, 4H), 7.67-7.74 (m, 1H), 7.91-7.96 (m, 2H), 8.24 (dd, $J = 1.5, 8.1$ Hz, 1H).



3-Bromo-2-phenylchromone (49). NBS (319 mg, 1.79 mmol) was added to a solution of **40** (362 mg, 1.63 mmol) in DMF (16 mL). The reaction mixture was heated in a microwave cavity at 60 °C for 30 min. The reaction mixture was quenched with $\text{Na}_2\text{S}_2\text{O}_3$ (aq., 10%) and the aqueous phase was extracted with ethyl acetate (3×20 mL). The combined organic phases were washed with brine (60 mL), dried over MgSO_4 and concentrated. The crude was purified by flash chromatography (heptane/ethyl acetate, gradient 20 \rightarrow 40% ethyl acetate) to afford **49** (256 mg, 52%) as an off-white powder. ^1H NMR (CDCl_3) δ 7.45-7.58 (m, 5H), 7.70-7.76 (m, 1H), 7.84-7.89 (m, 2H), 8.31 (dd, $J = 1.8, 8.1$ Hz, 1H).

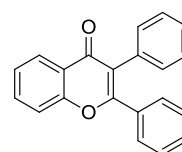


3-Iodo-2-phenylchromone (50). Iodine (42 mg, 0.17 mmol) and CAN (79 mg, 0.14 mmol) were added to a solution of **40** (32 mg, 0.14 mmol) in acetonitrile (2 mL). The mixture was heated in a microwave cavity at 65 °C for 30 min, 100 °C for 15 min and 130 °C for 15 min. The reaction mixture was quenched with Na₂S₂O₃ (aq., 10%), extracted with dichloromethane (3 × 5 mL), dried over MgSO₄, and concentrated. The crude was purified by flash chromatography (heptane/ethyl acetate, gradient 20 → 40% ethyl acetate) to afford **50** (34 mg, 67%) as a white solid. ¹H NMR (CDCl₃) δ 7.43-7.48 (m, 5H), 7.69-7.83 (m, 3H), 8.30 (dd, *J* = 1.7, 8.0 Hz, 1H).



General procedure for the synthesis of 3-arylflavones (55-56). The appropriate boronic acid (4 equiv) was added to a suspension of **49** (1 equiv) in PEG-400 (20 g/mmol aryl bromide) followed by the addition of Pd(OAc)₂ (0.2 equiv) and K₂CO₃ (2 equiv). The reaction mixture was heated in a microwave cavity at 60 °C for 30-60 min. The reaction mixture was poured over brine (5 mL), extracted with diethyl ether (3 × 5 mL) and washed with brine. The combined organic phases were dried over MgSO₄, filtered through Celite and concentrated. The crude product was purified by flash chromatography.

2,3-Diphenylchromone (55). The title compound was synthesized according to the general procedure. Compound **49** (59 mg, 0.20 mmol) and phenyl boronic acid (96 mg, 0.78 mmol) gave **55** (49 mg, 84%) as an off-white solid. The product was purified by flash chromatography using heptane/ethyl acetate (9:1). ¹H NMR (CDCl₃) δ 7.20-7.58 (m, 12H), 7.68-7.74 (m, 1H), 8.28-8.33 (m, 1H).



3-(4-Fluorophenyl)-2-phenylchromone (56). The title compound was synthesized according to the general procedure. Compound **49** (40 mg, 0.13 mmol) and 4-fluorophenyl boronic acid (74 mg, 0.53 mmol) gave **56** (24 mg, 53%) as an off-white solid. The product was purified by flash chromatography using heptane/ethyl acetate (gradient 10 → 20% ethyl acetate). ¹H NMR (CDCl₃) δ 6.96-7.04 (m, 2H), 7.15-7.48 (m, 8H), 7.52-7.57 (m, 1H), 7.68-7.75 (m, 1H), 8.29 (dd, *J* = 1.8, 8.1 Hz, 1H).

